LA-UR- 11-03026

Approved for public release; distribution is unlimited.

Title: Introduction to Free-Electron Laser Systems

Author(s): Dinh C. Nguyen

Intended for: AHPL Short Course
Santa Fe, NM
June 6, 2011

Los Alamos
NATIONAL LABORATORY
EST. 1943

Introduction to Free-Electron Laser Systems

AHPL Short Courses
6 June 2011
Santa Fe, NM

Dinh Nguyen
Los Alamos National Laboratory

Course Content

1. Introduction to FEL
2. Wigglers
3. Spontaneous Emission, Gain & Efficiency
4. Optical Architectures
5. Electron Beam Transport
6. RF Linear Accelerators
7. Electron Injectors
8. Backup Slides (Review Materials)

Los Alamos
NATIONAL LABORATORY
EST. 1943

Part 1
Introduction to FEL

Light are photons (individually) and EM waves (collectively)

Light consists of photons each with energy proportional to frequency

$$\mathcal{E} = h\nu = \frac{hc}{\lambda} \qquad \mathcal{E} = \frac{1.24eV \cdot \mu}{\lambda}$$

When there are many photons, light also behaves as a travelling electromagnetic (EM) wave

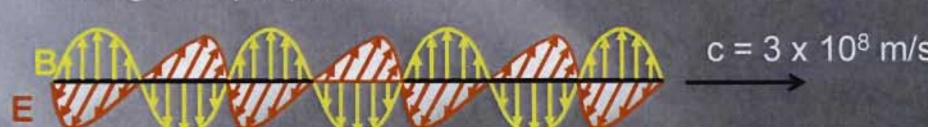

The electric field E and magnetic field B of plane-polarized light are perpendicular to each other and also to the direction of propagation

$$\mathbf{E}(z,t) = \hat{\mathbf{x}}E_0 \cos(kz - \omega t + \varphi)$$
$$\mathbf{B}(z,t) = \hat{\mathbf{y}}B_0 \cos(kz - \omega t + \varphi)$$

Light Amplification by Stimulated Emission of Radiation (LASER)

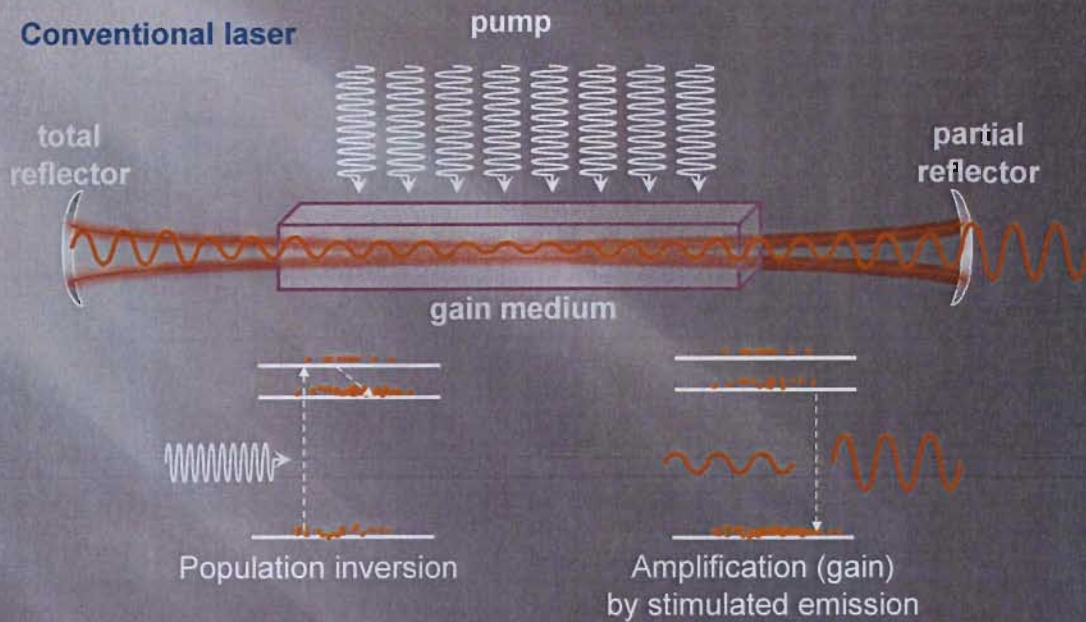

Quantum lasers use electrons bound to discrete atomic or molecular energy levels and thus produce fixed wavelengths

FEL gain medium is relativistic electrons traversing a wiggler

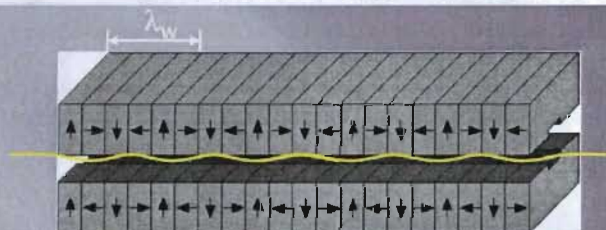

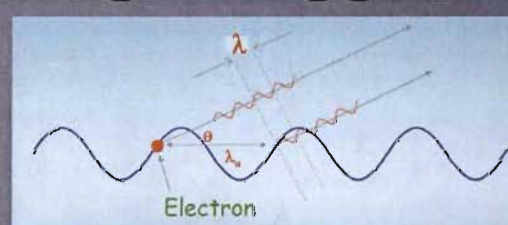

FEL use free electrons traveling near the speed of light through a series of alternating magnets called a wiggler. Electrons undulating in the wiggler radiate electromagnetic waves at wavelength λ as given by

$$\lambda = \frac{\lambda_w}{2\gamma^2}\left(1 + a_w^2 + \gamma^2\theta^2\right)$$

λ_w : wiggler period
γ : electron beam energy
a_w : dimensionless wiggler strength
θ : observation angle

Relativistic factor

$$\gamma = \frac{1}{\sqrt{1 - \frac{\upsilon_z^2}{c^2}}}$$

Electron average speed

$$\upsilon_z \approx c\left(1 - \frac{1 + a_w^2}{2\gamma^2}\right)$$

rms wiggler parameter

$$a_w = \frac{eB_0}{\sqrt{2}m_0 c}\left(\frac{\lambda_w}{2\pi}\right)$$

Resonance Wavelength

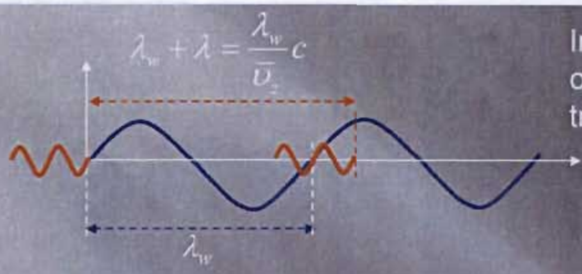

In the time it takes electrons to traverse one wiggler period, the light wave travels one period plus one wavelength

$$\lambda = \lambda_w \left(\frac{c}{\bar{\upsilon}_z} - 1 \right)$$

$$\bar{\upsilon}_z = c \left(1 - \frac{1 + a_w^2}{2\gamma^2} \right)$$

Wiggler period

rms wiggler parameter

Wavelength

$$\lambda = \frac{\lambda_w}{2\gamma^2} \left(1 + a_w^2 \right)$$

Electron kinetic energy

Total energy

$$\gamma = \frac{E_k + m_0 c^2}{m_0 c^2}$$

Electron rest energy (0.511MeV)

rms wiggler parameter in practical units

$$a_w = 0.66 B_0(T) \lambda_w(cm)$$

magnetic field

period

Wiggler Radiation

- Large deflection (K > 3)
- Large radiation cone angle

$$\Delta\theta = \frac{K}{\gamma}$$

- Broad spectral bandwidth
- Critical photon energy

$$e_c(keV) = 0.66 E(GeV)^2 B(T)$$

$$K = 0.983 B_0(T) \lambda_u(cm)$$

$$K = \sqrt{2} a_w$$

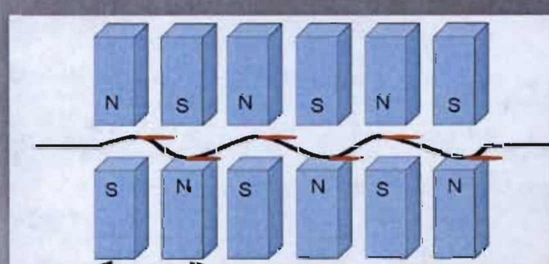

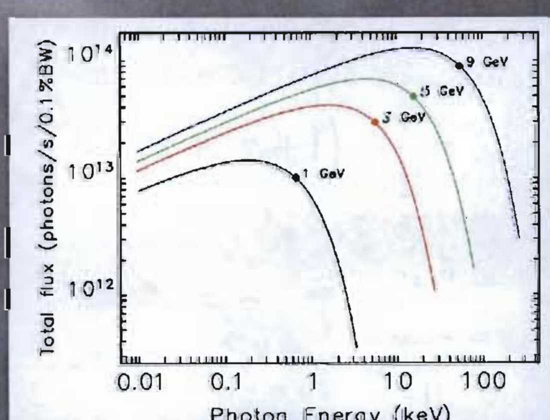

Undulator Radiation

- Small deflection (K ~ 1 – 3)
- Smaller cone angle

$$\Delta\theta = \frac{1}{\gamma\sqrt{N_w}}$$

- Narrow linewidth

$$\frac{\Delta\lambda}{\lambda} = \frac{1}{N_w}$$

- Wavelength

$$\lambda_m = \frac{\lambda_u}{2n\gamma^2}\left(1+\frac{K^2}{2}\right)$$

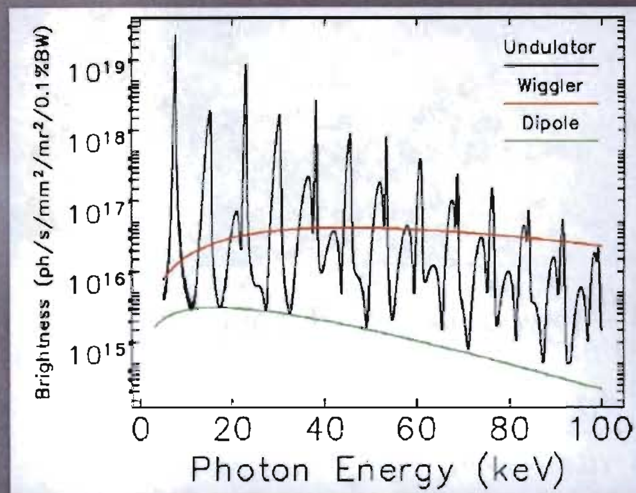

n : harmonic number

Undulator spectra contain many harmonics

Energy Transfer in FEL

Lorentz force on electrons

$$\mathbf{F} = -e\left[\mathbf{E} + (\mathbf{v}\times\mathbf{B})\right]$$

Magnetic field changes the electron beam's momentum but not its energy because the direction of magnetic force is always perpendicular to the electrons' motion. Energy transfer is possible with the light beam's electric field.

$$\Delta W = \int \mathbf{F}\cdot d\mathbf{s} = -\int e\mathbf{E}\cdot d\mathbf{s}$$

Light only has **transverse electric field**, so for energy transfer between co-propagating electron beam and light beam to occur, we need a **sinusoidal magnetic field** to give electrons **oscillatory transverse motion** to interact with the light beam's electric field.

Electron Beam Velocity and Motion inside a Wiggler

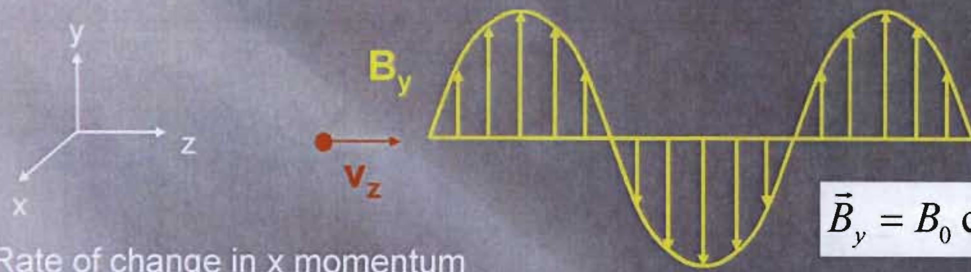

$$\vec{B}_y = B_0 \cos\left(k_w z\right)$$

Rate of change in x momentum

$$\frac{d}{dt}\left(\gamma m_0 \upsilon_x\right) = -e\upsilon_z B_o \cos\left(k_w z\right)$$

$$\frac{d\upsilon_x}{dt} \approx \frac{-ecB_0}{\gamma m_0}\cos\left(k_w z\right) \approx \frac{-ecB_0}{\gamma m_0}\cos\left(k_w\left(ct\right)\right)$$

$$K = \frac{eB_0}{m_0 c k_w}$$

Velocity in x direction

$$\upsilon_x = \frac{-eB_0}{\gamma m_0 k_w}\sin\left(k_w z\right) = \frac{-cK}{\gamma}\sin\left(k_w z\right)$$

Motion in x direction

$$x = \frac{K}{\gamma k_w}\cos\left(k_w z\right)$$

Energy Exchange between Electrons and Optical Field

$$\frac{dW}{dt} = -j_\perp \cdot E_s$$

Transverse electron current

$$j_\perp = ec\upsilon_x = -\frac{ecK}{\gamma}\sin\left(k_w z\right)$$

Plane-wave transverse electric field

$$E_s(z,t) = E_{s,0}\cos(kz - \omega t)$$

$$\frac{d\left(\gamma m_0 c^2\right)}{dt} = -\frac{ecKE_{s,0}}{\gamma}\sin\left(k_w z\right)\cos(kz - \omega t)$$

$$\frac{d\left(\gamma m_0 c^2\right)}{cdt} = -\frac{eKE_{s,0}}{\gamma}\sin\left(\left(k_w + k\right)z - \omega t\right)$$

Divide both sides by m_0c^2

$$\frac{d\gamma}{dz} = -\frac{eKE_{s,0}}{\gamma m_0 c^2}\sin\left(\left(k_w + k\right)z - \omega t\right)$$

Evolution of Energy Change with respect to Resonance Energy

Electron energy loss is small relative to its initial energy, i.e. $\Delta\gamma << \gamma$. Define change in energy as relative difference between the electron energy compared to the resonance energy

$$\frac{\Delta\gamma}{\gamma_R} = \frac{\gamma - \gamma_R}{\gamma_R}$$

$$\frac{d}{dz}\left(\frac{\Delta\gamma}{\gamma_R}\right) = \frac{d}{dz}\left(\frac{\gamma - \gamma_R}{\gamma_R}\right) = \frac{1}{\gamma_R}\left(\frac{d\gamma}{dz}\right)$$

Dimensionless optical field

$$a_s = \frac{eE_{s,0}}{km_0c^2}$$

Rewrite energy evolution in terms of relative change in energy to the resonance energy $\Delta\gamma/\gamma_R$ and a_s

$$\frac{d}{dz}\left(\frac{\Delta\gamma}{\gamma_R}\right) = -\frac{ka_sK}{\gamma_R^2}\sin\left[\left(k + k_w\right)z - \omega t\right]$$

Evolution of Electron Phase

Electron phase

$$\theta = \left(k_w + k\right)z - \omega t + \psi_i$$

Electron phase velocity

$$\frac{d\theta}{dt} = \left(k_w + k\right)\bar{\upsilon}_z - \omega$$

Average longitudinal velocity

$$\bar{\upsilon}_z = c\left(1 - \frac{1 + a_w^2}{2\gamma_R^2}\right)$$

$$\frac{d\theta}{dt} \approx k_w c - \frac{kc}{2\gamma_R^2}\left(1 + a_w^2\right)$$

Wiggler wave-number

$$k_w = \frac{2\pi}{\lambda_w} = k\frac{\left(1 + a_w^2\right)}{2\gamma^2}$$

$$\frac{d\theta}{dt} = \frac{kc}{2}\left(1 + a_w^2\right)\left(\frac{1}{\gamma_R^2} - \frac{1}{\gamma^2}\right)$$

$$\frac{1}{\gamma_R^2} - \frac{1}{\gamma^2} = \frac{\left(\gamma_R + \Delta\gamma\right)^2 - \gamma_R^2}{\gamma_R^2\gamma^2} \approx \frac{2\gamma_R\Delta\gamma}{\gamma_R^2}$$

$$\frac{d\theta}{dz} = \frac{k\left(1 + a_w^2\right)}{2\gamma_R^2}\left(\frac{2\Delta\gamma}{\gamma_R}\right) = 2k_w\left(\frac{\Delta\gamma}{\gamma_R}\right)$$

Trajectory in Phase Space

Evolution of energy difference relative to resonance energy depends on sine(phase)

$$\frac{d}{dz}\left(\frac{\Delta\gamma}{\gamma_R}\right) = -\Omega^2 \sin\theta$$

Evolution of phase depends on energy difference relative to resonance energy

$$\frac{d\theta}{dz} = 2k_w\left(\frac{\Delta\gamma}{\gamma_R}\right)$$

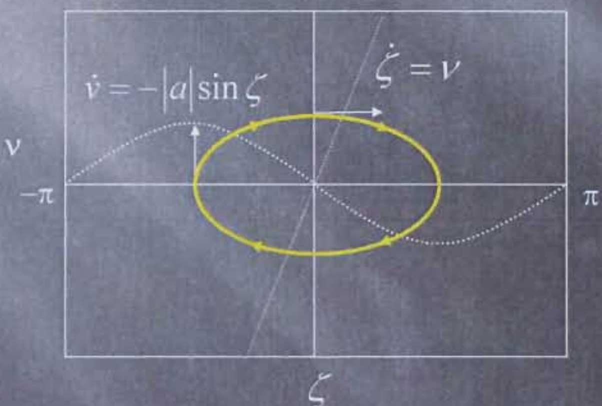

Dimensionless phase & velocity

$$\zeta = \frac{\theta}{2k_w} \qquad \nu = \frac{\Delta\gamma}{\gamma_R}$$

Coupled 1st order differential equations

$$\dot{\zeta} = \nu$$
$$\dot{\nu} = -|a|\sin\zeta$$

Particles follow **elliptical trajectories** corresponding to different energies.

Pendulum Equation

Hamiltonian = Total energy

$$H = \frac{\nu^2}{2} - \frac{g}{l}\cos\theta$$

The separatrix defines the boundary between closed (oscillatory motion) and open (rotational) orbits

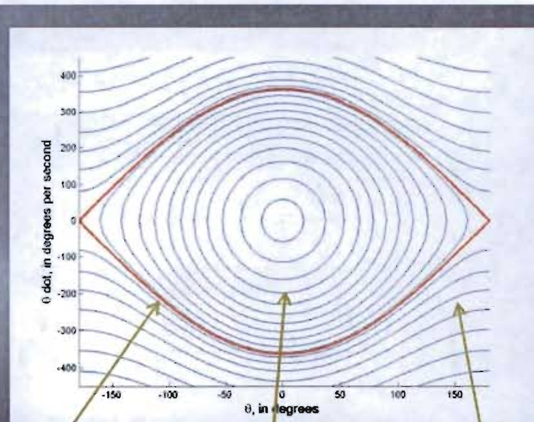

Separatrix

$$H = \frac{g}{l}$$

Closed orbits

$$-\frac{g}{l} < H < \frac{g}{l}$$

Open orbits

$$\frac{g}{l} < H$$

Courtesy of Wikipedia

Phase-space Motion of Electrons in Ponderomotive Wave

At z = 0
(wiggler entrance)

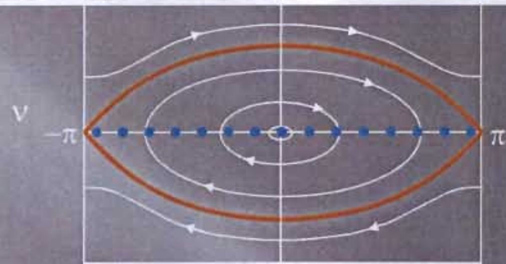

Electrons are unbunched

At z = 10 L_g
(middle of wiggler)

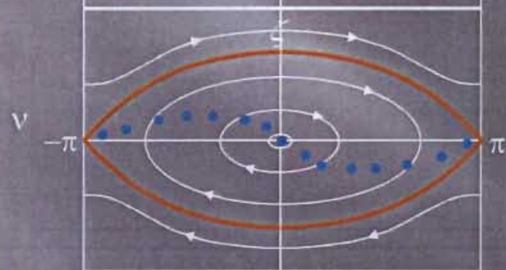

Electrons have energy modulation

At z = 16 L_g
(wiggler exit)

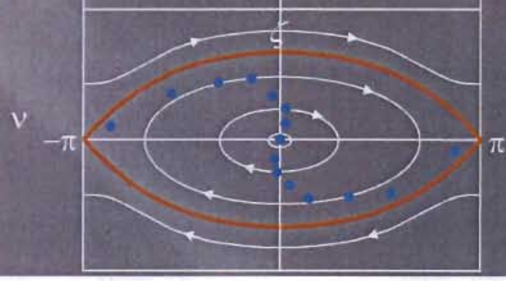

Electrons are bunched in time (density modulation)

Electrons are microbunched with periods of radiation wavelength

Phase space at wiggler entrance

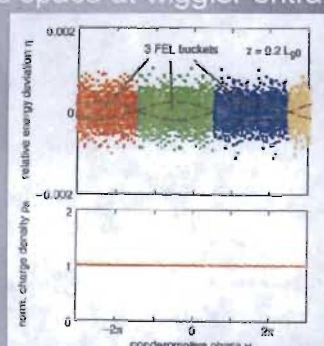

These phase space diagrams show three buckets, each one wavelength long, that grow in height as the FEL intensity increases. At z = $18L_g$, electrons become overbunched and start to absorb FEL light. The bucket height will decrease at longer z.

Phase space in wiggler and near saturation

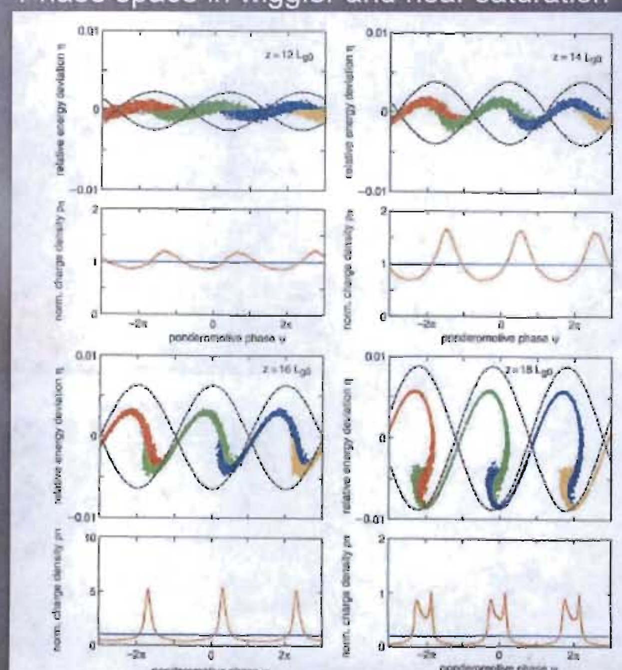

From Ultraviolet and Soft X-ray Free Electron Lasers

FEL (Bunched Beam) Radiation

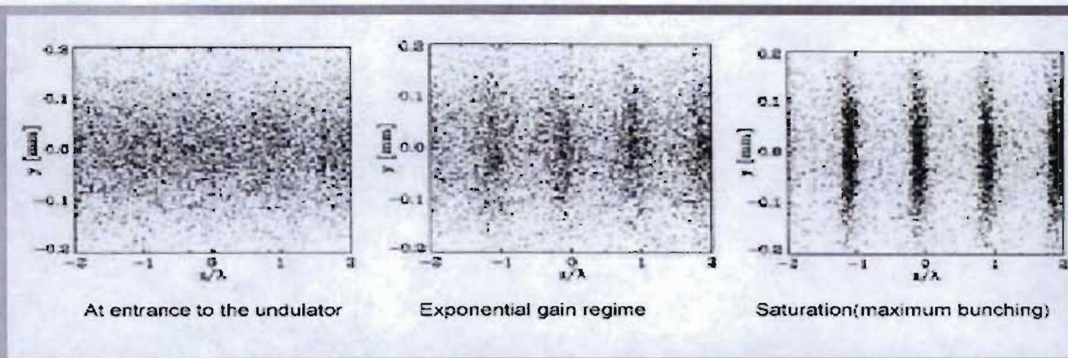

Undulator radiation

Electrons with random phases emit incoherent radiation

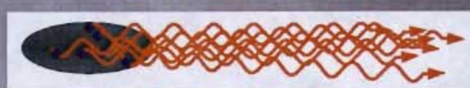

$E \propto \sqrt{N_e}$ $\quad I \propto N_e$

FEL radiation

Electrons bunched at radiation wavelength emit coherent light

$E \propto N_e$ $\quad I \propto N_e^2$

FEL radiation has 10^6 - 10^{10} more photons than undulator radiation

Courtesy of DESY and Michael Borland

Basic features of FEL

- Wavelength tunable
- Diffraction limited optical beam
- High power (GW peak, 10s of kW average)
- Flexible pulse format

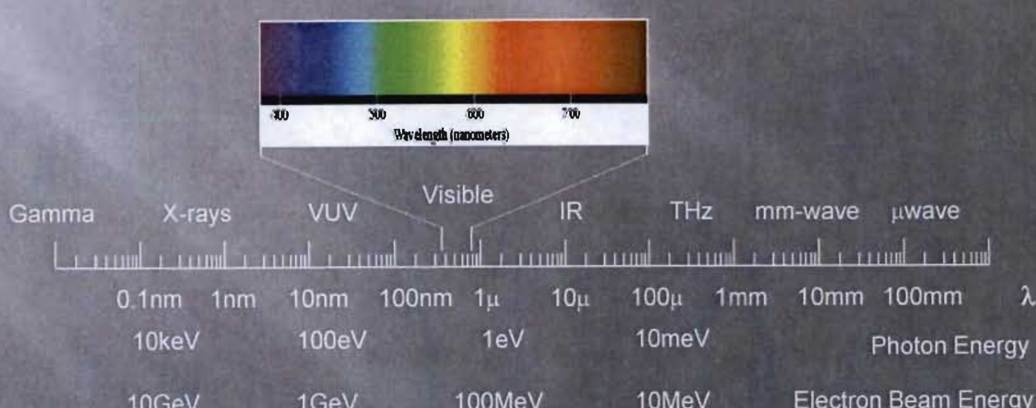

How an RF-linac FEL works

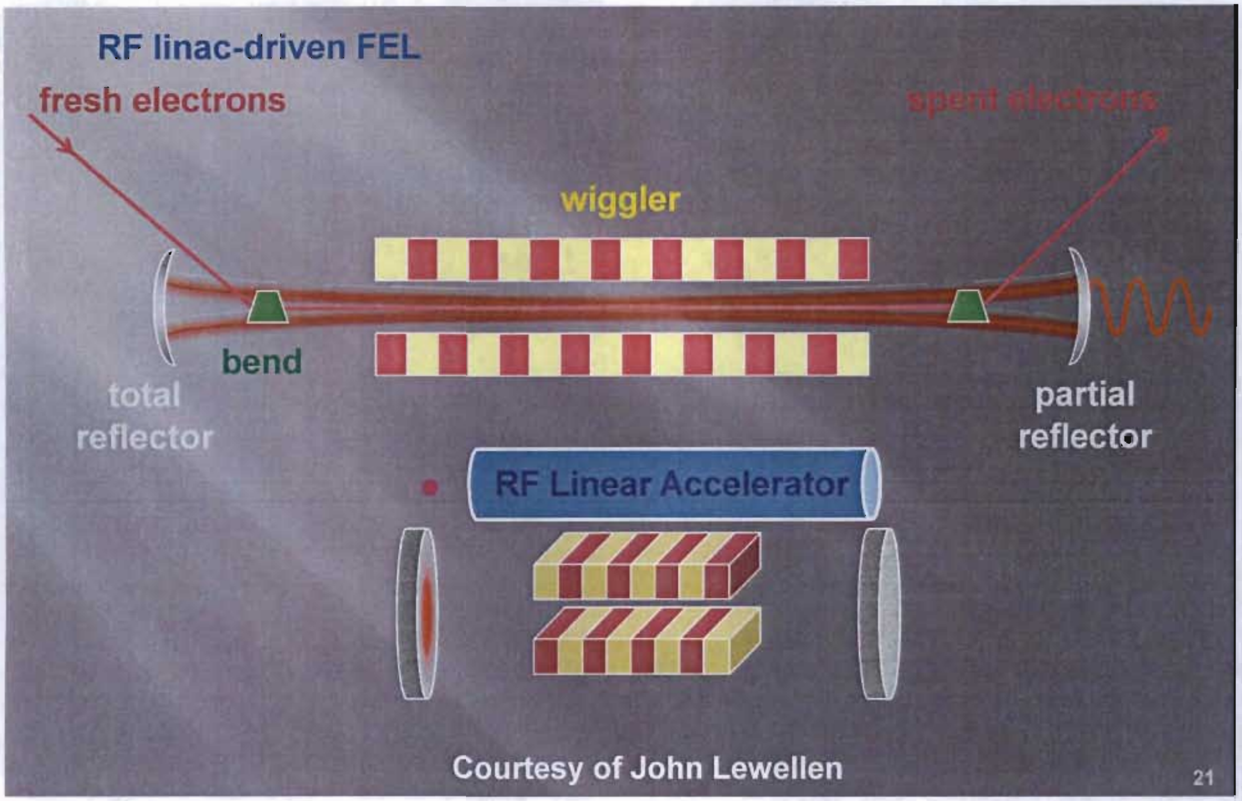

RF-linac FEL Pulse Format

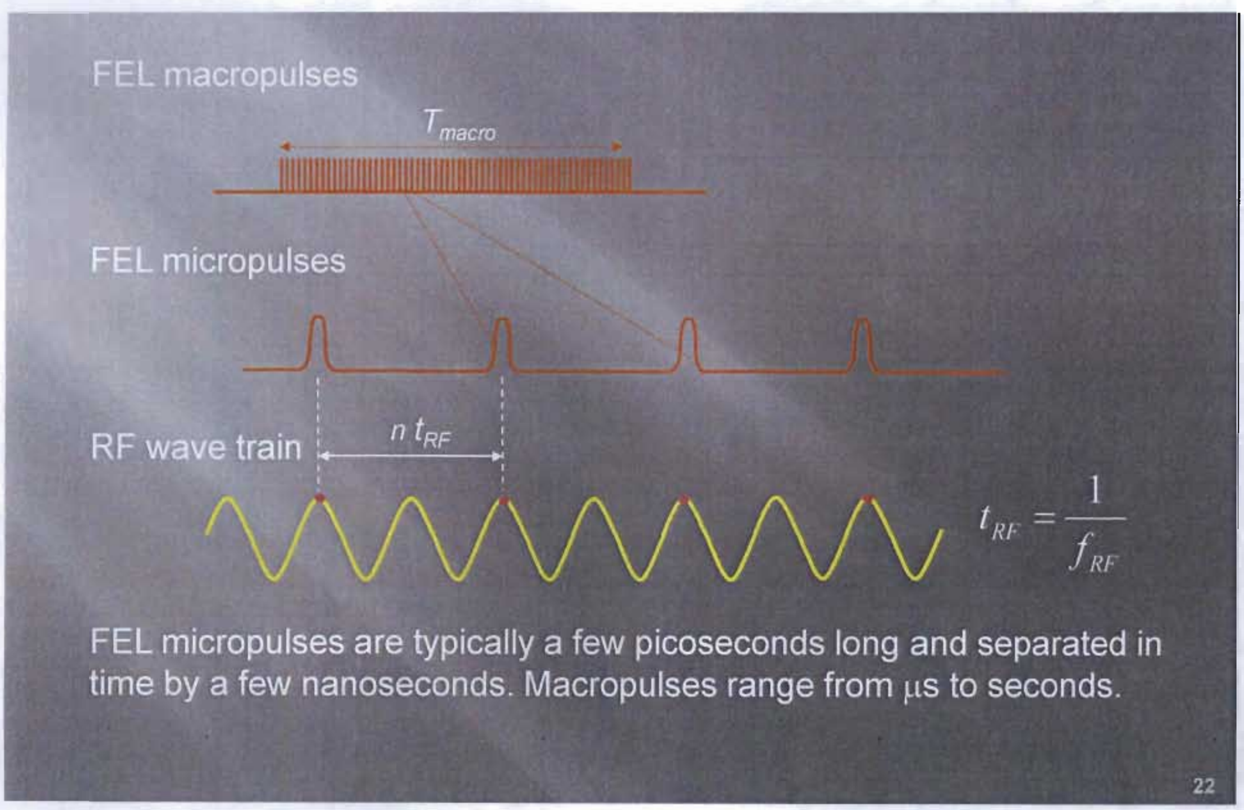

Brilliance

Brilliance = $\dfrac{\text{Number of photons}}{\text{time} \quad \text{bandwidth} \times \text{unit area} \times \text{unit solid angle}}$

longitudinal phase space

transverse phase space

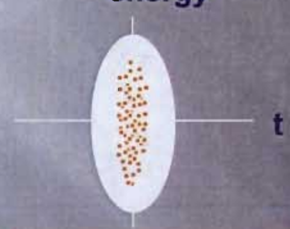

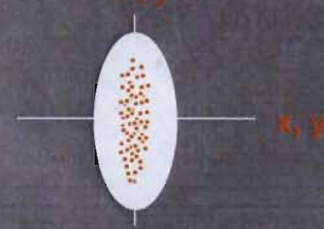

$$\sigma_z\left(\frac{\sigma_\gamma}{\gamma}\right) \le \left(\frac{\Delta\lambda}{\lambda}\right) c\sigma_t$$

Longitudinal emittance is expressed in time % bandwidth

$$\varepsilon_{x,y} \le \frac{\lambda}{4\pi}$$

Transverse emittance is expressed in microns

23

Transverse Emittance

Root-mean-square x emittance

$$\varepsilon_{rms,x} = \sqrt{\langle x^2\rangle\langle x'^2\rangle - \langle xx'\rangle^2}$$

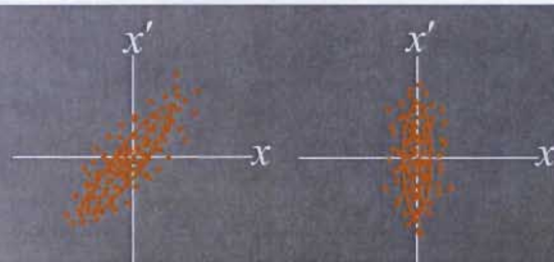

<x-x'> ≠ 0 <x-x'> = 0

Emittance is defined using ensemble averages, denoted by < >, of x^2 and x'^2 and x'-x correlation. The correlation vanishes at the waist (upright ellipse) and rms beam emittance becomes $\sigma_x\sigma_{x'}$ where $\sigma_x = \sqrt{\langle x^2\rangle}$ is the rms radius in x and $\sigma_{x'} = \sqrt{\langle x'^2\rangle}$ is the rms spread in x'.

Ensemble average of x^2

$$\langle x^2\rangle = \frac{1}{N}\sum_{j=1}^{N}\left(x_j - x_0\right)^2$$

At the beam waist

$$\varepsilon_{rms,x} = \sigma_x\sigma_{x'}$$

24

Longitudinal Emittance

Electron beam's energy spread must be smaller than the electrons' velocity spread over the interaction length.

For oscillator FEL, interaction length ~ wiggler length

$$\frac{\Delta\gamma}{\gamma} \le \frac{1}{2N_w}$$

For SASE and amplifier FEL, interaction length ~ gain length

$$\frac{\Delta\gamma}{\gamma} \le \rho$$

Uncompressed electron beams have small energy spread and low peak current. Compressed beams have high current and large energy spread.

FEL and SR Peak Brilliance

Brilliance

$$\mathfrak{B} = \frac{N_p}{\pi^2 \varepsilon_x \varepsilon_y \Delta t \frac{\Delta\omega}{\omega}}$$

Un-normalized emittance

$$\varepsilon_x = \frac{\varepsilon_{x,n}}{\gamma}$$

FEL peak brilliance is orders of magnitude above SR thanks to low emittance, sub-ps bunch length, and FEL amplification.

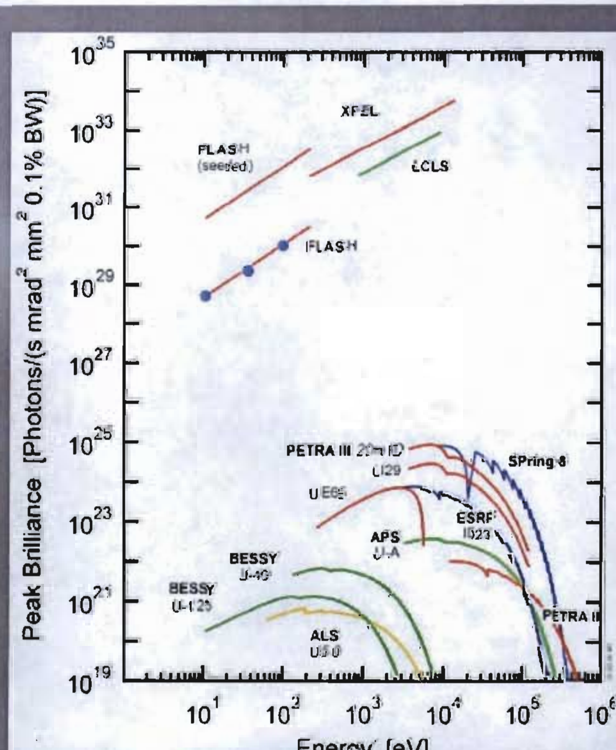

Los Alamos
NATIONAL LABORATORY
EST. 1943

Part 2
Wigglers

27

Linac Coherent Light Source Wiggler (Undulator)

28

Magnetic Flux Density B and Magnetizing Force H

Magnetic flux density B (aka magnetic induction) is in unit of tesla (T). Magnetizing force H (aka magnetic field strength) is in unit of A/m. In vacuum, B and H are related by the permeability of free space, μ_0

$$\mathbf{B} = \mu_0 \mathbf{H} \qquad \mu_0 = 4\pi \times 10^{-7}\ \text{T-m A}^{-1}$$

Magnetic flux density is increased in the presence of a ferromagnetic material by its relative magnetic permeability, μ_r

$$\mathbf{B} = \mu_r \mu_0 \mathbf{H}$$

Relative permeability of common magnet materials ~ 1.05

Relative permeability of vanadium permendur ~ 7,000

B-H Curve of Magnet Materials

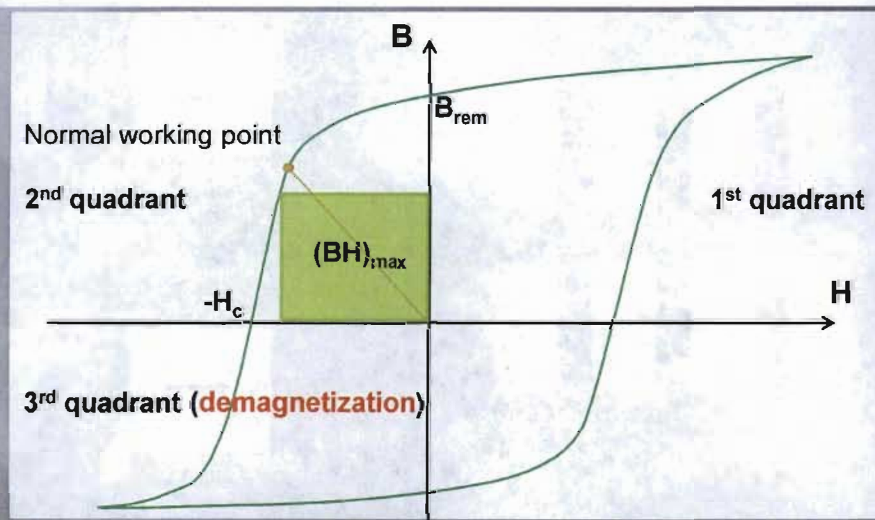

Remanence - coercivity trade-off

SmCo have high H_c and lower B_{rem}

NdFeB have high B_{rem} but low H_c

PM Material	$(BH)_{max}$ (kJ/m^3)	Remanence (mT)	H_c Coercivity (kA/m)	Radiation Hardness
$SmCo_5$	170	800-1000	2400	High
Sm_2Co_{17}	220	1000-1100	2000	Medium
NdFeB	300	1100-1400	1400	Low - Medium

Permanent Magnet Wiggler Designs

Hallbach Design

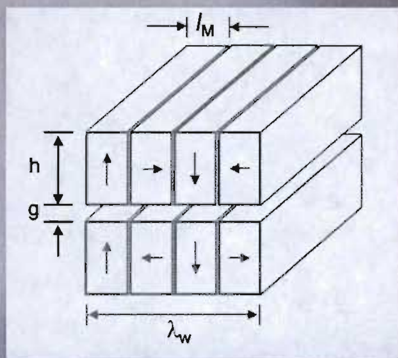

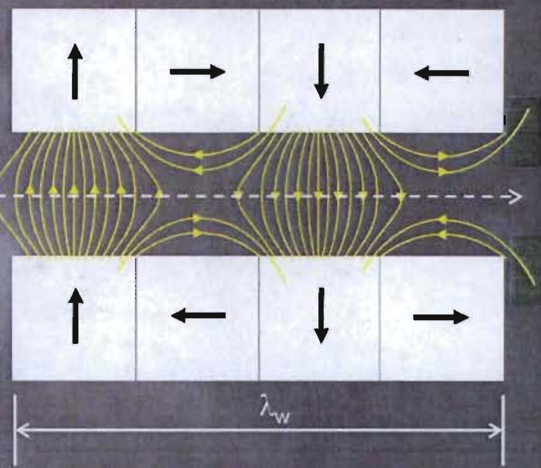

Peak magnetic field on axis

$$B_0 = (1.78T) B_r e^{-\frac{\pi \cdot g}{\lambda_w}}$$

Note magnetic field increases as we go away from electron beam axis

To maintain high field, wiggler gap must not be larger than ⅓ wiggler period

Hybrid Wiggler Design

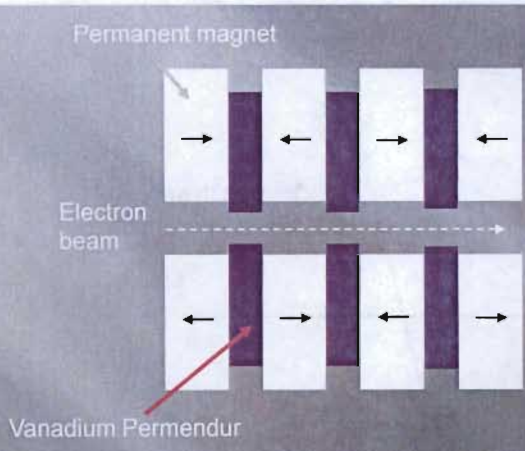

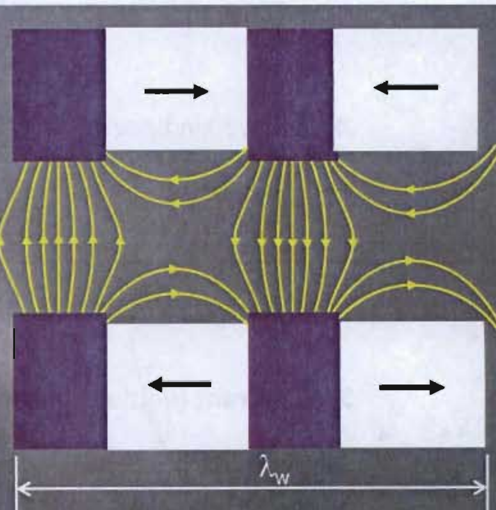

Hybrid wiggler design replaces up/down magnets with vanadium permendur

$$B_0 = (3.69T) e^{-\frac{g}{\lambda_w}\left(5.07-1.5\left(\frac{g}{\lambda_w}\right)\right)}$$

Planar wigglers focus e- beams in the y (vertical) plane

Planar wiggler with infinite x dimension

$$B_x = 0$$
$$B_y = \hat{y} B_0 \cosh(k_w y)\cos(k_w z)$$
$$B_z = -\hat{z} B_0 \sinh(k_w y)\sin(k_w z)$$

Equation of motion in the y direction

$$\frac{d(\gamma m_0 v_y)}{dt} = e\left(\overline{v_x B_z} - \overline{v_z B_x}\right)$$

Velocity in x

$$v_x = -\left(\frac{a_w c}{\gamma}\right)\sin(k_w z)$$

B_x is zero

Expand B_z about y=0

$$B_z = B_0 k_w y \sin(k_w z)$$

$$\ddot{y} = -\left(\frac{e B_0 k_w c}{\sqrt{2} m_0 \gamma}\right)\left(\frac{a_w}{\gamma}\right) y$$

Divide both sides by c^2 to convert to 2nd derivative with respect to z

$$y'' = -\left(\frac{k_w a_w}{\gamma}\right)^2 y$$

Betatron Motion

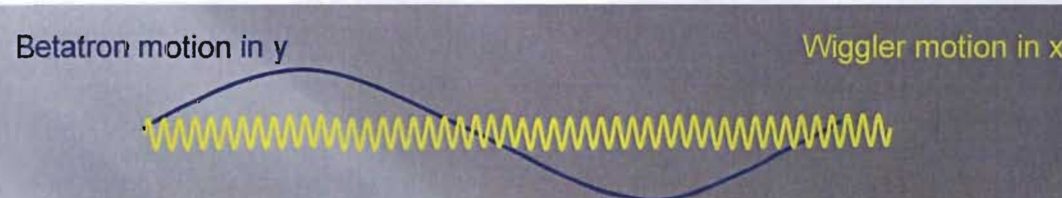

$$y'' + k_\beta^2 y = 0$$

$$x'' + k_w x = 0$$

$$k_\beta = \frac{k_w a_w}{\gamma}$$

Betatron motion is slow, large amplitude motion in the y direction over many wiggler periods due to gradient of B_y along the y direction. The field amplitude is proportional to the square of deviation from the center.

$$B_y = B_0\left[1 + (k_w y)^2\right]\cos(k_w z)$$

Single-Plane Focusing

- Vertical envelope equation with emittance

$$\frac{d^2R_y}{dz^2} + k_\beta^2 R_y = \left(\frac{\varepsilon_{ny}}{\gamma}\right)^2 \frac{1}{R_y^3}$$

- Find matched beam envelope radius by setting $\frac{d^2R_y}{dz^2}$ to zero

$$R_{y0}^4 = \left(\frac{\varepsilon_{ny}}{\gamma k_\beta}\right)^2 \rightarrow k_\beta = \frac{k_w a_w}{\gamma} \rightarrow R_{y0} = \sqrt{\frac{\varepsilon_{ny}}{k_w a_w}}$$

Matched beam rms radius

With single-plane focusing (planar) wiggler, the electron beam is focused in y at the entrance and in x in the wiggler of the wiggler. The beam is elliptical at the entrance and exit, and round in the middle.

Two-Plane Weak Focusing

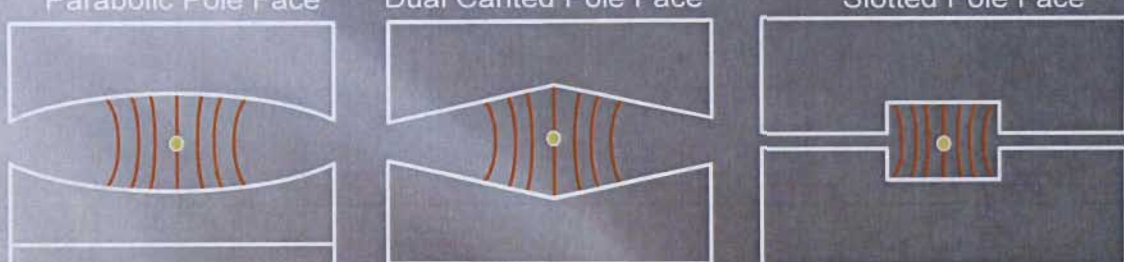

Quadratic x^2 dependence   Approximate x^2 dependence of B_y at the center

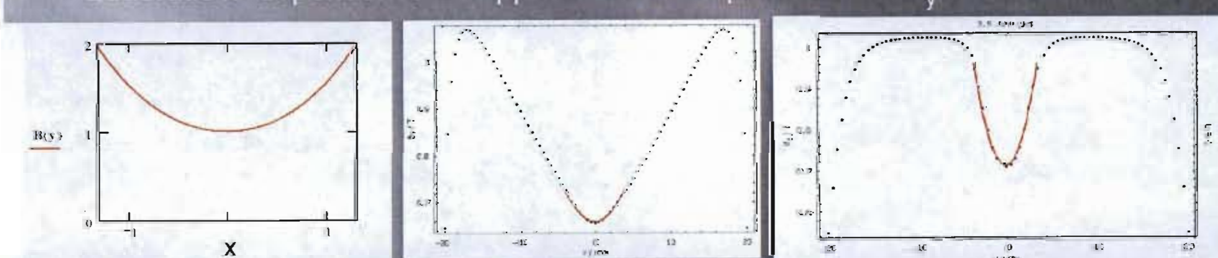

$$B_y = B_0\left[1 + \frac{(k_w x)^2}{2}\right]$$

Magnetic field along the x axis in a two-plane focusing wiggler. Note the parabolic dependence similar to the field of a sextupole magnet.

Matched Beam for Two-plane (Weak) Focusing Wiggler

Equations for x and y envelope radii in two-plane focusing wigglers

$$\frac{d^2R_x}{dz^2}+k_x^2R_x=\left(\frac{\varepsilon_{nx}}{\gamma}\right)^2\frac{1}{R_x^3}$$

$$\frac{d^2R_y}{dz^2}+k_y^2R_y=\left(\frac{\varepsilon_{ny}}{\gamma}\right)^2\frac{1}{R_y^3}$$

where

$$k_x^2+k_y^2=k_\beta^2$$

Equal two-plane focusing

$$k_x=k_y=\frac{k_\beta}{\sqrt{2}}$$

Matched beam rms radii in x and y

$$R_{x0}=\sqrt{\frac{\sqrt{2}\varepsilon_{nx}}{k_wa_w}}$$

$$R_{y0}=\sqrt{\frac{\sqrt{2}\varepsilon_{ny}}{k_wa_w}}$$

Focusing in y is distributed to focusing in x in natural focusing wigglers.

Transverse and Longitudinal Velocities

Transverse velocity in x

$$\upsilon_x=-\frac{\sqrt{2}ca_w}{\gamma}\sin(k_wz)$$

The average electron velocity is constant, so the longitudinal velocity is reduced when transverse velocity increases

$$\upsilon_z=\sqrt{\beta^2c^2-\upsilon_x^2}$$

Use small x approximation $(1 + x)^{1/2} \approx 1 + \frac{1}{2}x$

Longitudinal velocity

$$\upsilon_z=c\left[1-\frac{1}{2\gamma^2}\left(1+2a_w^2\sin^2(k_wz)\right)\right]$$

$$\upsilon_z=c\left[1-\frac{1}{2\gamma^2}\left(1+a_w^2-a_w^2\cos(2k_wz)\right)\right]$$

Figure 8 motion

Average velocity of electrons

$$\bar{\upsilon}_z = c\left(1 - \frac{\left(1 + a_w^2\right)}{2\gamma^2}\right)$$

Motion in electron's rest frame

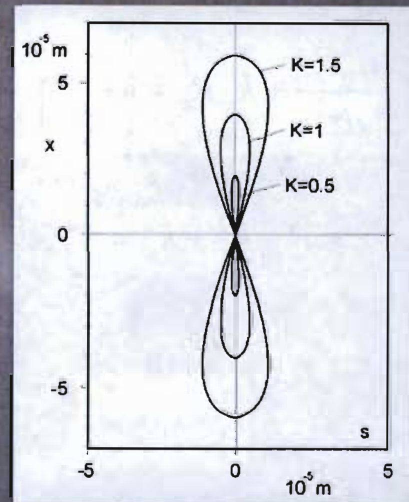

Electrons' velocity is modulated at twice the wiggler period

$$\upsilon_z = \bar{\upsilon}_z + \frac{c a_w^2}{2\gamma^2}\cos\left(2k_w z\right)$$

Figure 8 motion gives rise to harmonics in undulator radiation and reduced FEL interaction strength in a planar wiggler

Double Bessel JJ Factor

Difference between J_0 and J_1 Bessel functions

$$JJ(\xi) = J_0(\xi) - J_1(\xi)$$

where

$$\xi = \frac{a_w^2}{2\left(1 + a_w^2\right)}$$

Approximation for small ξ

$$J_0(\xi) \approx 1 - \frac{\xi^2}{4}$$

$$J_1(\xi) \approx \frac{\xi}{2}$$

$$\left[JJ(\xi)\right] \approx 1 - \frac{\xi}{2} - \frac{\xi^2}{4}$$

$JJ(\xi) < 1 \rightarrow$ gain reduction due to figure 8 motion

J_0 - J_1 versus a_w

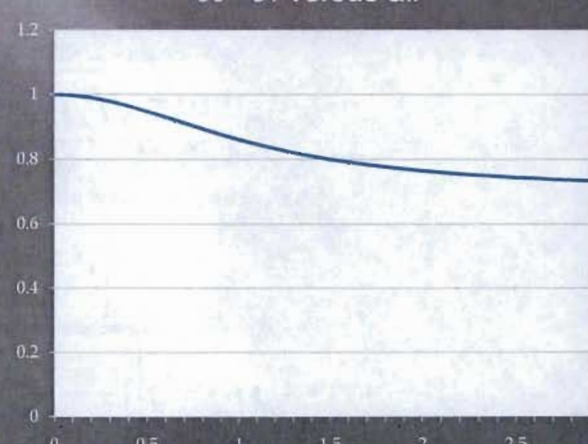

Los Alamos
NATIONAL LABORATORY
EST. 1943

Part 3
Spontaneous Emission, Gain & Efficiency

Spontaneous Emission Spectrum

$$\frac{dW}{d\omega d\Omega} = \frac{e^2\gamma^2 N_w^2 N_e}{2\pi\varepsilon_0 c}[JJ(a_w)]^2\left(\frac{a_w}{1+a_w^2}\right)^2\left(\frac{\sin \Delta/2}{\Delta}\right)^2$$

$$\Delta = \pi N_w\left(\frac{\Delta\gamma}{\gamma_R}\right) = 2\pi N_w\left(\frac{\Delta\omega}{\omega_R}\right)$$

A wave train with N_w wavelengths has relative bandwidth equal to the inverse of N_w

Spontaneous spectrum is the Fourier transform of a rectangular train of N_w waves

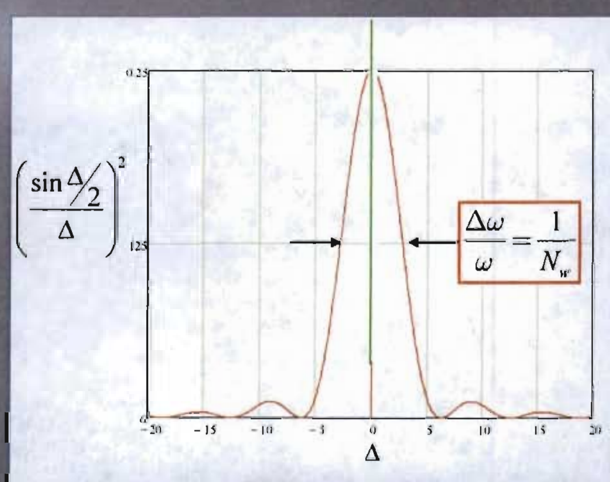

Number of Coherent Photons in Spontaneous Emission

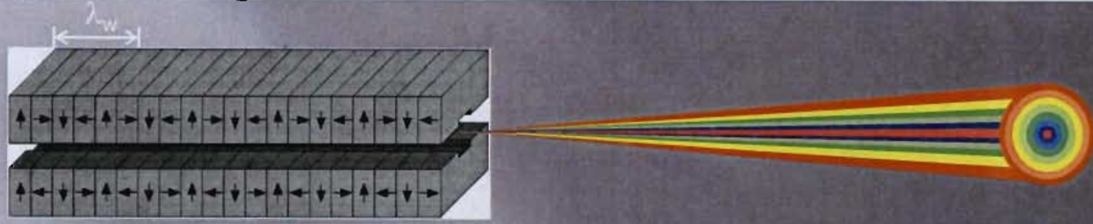

Coherent spectral bandwidth

$$\frac{\Delta\omega}{\omega} = \frac{1}{N_w}$$

Coherent angle

$$\theta = \sqrt{\frac{\lambda}{L_w}}$$

Solid angle

$$\pi\theta^2 = \frac{\pi\lambda}{N_w \lambda_w}$$

Number of coherent spontaneous photons per electron does not depend on N_w

where α = fine structure constant

$$\alpha = \frac{e^2}{\hbar c 4\pi\varepsilon_0} \approx \frac{1}{137}$$

$$\frac{N_{photon}}{N_e} = \pi\alpha\left[JJ(a_w)\right]^2 \left(\frac{a_w}{1+a_w^2}\right)^2$$

Spontaneous emission has several harmonics of fundamental frequency

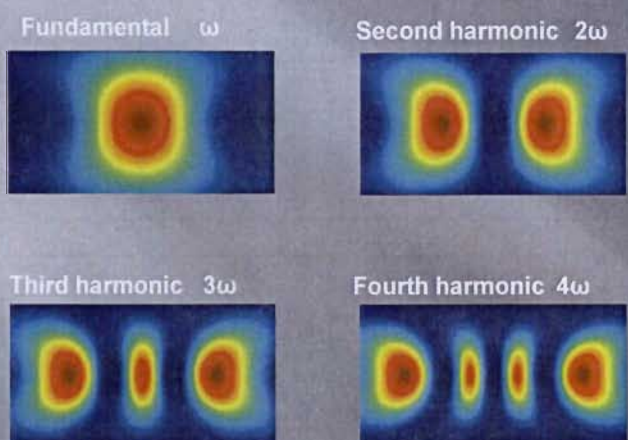

Color codes depict radiation intensity not wavelength

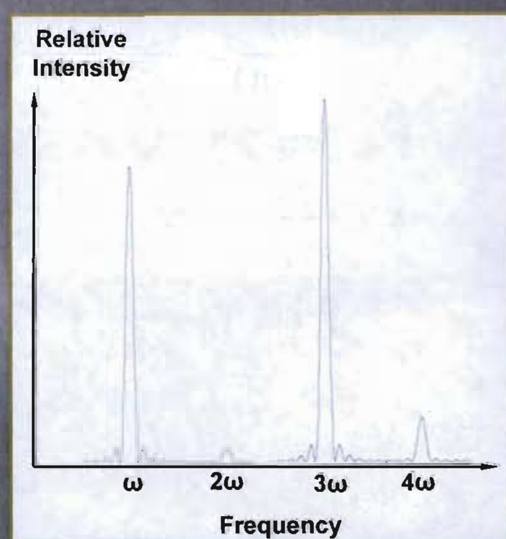

Harmonics are produced by figure 8 motion of electrons in planar wigglers (spontaneous emission of helical wigglers does not have harmonics)

Madey's Theorem

Madey's theorem: The FEL gain spectrum (gain versus energy detuning) is the derivative of the spontaneous emission spectrum.

$$g_{ss}(\Delta) = \frac{4(4\pi\rho N_w)^3}{\Delta^3}\left(1-\cos\Delta-\frac{\Delta}{2}\sin\Delta\right)$$

Maximum gain occurs at **positive detuning = 2.6**, zero on resonance and negative (absorption) at negative detuning.

$$\Delta = 2\pi N_w\left(\frac{\Delta\lambda}{\lambda}\right)$$

Madey's theorem predicts equal gain and absorption off resonance.

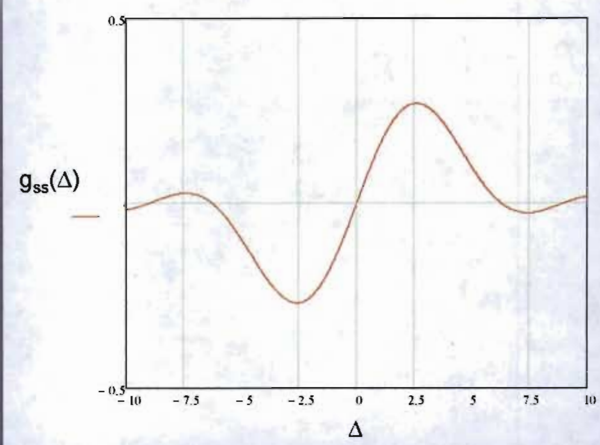

Phase-space Illustration of Madey's Theorem

Electrons' energy > Resonance energy

Electrons' energy = Resonance energy

Electrons' energy < Resonance energy

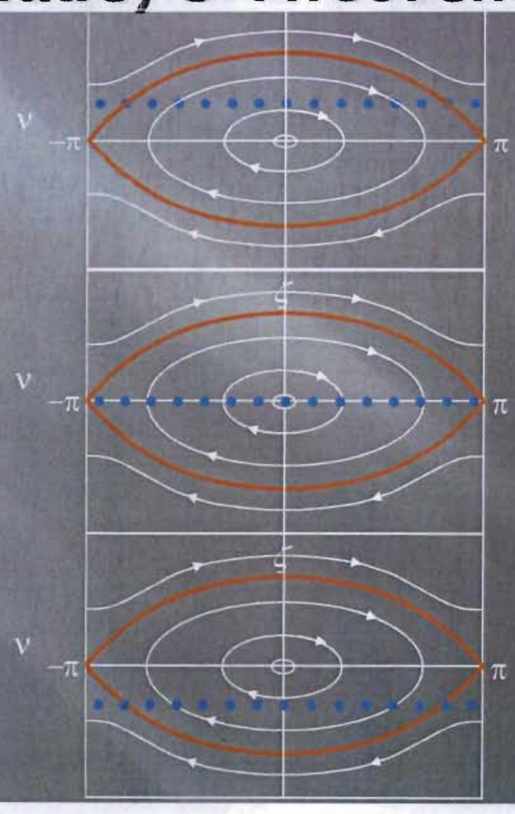

FEL gain > 0

FEL gain = 0

FEL gain < 0

Low-Gain, Small-Signal (Low-Field) Gain Spectrum

Small-signal gain at peak

$$g_{ss} = \left(\frac{2\pi N_w}{\gamma}\right)^3 \left(\frac{[JJ]a_w}{\sigma k_w}\right)^2 \left(\frac{I}{I_A}\right)$$

Gain scales linearly with peak current (not average)

Amplification

$$P_{out} = (1 + g_{ss}) P_{in}$$

Peak of gain curve shifts toward larger detuning (~3 instead of 2.6) due to optical diffraction. Gain is negative (absorption) at resonance wavelength.

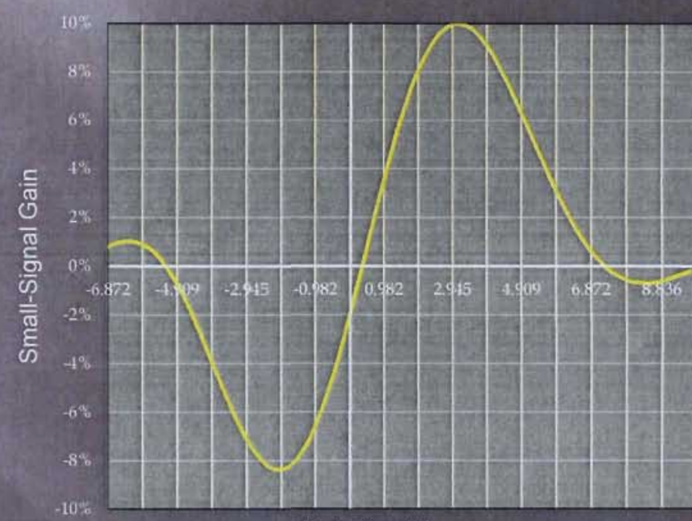

Low-Gain, Large-Signal (High-Field) Gain Spectrum

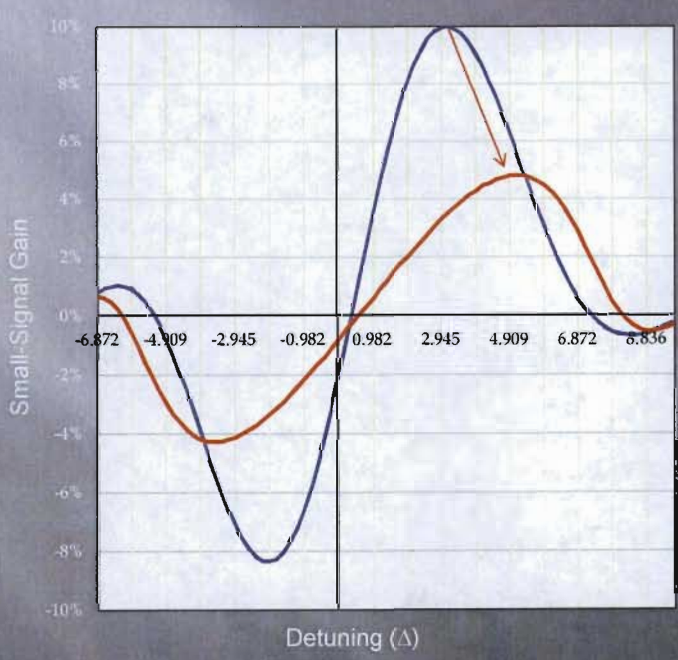

Gain curve shifts to longer wavelength (larger Δ)

Peak gain is reduced

Gain spectrum is broadened

Gain Saturation

Gain decreases at high input power

Power saturates when gain = loss

For oscillator FEL, this is intracavity power, not output FEL power

Optimum outcoupling ~ ¼ of g_{ss}

As an example, if the outcoupling is 2%, the intra-cavity power saturates at 3 GW and FEL external power is 60 MW.

Note these numbers denote peak power; to get FEL pulse energy, multiply peak power by the electron pulsewidth (FWHM for a gaussian pulse).

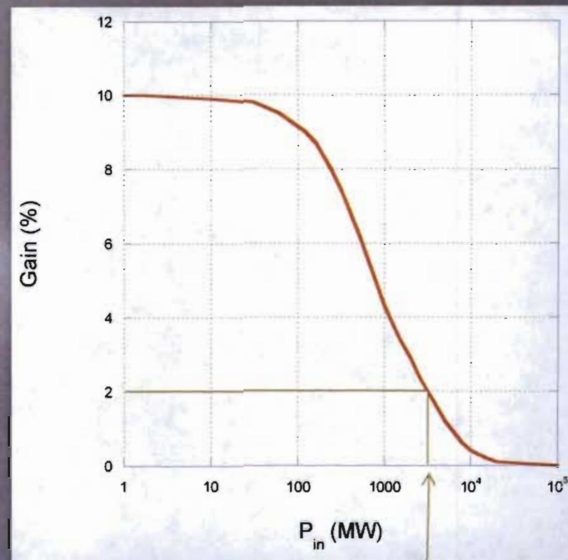

Saturated P_{in} at 2% OC

FEL Gain (Pierce) Parameter

Dimensionless Pierce parameter

$$\rho = \frac{1}{2\gamma}\left(\frac{[JJ]a_w}{\sigma k_w}\right)^{\frac{2}{3}}\left(\frac{I}{I_A}\right)^{\frac{1}{3}}$$

Small-signal gain relationship to ρ

$$g_{ss} = 2\left(2\pi N_w \rho\right)^3$$

The small-signal gain is proportional to the cube of the interaction length in the low-gain regime. As the number of wiggler periods increases, FEL power grows exponentially with z instead of z^3. With exponential power growth, the FEL is in the high-gain regime.

High-Gain FEL

Gain length is wiggler length needed for power to grow by 2.7

$$L_G = \frac{\lambda_w}{4\pi\sqrt{3}\rho}$$

Seed laser power is reduced by 9 due to mode competition (growing, decaying and oscillatory modes).

In a long wiggler, power grows exponentially with wiggler length

$$P = \frac{P_0}{9}\exp\left(\frac{z}{L_G}\right)$$

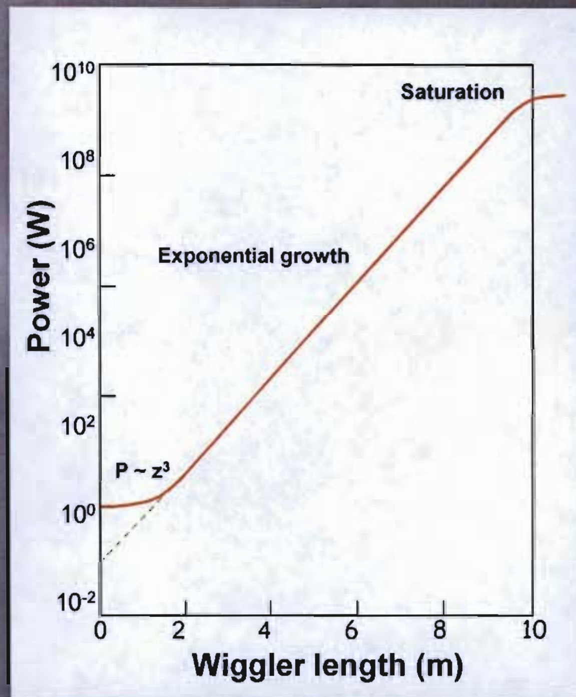

High Gain Spectrum

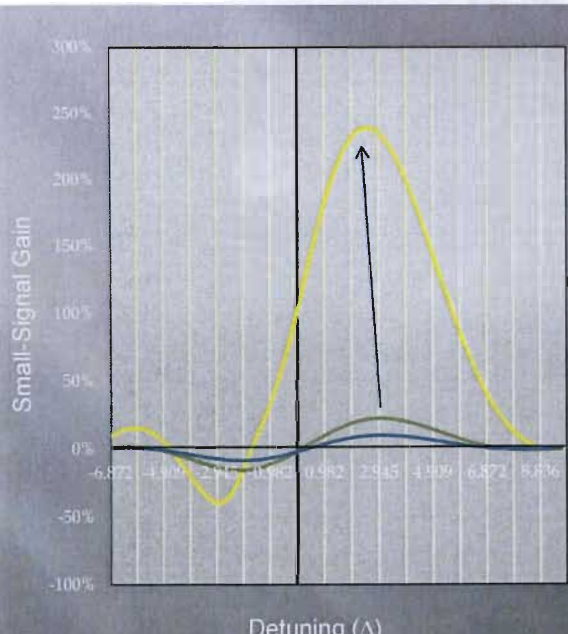

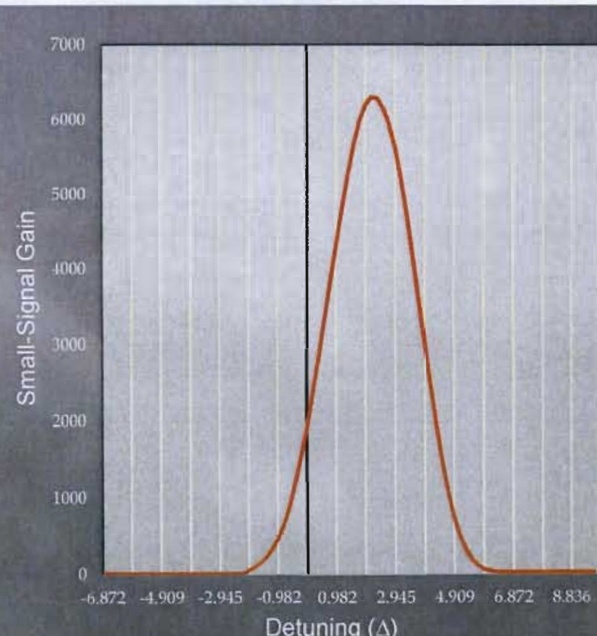

Gain curve shifts to shorter wavelength (smaller Δ) and higher peak gain (diffraction is reduced by optical guiding). There is gain at resonance wavelength.

FEL Extraction Efficiency

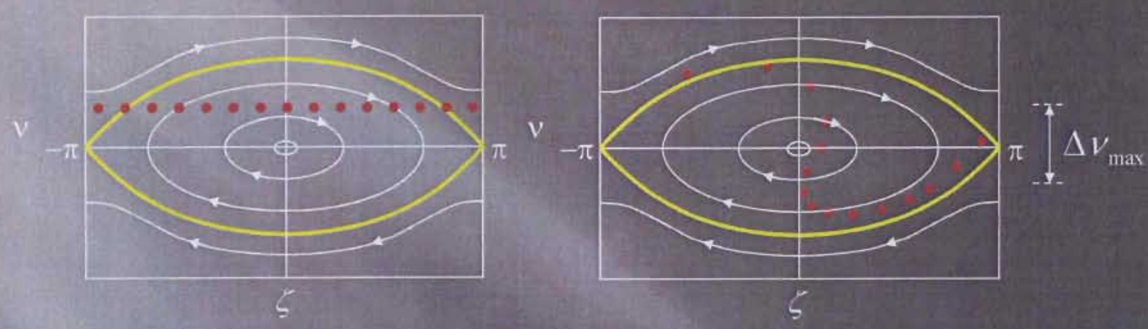

Low-gain oscillator

$$\Delta \nu_{max} = \frac{1}{2N_w}$$

High-gain amplifier

$$\Delta \nu_{max} = \rho$$

Example:

JLab FEL oscillator

$N_w = 30$
$\Delta \nu_{max} = 1.6\%$

Tapering Wiggler Period/Field

As the electron beam's energy is reduced along the wiggler, the resonance condition is shifted toward lower beam energy. To maintain resonance, the wiggler period or a_w must be reduced. It is easier to change the wiggler gap g to change the wiggler parameter a_w and thus the resonance energy.

Resonance condition at z_0

$$\lambda = \frac{\lambda_w}{2\gamma^2}\left(1 + a_w^2\right)$$

Resonance condition at $z_0 + \Delta z$

$$\lambda = \frac{\lambda_w}{2(\gamma - \Delta\gamma)^2}\left[1 + (a_w - \Delta a_w)^2\right]$$

Rate of resonance energy change with respect to z

$$\frac{d}{dz}\gamma_R^2 = -k_w a_w a_s [JJ] \sin\phi_R$$

Energy taper vs. taper in a_w

$$\frac{d}{dz}\left(\frac{\Delta\gamma}{\gamma}\right) \approx \frac{a_w^2}{1 + a_w^2}\frac{d}{dz}\left(\frac{\Delta a_w}{a_w}\right)$$

Ponderomotive Potential

$$H = \frac{\nu^2}{2} + V(\zeta)$$

Uniform Wiggler

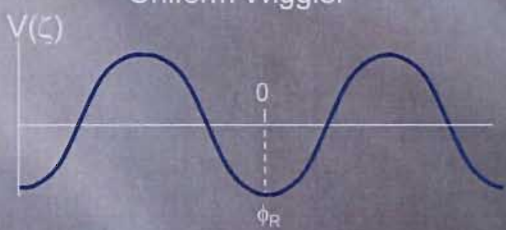

Linearly Tapered Wiggler

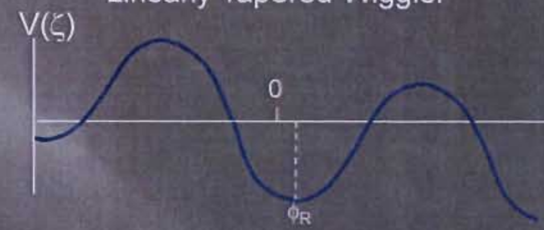

$$V(\zeta) = -|a|\cos\zeta$$

$$V(\zeta) = -|a|\cos(\zeta + \phi_R) + \zeta\sin\phi_R$$

$$\dot{\nu} = -\frac{\partial H}{\partial \zeta} = -|a|\sin\zeta$$

$$\dot{\nu} = -\frac{\partial H}{\partial \zeta} = -|a|\sin(\zeta + \phi_R) + \sin\phi_R$$

Tapered Wiggler Phase Space

Tapered wiggler pendulum equation

$$\dot{\nu} = |a|\sin(\zeta + \phi_R) + \delta$$

Energy exchange amplitude

$$|a| = \frac{k a_s a_w}{\gamma^2}$$

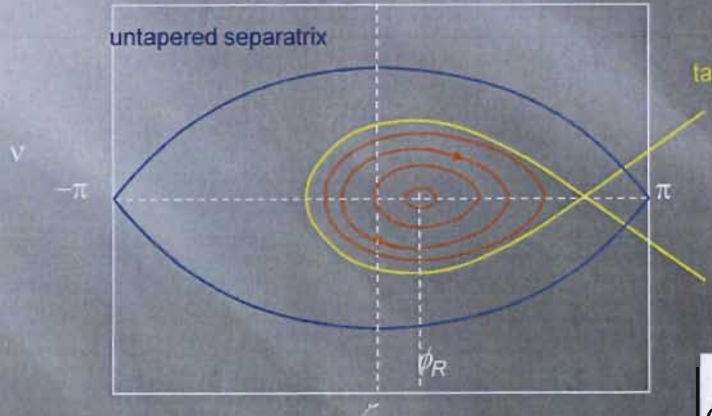

New term in pendulum eq.
= phase acceleration

Phase acceleration

$$\delta = \sin\phi_R = \frac{1}{k_w a_s a_w}\frac{d}{dz}\left(\frac{\Delta\gamma}{\gamma_R}\right)$$

Efficiency Enhancement with a Linearly Tapered Wiggler

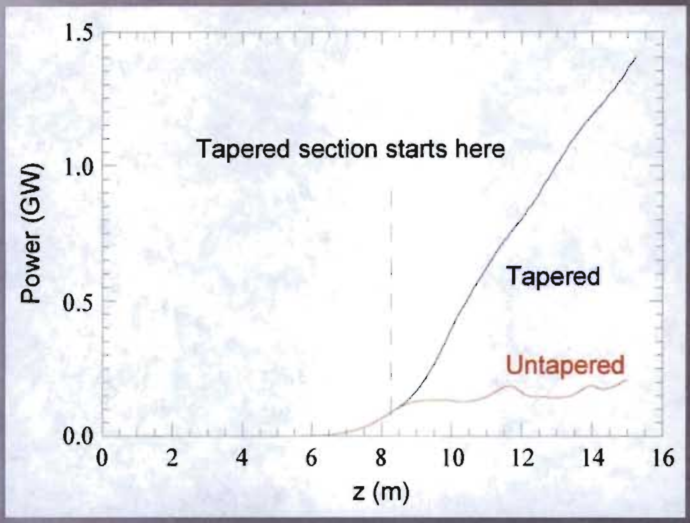

Depending on the trapping fraction and taper length, tapering can increase the power by 2 – 5. The electron trapping fraction decreases with increasing resonant phase and becomes zero if resonant phase = π.

Courtesy of Henry Freund

Efficiency Enhancement with Energy Recovery

Oscillator FEL efficiency is typically 1%. The spent electron beams still have ~99% of the initial energy. Dumping the high-power electron beam is wasteful and creates radiation hazards (E_{dump} is beam energy before the beam dump).

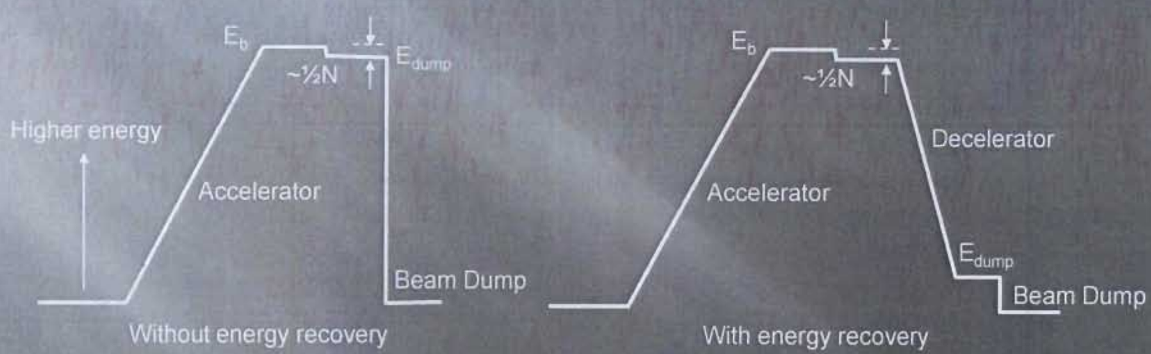

With energy recovery, the efficiency of electron-to-FEL conversion is enhanced by the ratio of beam energy at the wiggler to beam dump energy.

$$\eta_{electron-FEL} = \frac{E_b}{2N_w E_{dump}}$$

Part 4
Optical Architectures

Gain & mirror relectivity determine optical architecture

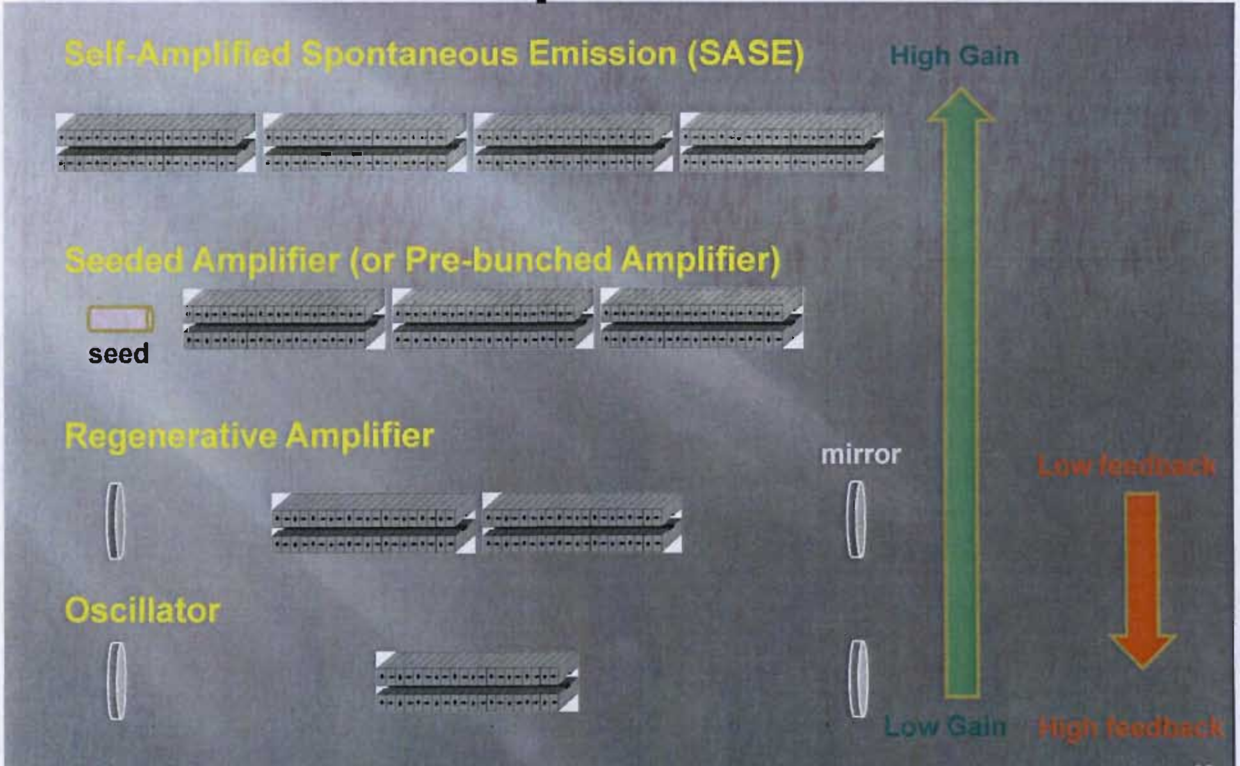

Self-Amplified Spontaneous Emission (SASE)

- Start from spontaneous emission (noise)
- Use very long wiggler (undulator)
- Rely on very high brightness electron beams
- Saturate in a single pass

LCLS Undulator

Courtesy of P. Emma

SASE Power vs. Length

About 20 gain lengths are needed to reach saturation

Saturation Power

$$P_{sat} = \frac{\rho I_p E_b}{e}$$

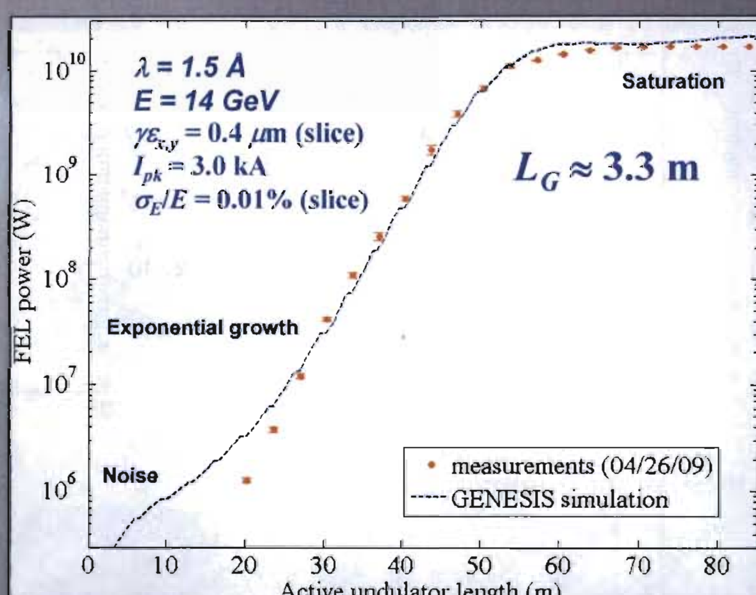

Courtesy of Paul Emma

SASE output is chaotic temporally and spectrally

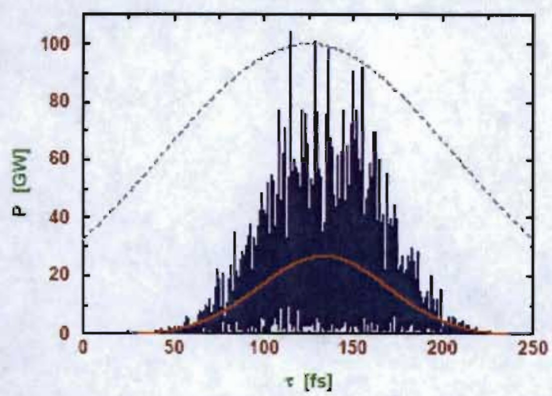

Temporal profile

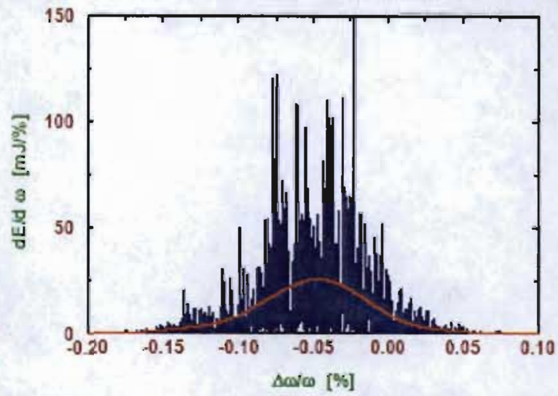

Spectral profile

SASE temporal profile consists of several spikes. The corresponding spectral profile FWHM is inversely proportional to the spikes' temporal width. The narrow spectral line is the inverse of the full temporal pulse.

SASE spectrum is slightly narrower than spontaneous emission

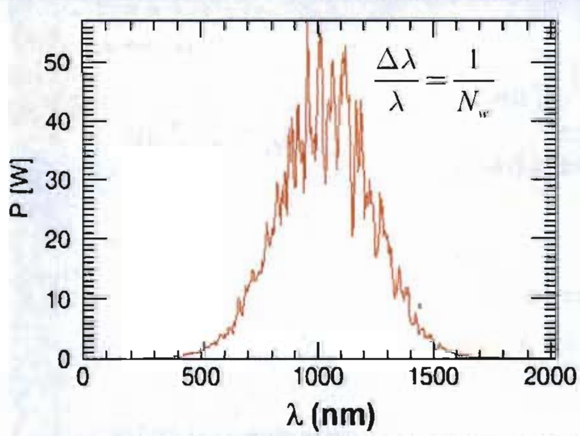

Incoherent Spontaneous Emission

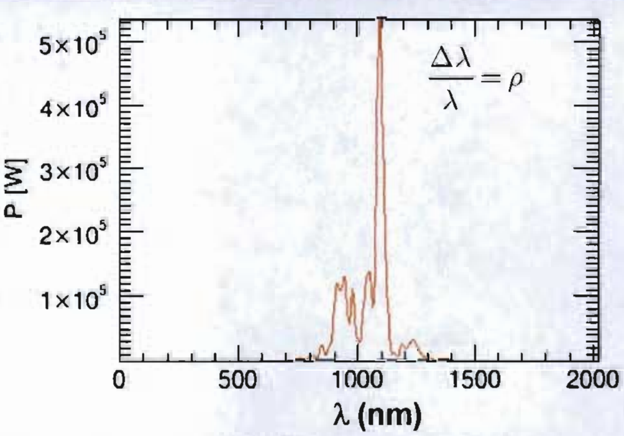

SASE near saturation

Shot-to-shot fluctuations depend on the number of spikes in the radiation pulse.

$$\frac{\Delta I}{I} = \frac{1}{\sqrt{M}}$$

Courtesy of Phil Sprangle

Seeded Amplifier

- Start from a coherent optical beam from a seed laser
- Reduce wiggler length needed to reach saturation
- Reduce spectral width and fluctuations, increase coherence

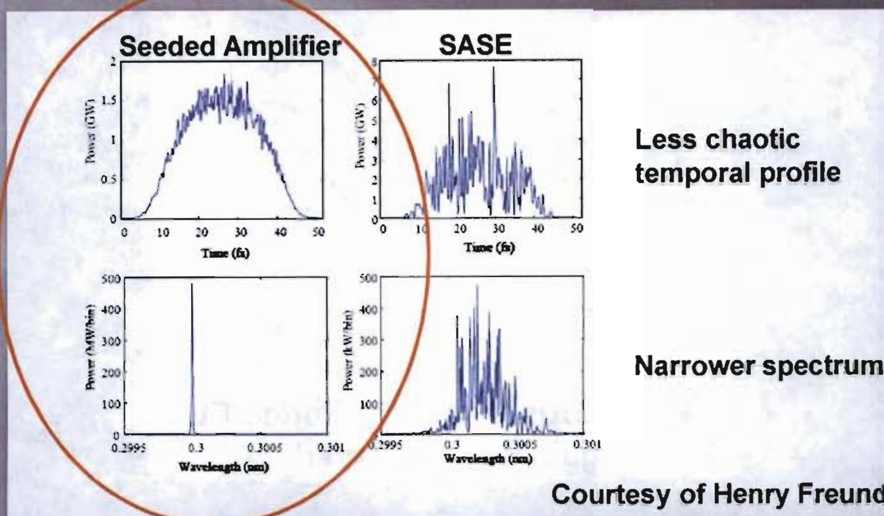

Seeded amplifier reduces wiggler length needed to saturate

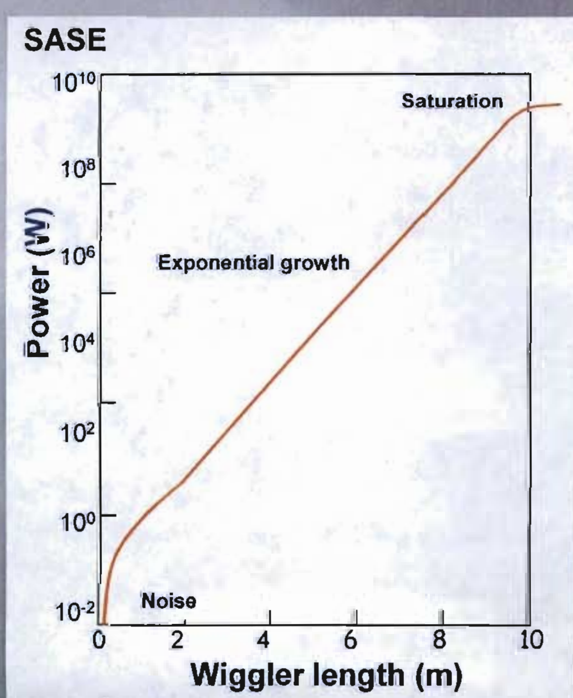

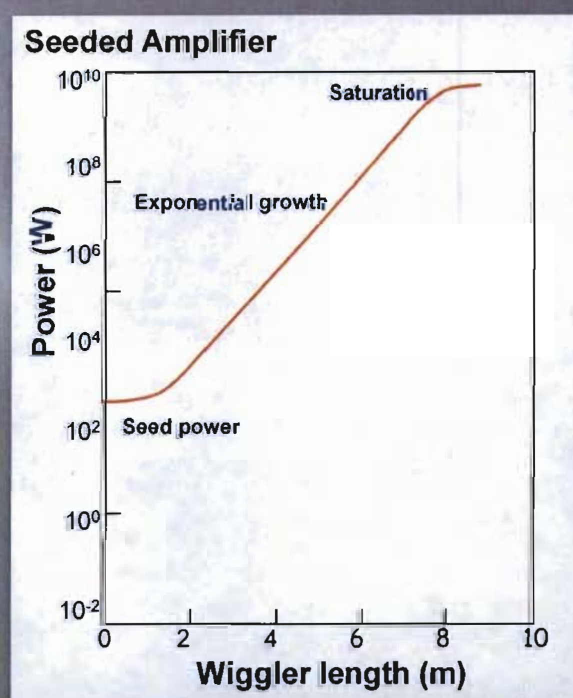

Seeded Amplifier Experiments with Different Seed Power

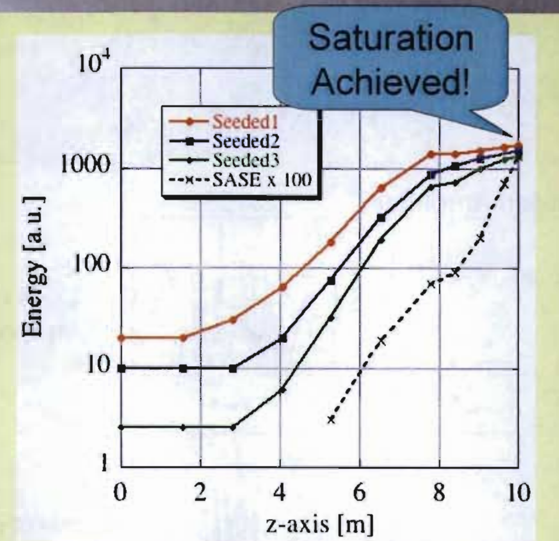

Three orders of magnitude FEL gain was observed.

Courtesy of Jim Murphy

Prebunched Amplifier

- Start from electron beams that have density modulations
- Reduce wiggler length needed to reach saturation
- Rely on some electron microbunching schemes

Start-up power without a seed laser depends on the number of correlated electrons, characterized by the initial bunching coefficient, and the resulting equivalent start-up power.

$$b_1 = \frac{1}{N_e}\sum_{k=1}^{N_e} e^{i\omega t_k(0)}$$

$$P_{startup} = |b_1|^2 N_e^2 P_e$$

For SASE, the initial bunching is due to shot noise so the square of b_1 is simply $1/N_e$ and the SASE start-up is spontaneous emission. For pre-bunched electrons, the start-up power is

$$P_{prebunch} = 0.22|b_1|^2 \rho\left(\frac{IE_b}{e}\right)$$

Pre-bunched Amplifiers also Have Shorter Saturation Lengths

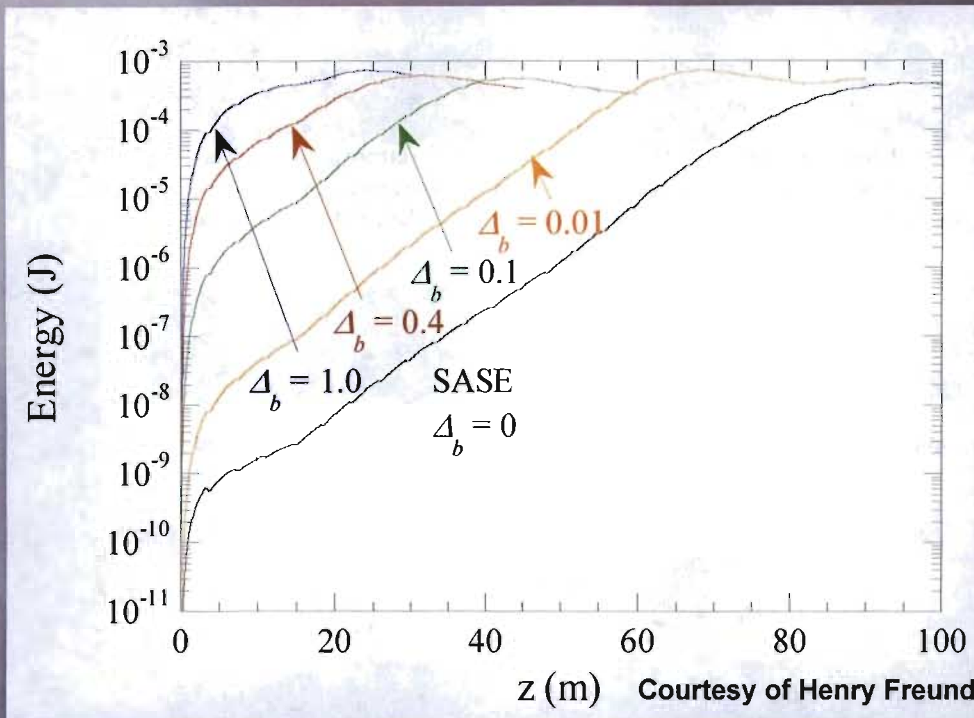

Optical Klystron

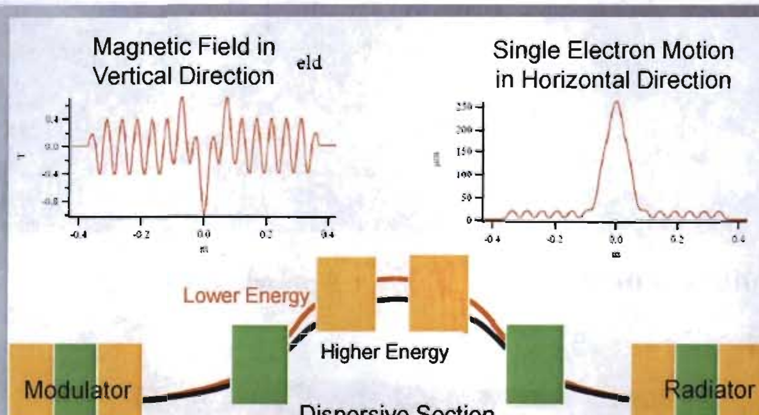

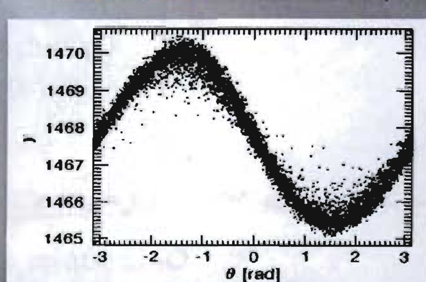

Energy modulation

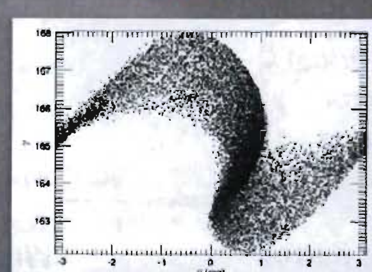

Density modulation

High Gain Harmonic Generation

HGHG is a way to generate short wavelength radiation using a low energy electron beam and a long-wavelength seed. HGHG requires high quality electron beams (ones with low emittance and energy spread).

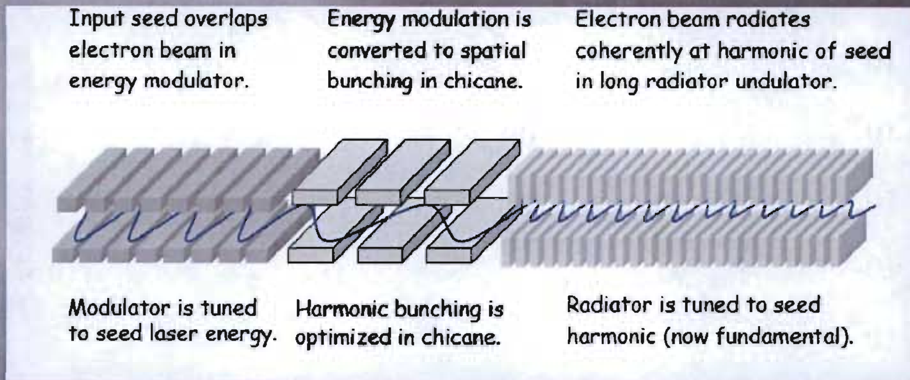

$$\lambda_{\text{mod}} = \frac{\lambda_{w1}}{2\gamma^2}\left(1+a_1^2\right)$$

$$\lambda_{\text{rad}} = \frac{\lambda_{wh}}{2\gamma^2}\left(1+a_h^2\right) = \frac{\lambda_{\text{mod}}}{h}$$

Regenerative Amplifier

- Use mirrors to feedback a small fraction (<1%) of FEL beam
- Similar to Seeded Amplifier except it does not need a seed laser
- Cavity length has to be multiple of electron bunch arrival time

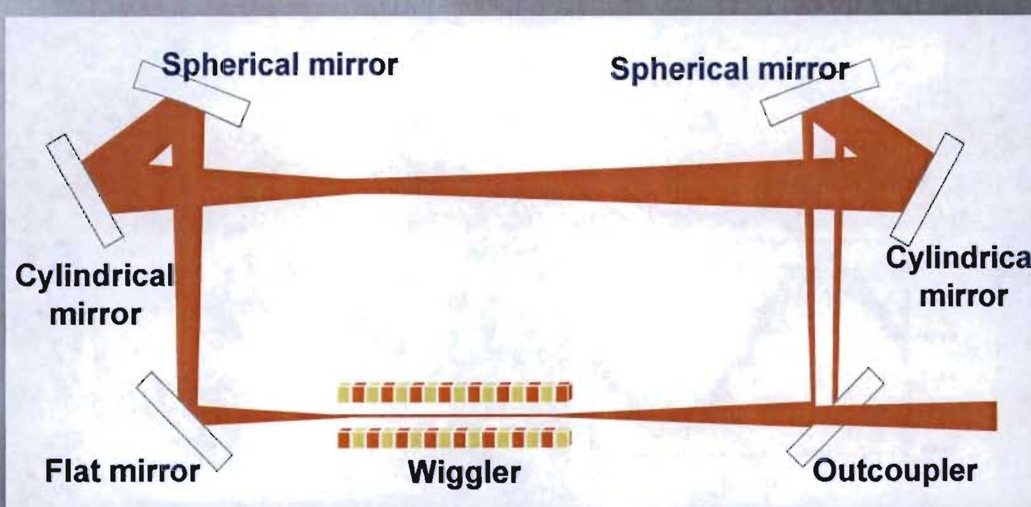

RAFEL saturates with a few electron bunches through the wiggler

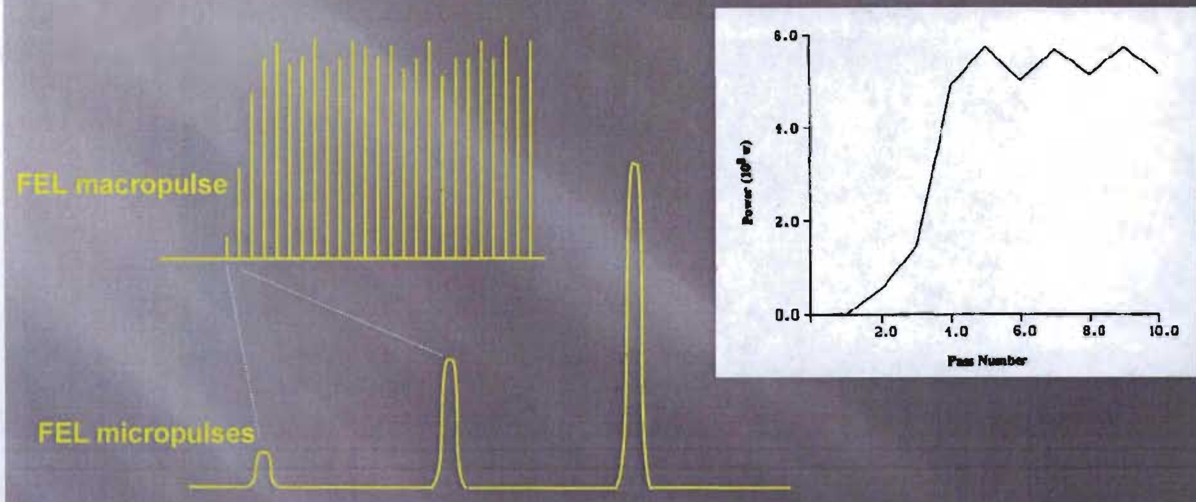

RAFEL micropulse power fluctuates between high and low values, caused by feedback fraction exceeding the optimum value.

RAFEL output power peaks at low feedback power

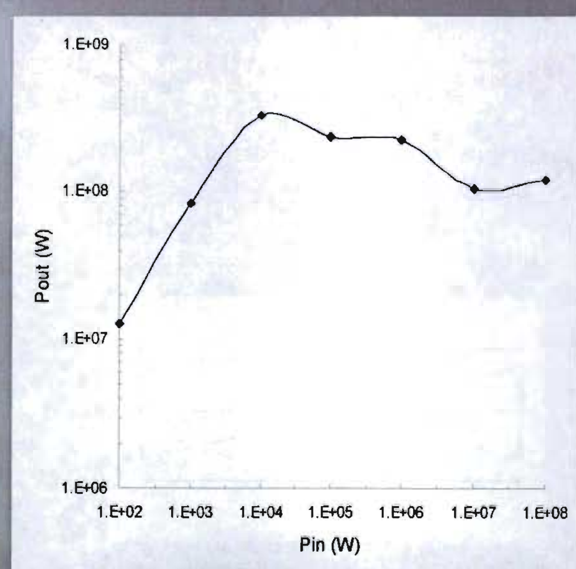

Optimum feedback fraction is only 10^{-4} which makes RAFEL possible with poor mirrors (such as mirrors at x-ray wavelengths).

Oscillator

- Use mirrors to feedback a large fraction (>80%) of FEL beam
- If cavity loss is low, the remaining power exits optical cavity
- Can tolerate a low-quality electron beam
- Optical cavity determines the optical mode to a good approximation
- Cavity length has to be exactly multiple of electron bunch arrival time
- Oscillator has the highest average power than any other architectures

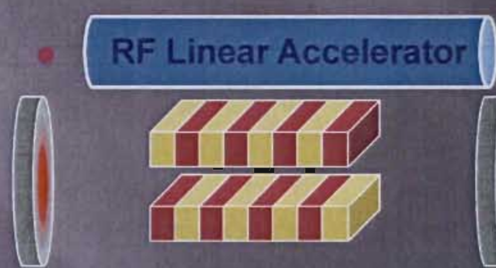

Optical Resonator

- The optical resonator consists of two concave mirrors with radii of curvature R_1 and R_2. The mirrors are separated by a distance D.

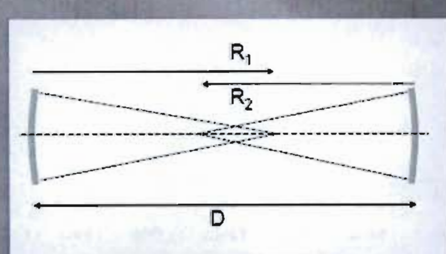

- A measure of stability is the overlap between two foci of the mirrors.
- The Rayleigh length is a measure of the FEL beam's divergence. The shorter the Rayleigh length, the larger the divergence.

Slippage and Lethargy in FEL

Resonance condition dictates that the FEL pulse slips ahead of electron pulse one wavelength every wiggler period.

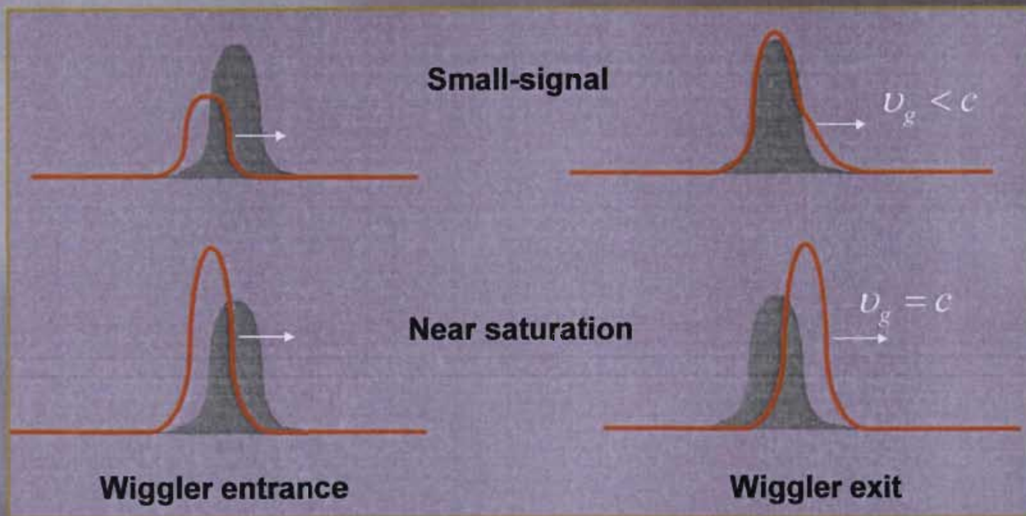

In the small-signal regime, FEL pulse is pulled back by slower electrons. Near saturation, FEL pulse travels at speed *c* as gain is reduced.

Cavity Length Detuning

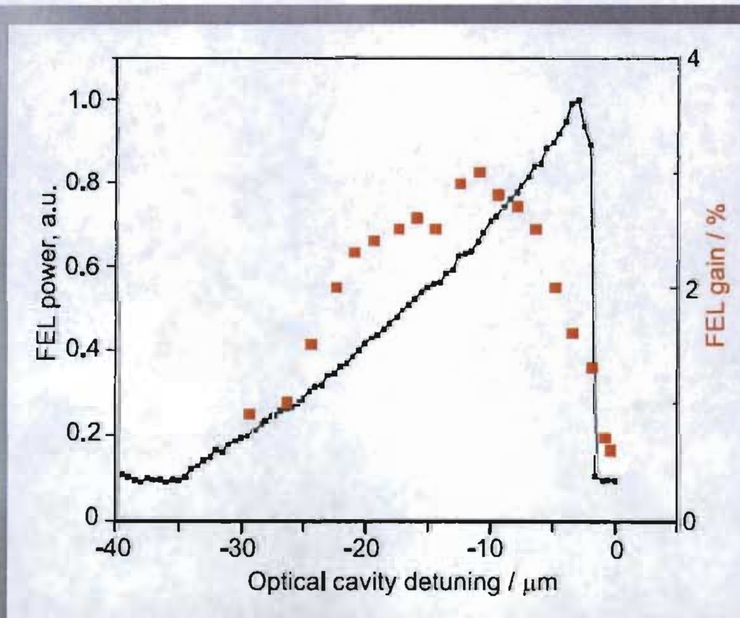

Cavity length must be within a few wavelengths of the correct length. Cavity length for max gain is slightly shorter than that for max power.

Jefferson Laboratory FEL

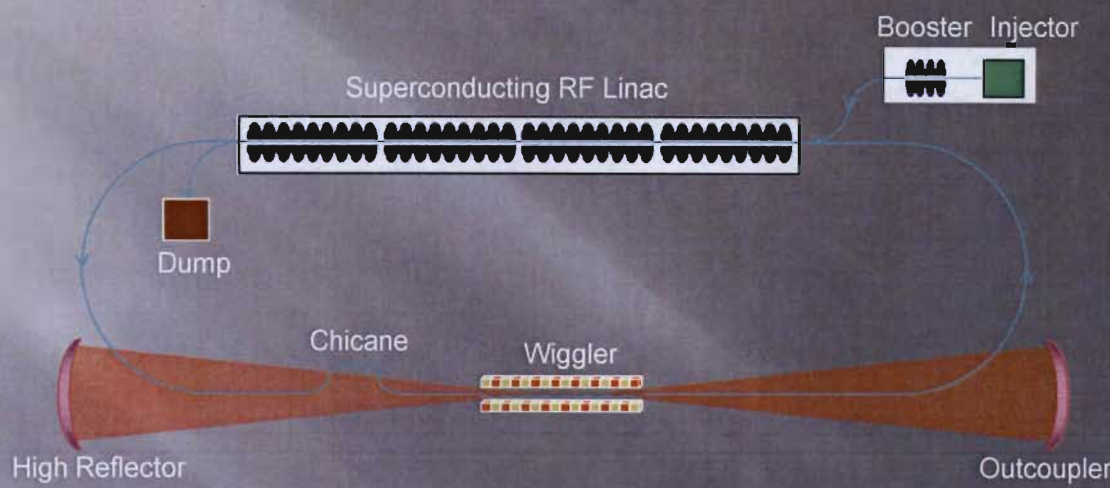

Jefferson Laboratory FEL has produced 14kW, the world record of FEL average power, thanks to energy recovery linac design.

Los Alamos
NATIONAL LABORATORY
EST. 1943

Part 5
Electron Beam Transport

Curvilinear Coordinate

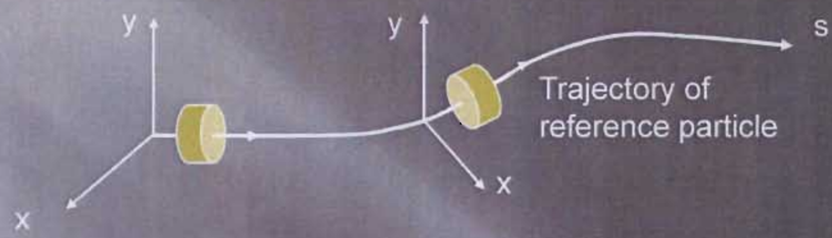

Electrons travel in the s direction. Use (x, y, s) coordinate system to follow the reference electron, an ideal particle at the beam center with a curvilinear trajectory. The reference particle trajectory takes into account only pure dipole fields along the beam line. The x and y of the reference trajectory are thus affected only by the placement and strength of the dipole magnets.

For other electrons, define x' and y' as the slopes of x and y with respect to s

$$x' = \frac{dx}{ds} \qquad y' = \frac{dy}{ds}$$

Phase Space Ellipse & Emittance

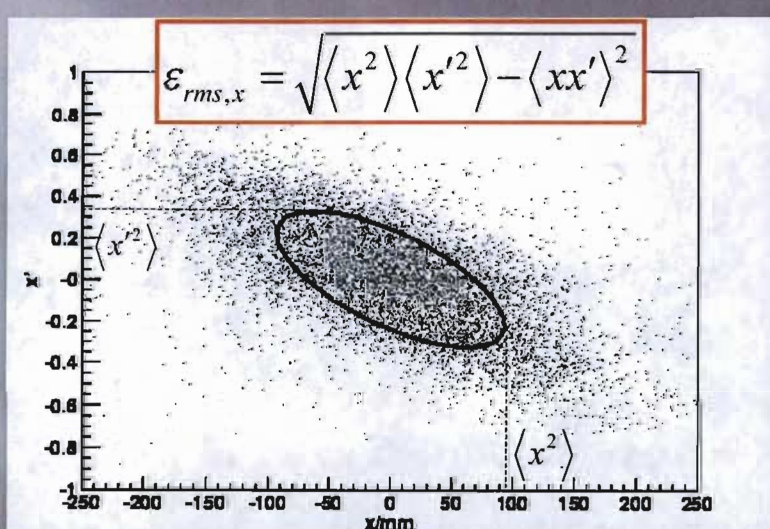

Beams are treated as a statistical distribution of particles in *x'*-*x* (also in *y'*-*y* and γ-*ct*) phase space (particles on x'-x plot). We can draw an ellipse around the particles such that 50% of the particles are found within the ellipse. The area of this ellipse is π times the beam emittance.

Beam Envelope

Consider x and x' phase space in a drift after a quadrupole lens

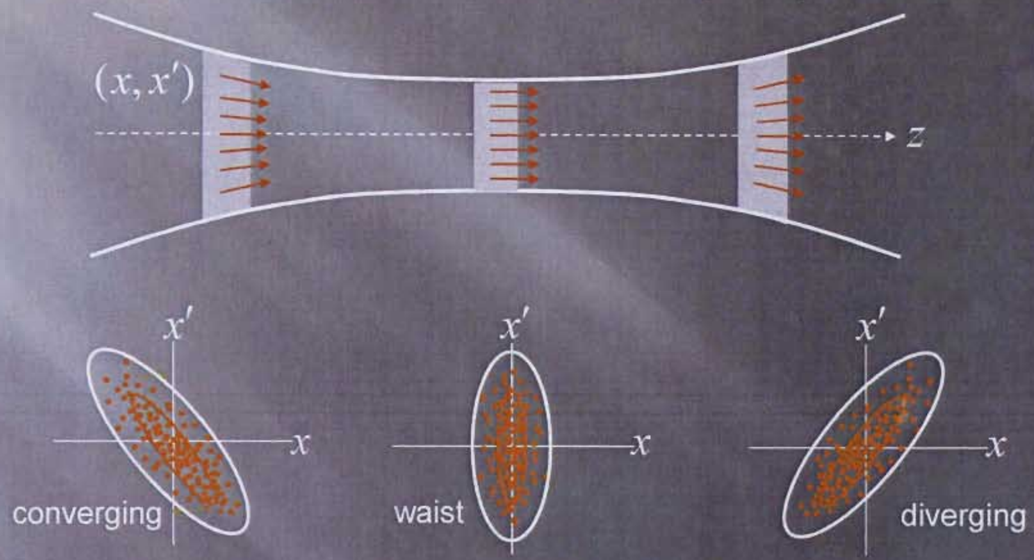

Electrons with x' > 0 drift to the right; those with x' < 0 drift left

83

Electron Beam Focusing

rms electron beam's radius at the waist

$$\sigma_{x0} = \sqrt{\beta_x \varepsilon_x}$$

β function
Property of the lattice

Emittance (un-normalized)
Property of the beam

The beta function is useful because it describes the beam's size (square root of beta) and the maximum amplitude of beam's envelope, and it also tells us where the beam is sensitive to perturbations.

84

Single quadrupoles focus electron beams in one direction

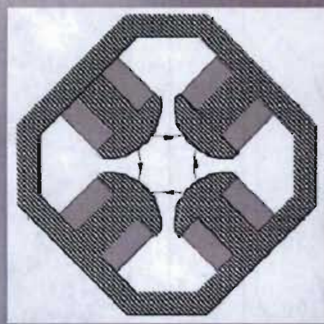

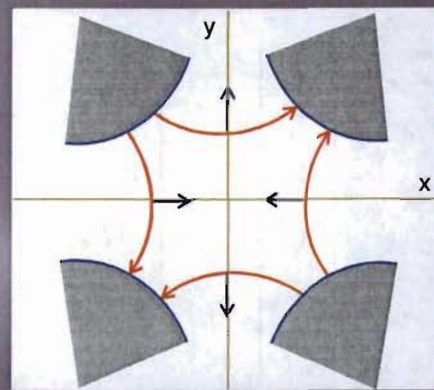

Quadrupoles focus electron beam in one plane, defocus it in the other plane. A round beam becomes elliptical after traversing a quadrupole.

Dipoles bend electron beams

Dipoles bend electron beam at an angle depending on its energy

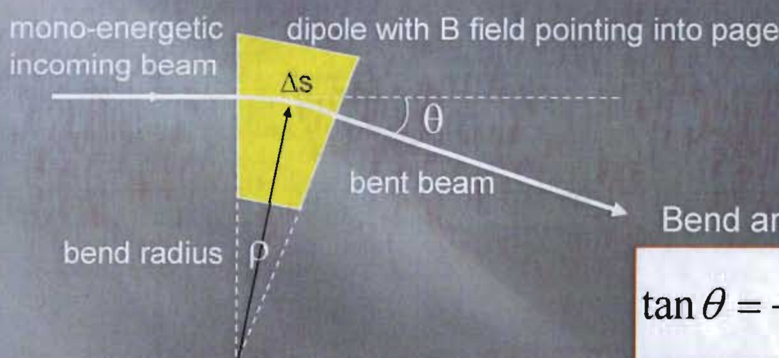

Bend angle

$$\tan\theta = -\frac{ecB\Delta s}{E_b}$$

Bend radius

$$\frac{1}{\rho}\left(m^{-1}\right) = 299.8\frac{B(T)}{E_b\left(MeV\right)}$$

Magnetic rigidity

$$B\rho = \frac{\beta\gamma m_0 c}{e} = \frac{E_b}{c}$$

Beam Transfer Matrix

$$\begin{bmatrix} x \\ x' \\ y \\ y' \\ \delta \\ ct \end{bmatrix}_{out} = \begin{pmatrix} M_{11} & \cdots & M_{16} \\ \vdots & \ddots & \vdots \\ M_{51} & \ddots & M_{56} \\ M_{61} & \cdots & M_{66} \end{pmatrix} \begin{bmatrix} x \\ x' \\ y \\ y' \\ \delta \\ ct \end{bmatrix}_{in}$$

$$\delta = \frac{E - E_0}{E_0}$$

$$\tau = t - t_0$$

Dispersion

Bunch compression element

Transfer matrix is a 6x6 matrix that performs linear transform of a beam vector at the input location to another beam vector at the output location.

87

2x2 Transfer Matrices of an F(ocusing) Quadrupole

$$x'' + kx = 0$$

F quad focuses beam in x

$$\begin{bmatrix} x \\ x' \end{bmatrix}_{out} = \begin{pmatrix} \cos\left(\sqrt{k}l\right) & \frac{1}{\sqrt{k}}\sin\left(\sqrt{k}l\right) \\ -\sqrt{k}\sin(kl) & \cos\left(\sqrt{k}l\right) \end{pmatrix} \begin{bmatrix} x \\ x' \end{bmatrix}_{in}$$

$$y'' - ky = 0$$

F quad defocuses beam in y

$$\begin{bmatrix} y \\ y' \end{bmatrix}_{out} = \begin{pmatrix} \cosh\left(\sqrt{k}l\right) & \frac{1}{\sqrt{k}}\sinh\left(\sqrt{k}l\right) \\ -\sqrt{k}\sinh\left(\sqrt{k}l\right) & \cosh\left(\sqrt{k}l\right) \end{pmatrix} \begin{bmatrix} y \\ y' \end{bmatrix}_{in}$$

Thin lens transfer matrix

$$\begin{bmatrix} x \\ x' \end{bmatrix}_{out} = \begin{pmatrix} 1 & 0 \\ -\frac{1}{f} & 1 \end{pmatrix} \begin{bmatrix} x \\ x' \end{bmatrix}_{in}$$

Focusing strength

$$k = \left|\frac{B'}{B\rho}\right|$$

Field gradient

Magnetic rigidity

88

Triplets focus electron beams in both x and y directions

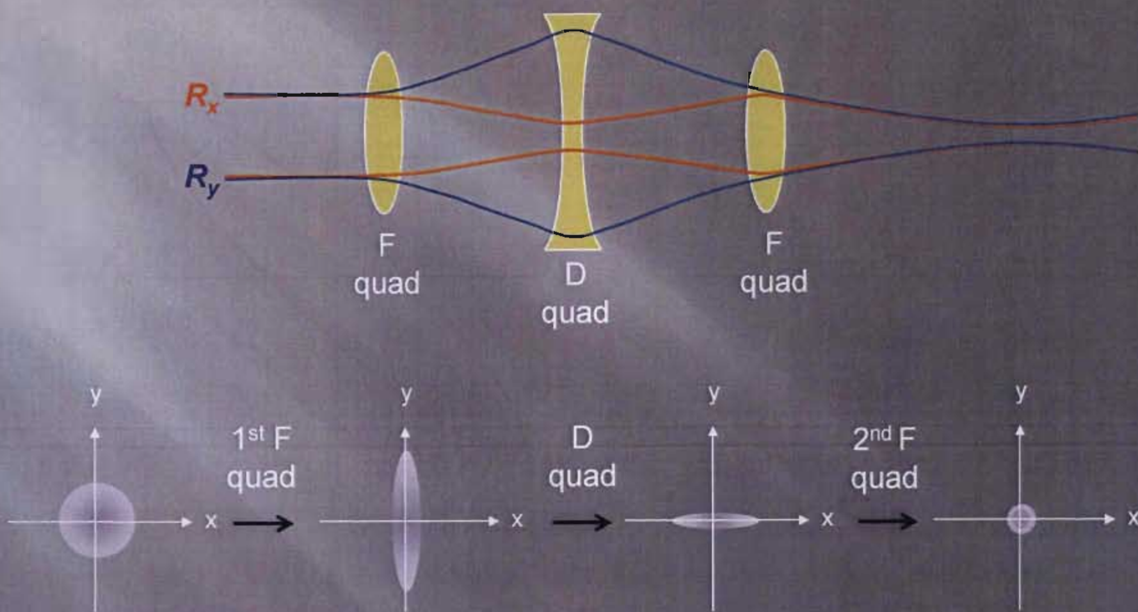

Evolution of electron beam envelope through a quadrupole triplet

89

Transfer Matrices of a Quadrupole Triplet

Combining matrices in the order: elements closest to the input beam on the right hand side (next to input vector) and work toward the left.

Transfer matrix in x plane

$$A_x = \begin{pmatrix} \cos\varphi_5 & \frac{1}{\sqrt{k_5}}\sin\varphi_5 \\ -\sqrt{k_5}\sin\varphi_5 & \cos\varphi_5 \end{pmatrix} \begin{pmatrix} 1 & l_4 \\ 0 & 1 \end{pmatrix} \begin{pmatrix} \cosh\varphi_3 & \frac{1}{\sqrt{k_3}}\sinh\varphi_3 \\ -\sqrt{k_3}\sinh\varphi_3 & \cosh\varphi_3 \end{pmatrix} \begin{pmatrix} 1 & l_2 \\ 0 & 1 \end{pmatrix} \begin{pmatrix} \cos\varphi_1 & \frac{1}{\sqrt{k_1}}\sin\varphi_1 \\ -\sqrt{k_1}\sin\varphi_1 & \cos\varphi_1 \end{pmatrix}$$

Transfer matrix in y plane

$$A_y = \begin{pmatrix} \cosh\varphi_5 & \frac{1}{\sqrt{k_5}}\sinh\varphi_5 \\ -\sqrt{k_5}\sinh\varphi_5 & \cosh\varphi_5 \end{pmatrix} \begin{pmatrix} 1 & l_4 \\ 0 & 1 \end{pmatrix} \begin{pmatrix} \cos\varphi_3 & \frac{1}{\sqrt{k_3}}\sin\varphi_3 \\ -\sqrt{k_3}\sin\varphi_3 & \cos\varphi_3 \end{pmatrix} \begin{pmatrix} 1 & l_2 \\ 0 & 1 \end{pmatrix} \begin{pmatrix} \cosh\varphi_1 & \frac{1}{\sqrt{k_1}}\sinh\varphi_1 \\ -\sqrt{k_1}\sinh\varphi_1 & \cosh\varphi_1 \end{pmatrix}$$

element	5	4	3	2	1
	F quad	drift	D quad	drift	F quad

90

Twiss Parameters

β ~ (beam envelope)^2

γ ~ (beam divergence)^2

ϕ ~ angle in phase space

$$\tan(2\phi) = \frac{\alpha}{\gamma - \beta}$$

α = 0 upright ellipse (waist)

α > 0 diverging beam

α < 0 converging beam

Courant-Snyder invariant

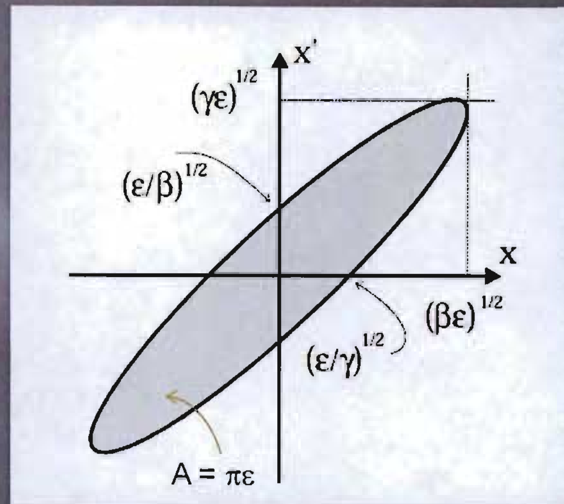

$$\gamma x^2 + 2\alpha x x' + \beta x'^2 = \varepsilon$$

Dipole's dispersion spreads electron beam in the bend plane

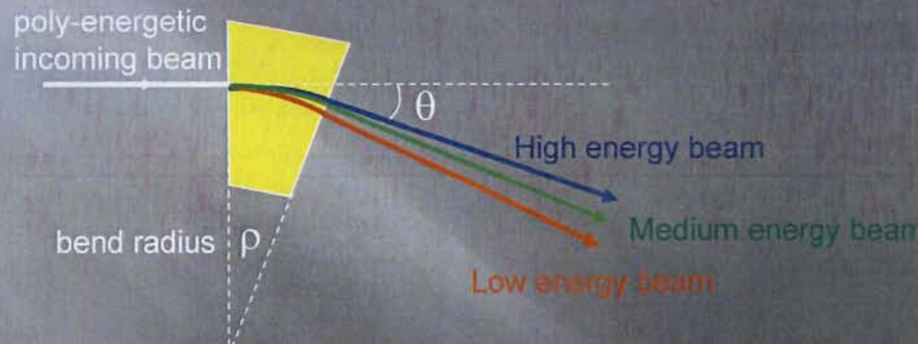

Dipoles are used as **energy spectrometers** to measure beam's energy (from known bend radius and magnetic field) and energy spread.

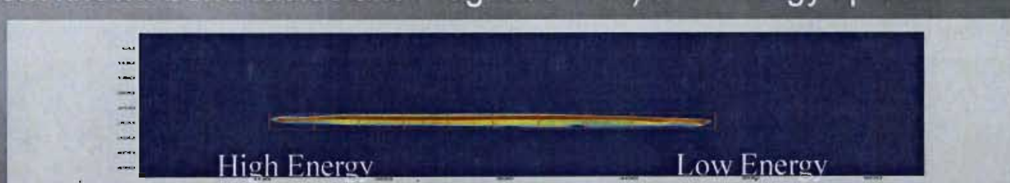

Two dipoles translate & disperse electron beam into a new line

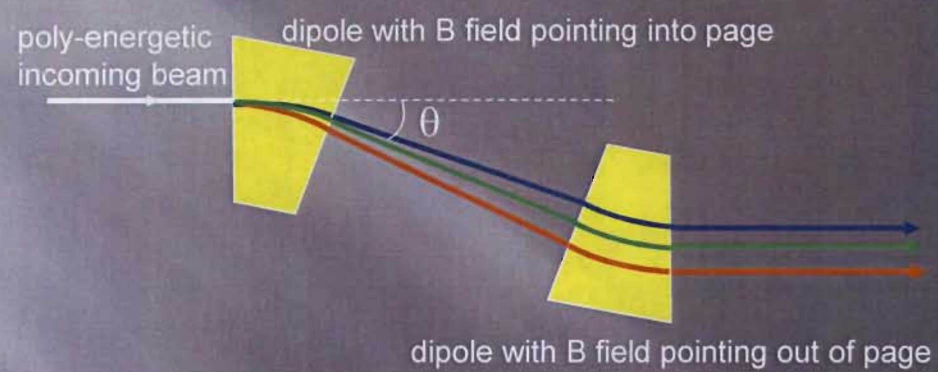

Achromatic: different energies come back together in space
Isochronous: different energies come back together in time

The above two-dipole bend is neither achromatic nor isochronous; low-energy beam (red) takes longer path than high-energy (blue).

Achromatic Bunch Compressor

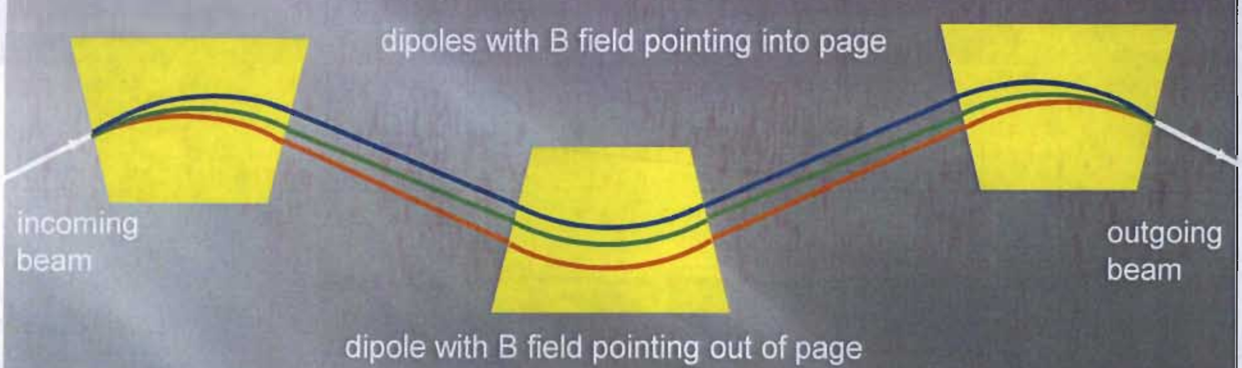

This two-dipole bend is achromatic but not isochronous.
Three dipole bend can be used to compress electron bunch via M_{56}

$$c\Delta\tau = M_{56}\frac{\Delta E}{E}$$

Chicane Compressor

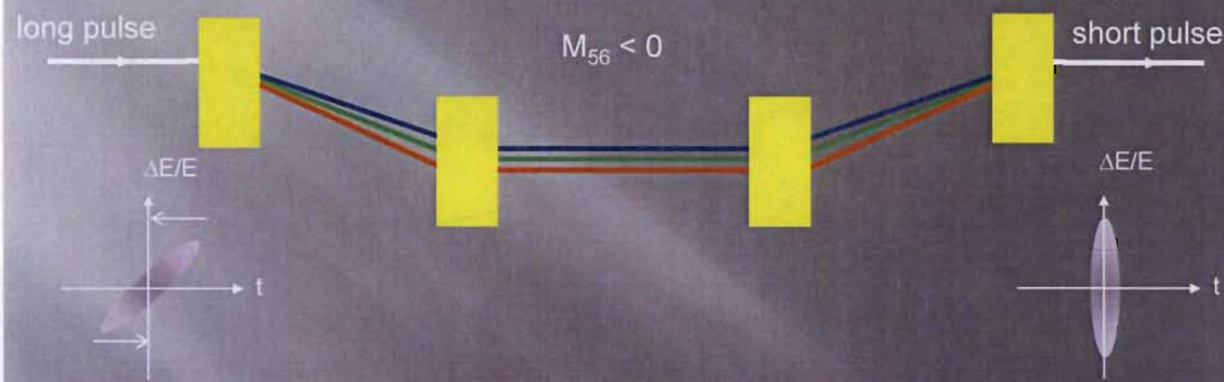

- Chirp electron bunch by accelerating it off-crest so the leading edge (left) has lower energy than the trailing edge (right)
- Put energy-chirped electron bunch through a chicane
- Chicane compresses long bunch to shorter bunch (higher peak current)

Coherent Synchrotron Radiation (CSR)

- Short bunches radiates coherent synchrotron radiation (CSR) that catches up with the bunches and causes energy change

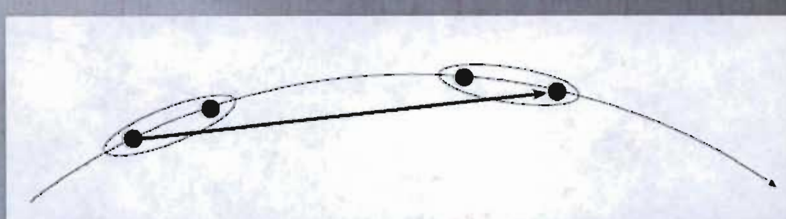

- CSR-induced energy change

$$\frac{d\mathcal{E}}{d(ct)} = \frac{1}{4\pi\varepsilon_0} \frac{2eQ}{3^{\frac{1}{3}}(2\pi)^{\frac{1}{2}} R^{\frac{2}{3}} \sigma_z^{\frac{4}{3}}} f(\xi)$$

- CSR-induced energy change combines with dispersion in the bunch compressor to produce an emittance growth.

Ideal Bunch Compressor

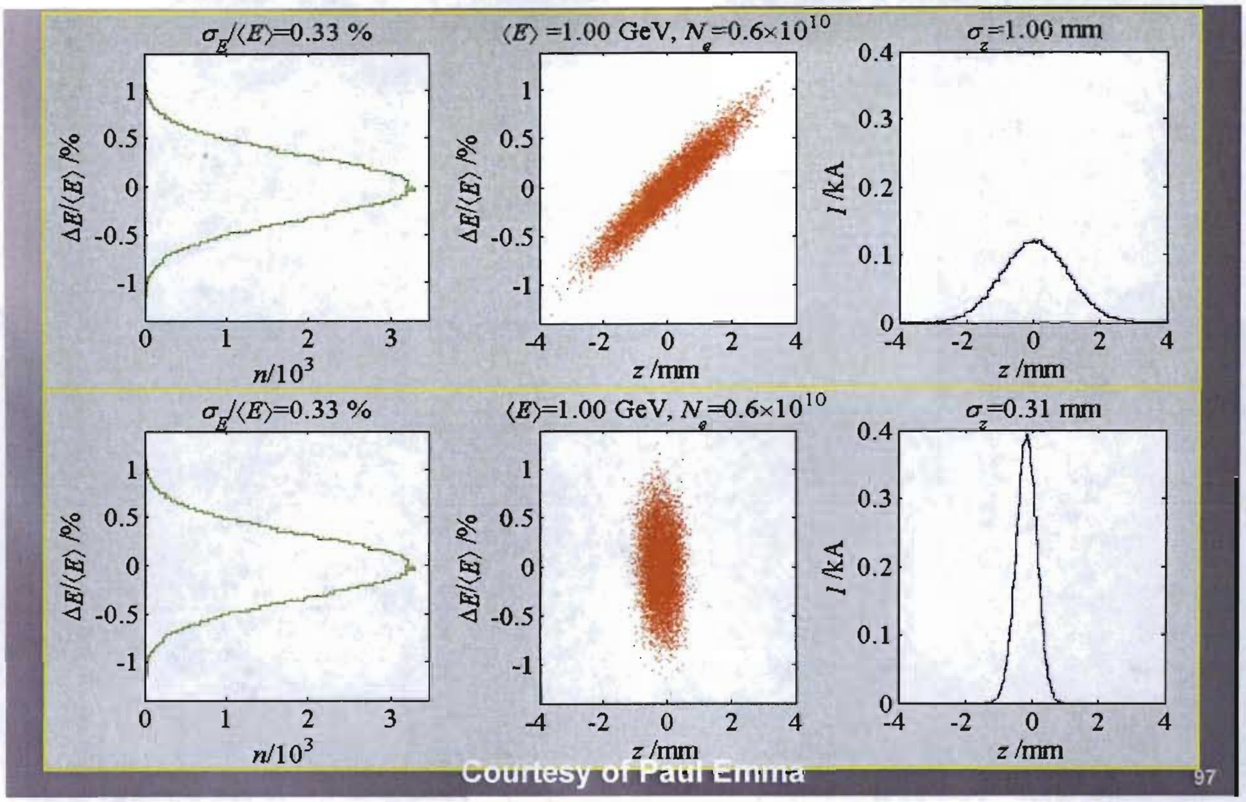

Real Bunch Compressor

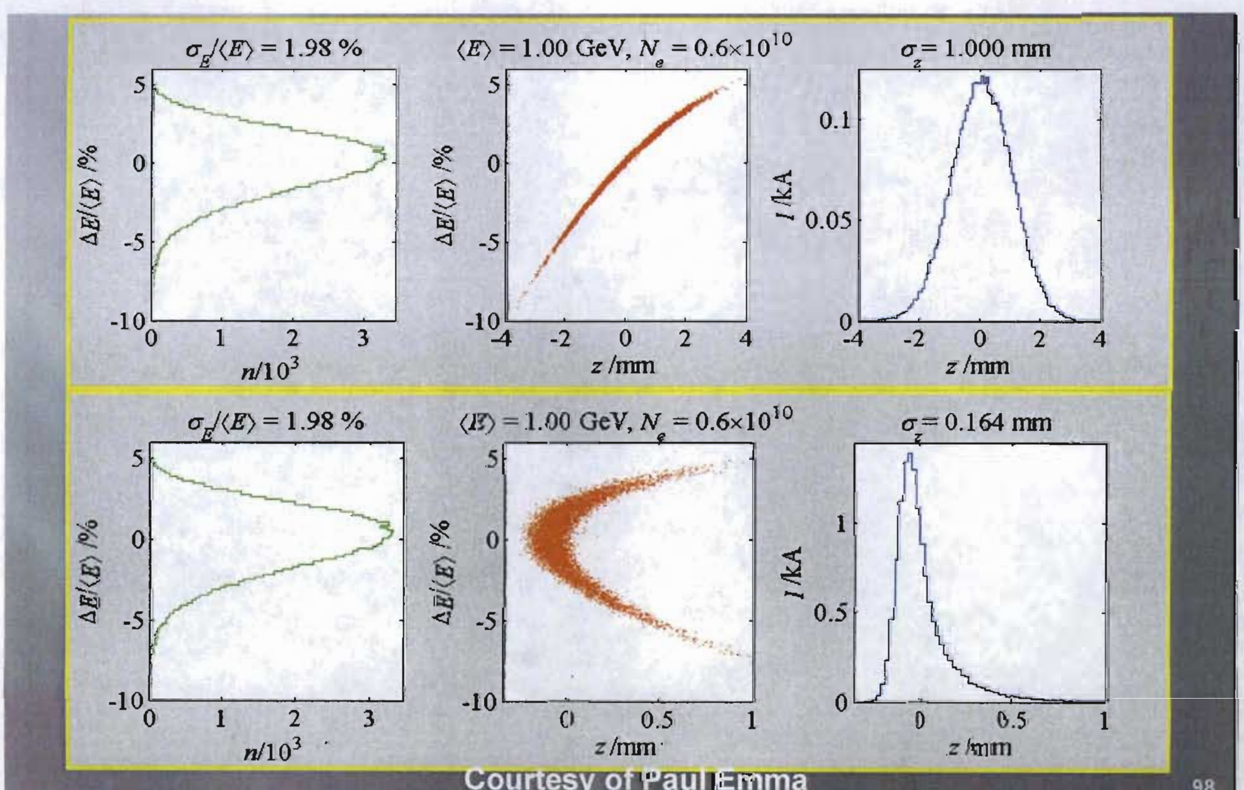

CSR increases electron beam's emittance and energy spread

Peak Current

CSR-induced energy change

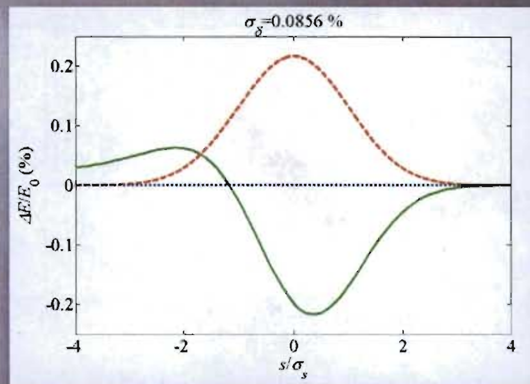

CSR-induced energy spread

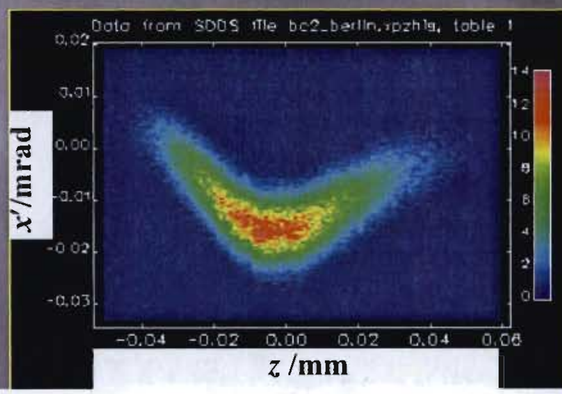

CSR-induced emittance

Los Alamos NATIONAL LABORATORY EST. 1943

Part 6 RF Linear Accelerators

RF Waveguide Modes

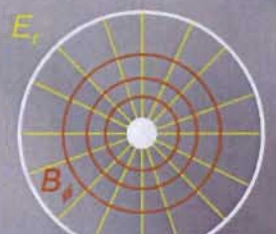

TEM
Transverse electric, magnetic

TEM modes in coaxial transmission lines; used for power transmission

TM
Transverse magnetic

TM modes in cylindrical waveguides; used for **acceleration**

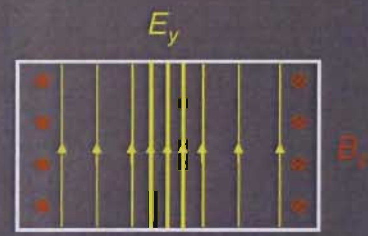

TE
Transverse electric

TE modes in rectangular waveguides; used for high-power transmission

101

How an RF accelerator works

Electric field accelerates electrons and increases their energy.

$$\Delta W = \int \mathbf{F} \cdot d\mathbf{s} = -\int e\mathbf{E} \cdot d\mathbf{s}$$

RF cavities store electromagnetic energy to produce high electric fields. Electric fields are maximum on axis and magnetic fields are maximum near the equator.

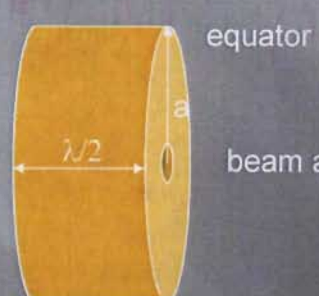

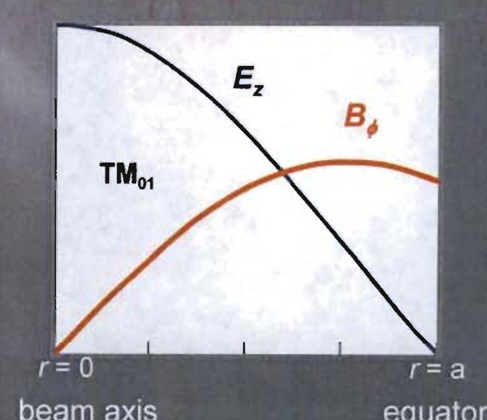

$$E_z(r,z,t) = E_0 J_0(k_c r)\cos(kz - \omega t)$$

$$B_\phi(r,z,t) = \frac{E_0}{c}\frac{\omega}{\omega_c} J_1(k_c r)\sin(kz - \omega t)$$

102

Standing-wave π-mode Cavity

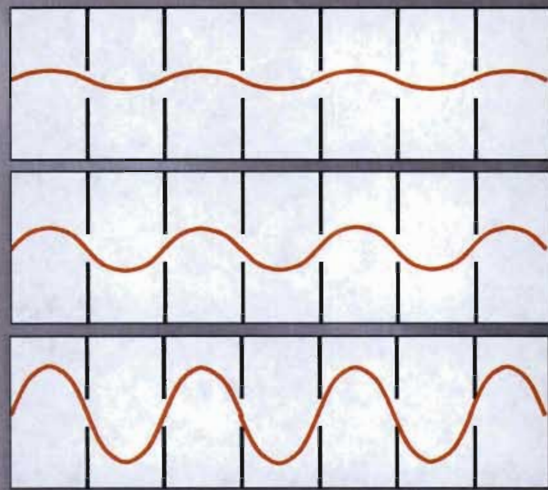

Standing waves exist in multi-cell cavity if each cell is one-half wavelength long. The waves' absolute amplitude are time-dependent but the relative amplitudes remain constant with time. Electrons injected at the correct phase are accelerated during their transit through the accelerator cavity.

Single Pillbox Cavity

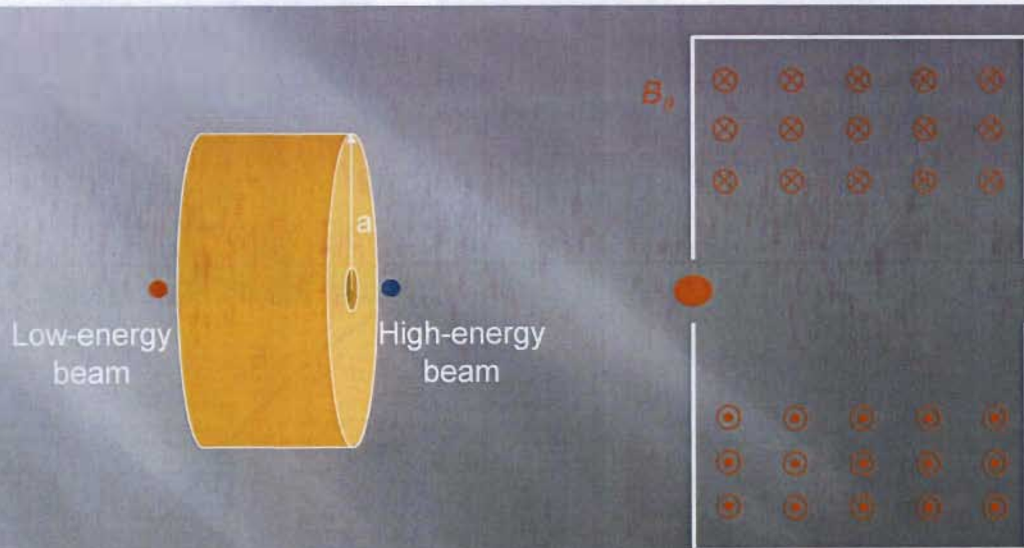

The color of the electron bunch denotes its energy (red = low; blue = high)

Single Pillbox Cavity

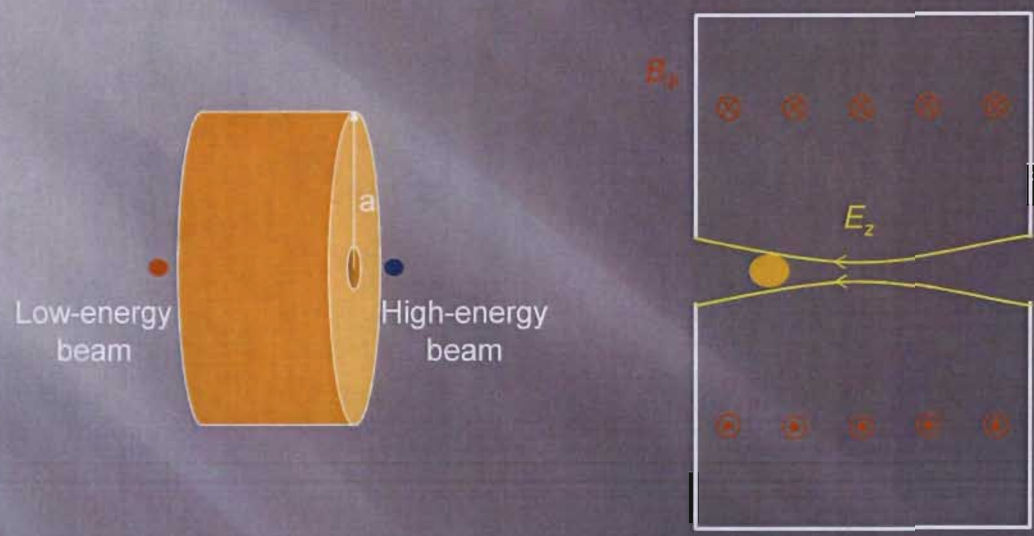

The color of the electron bunch denotes its energy (red = low; blue = high)

Single Pillbox Cavity

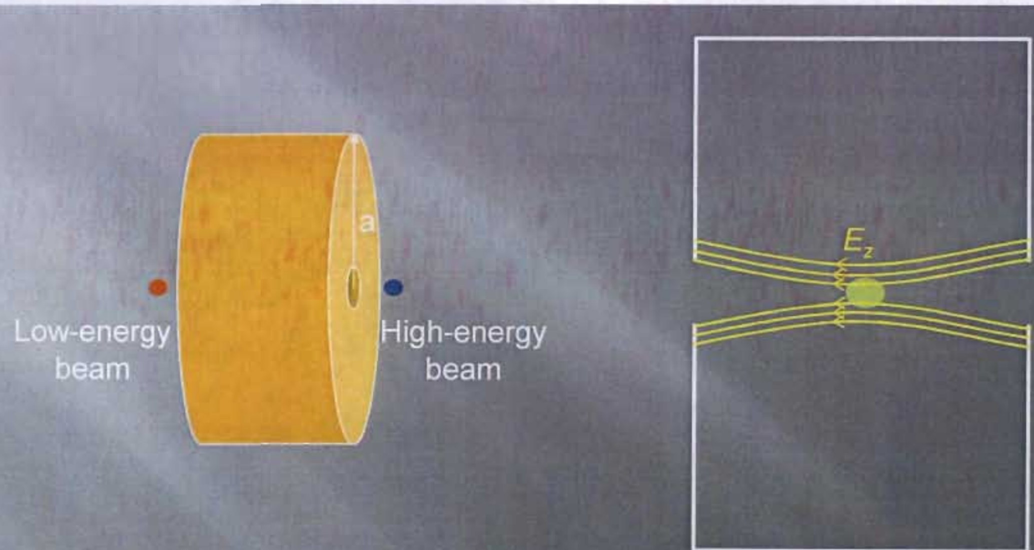

The color of the electron bunch denotes its energy (red = low; blue = high)

Single Pillbox Cavity

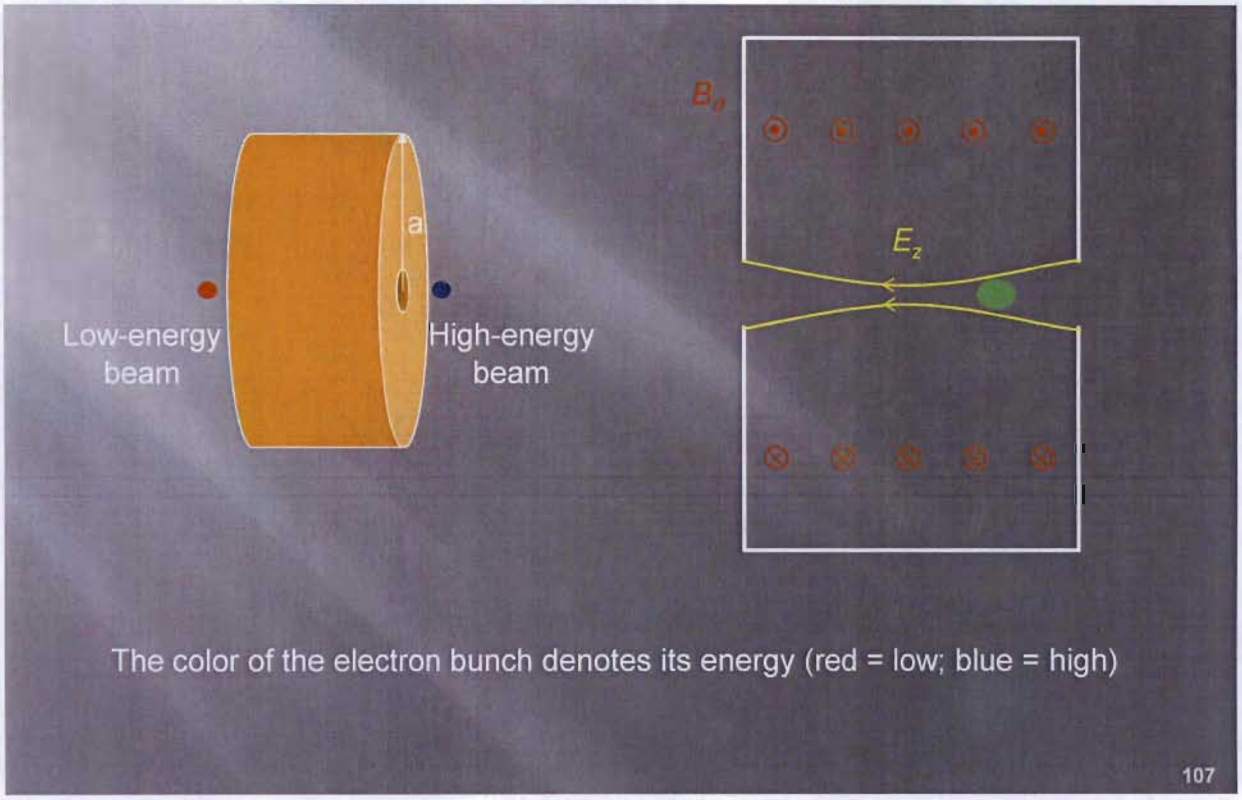

Single Pillbox Cavity

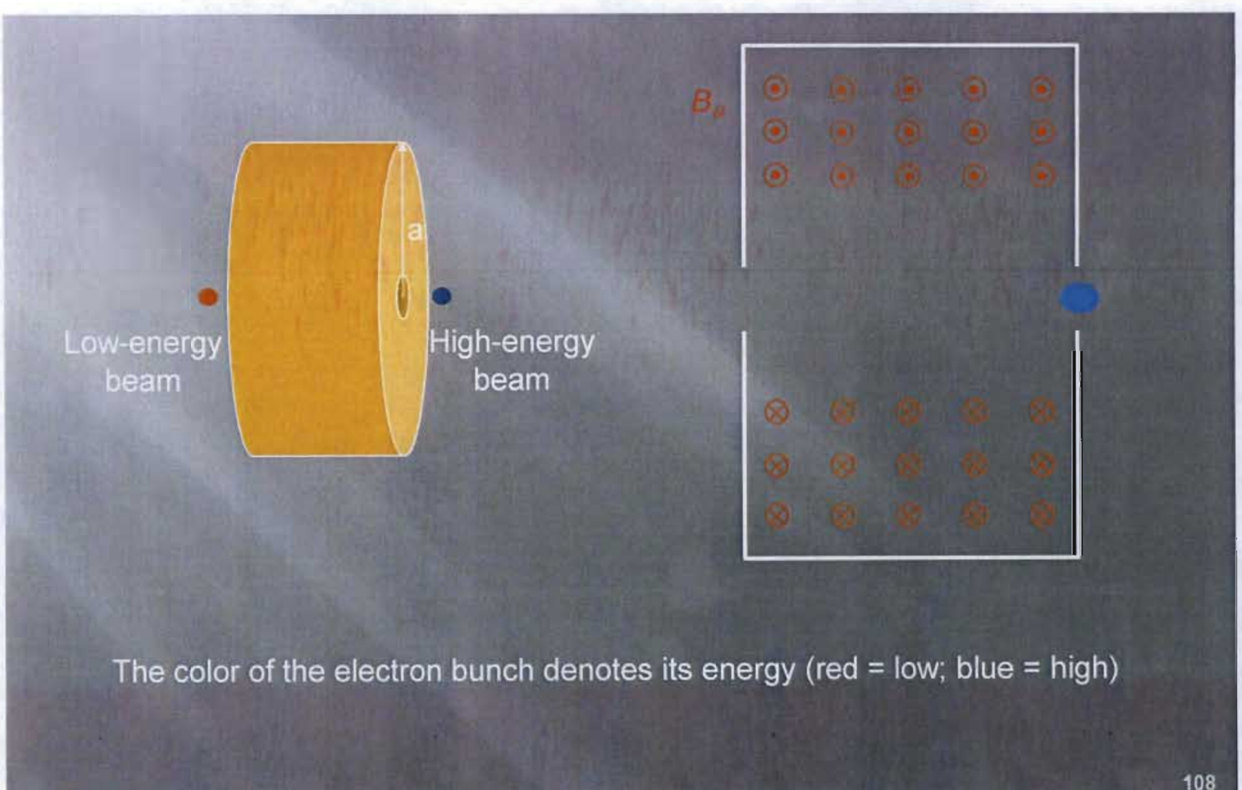

Multi-cell Acceleration

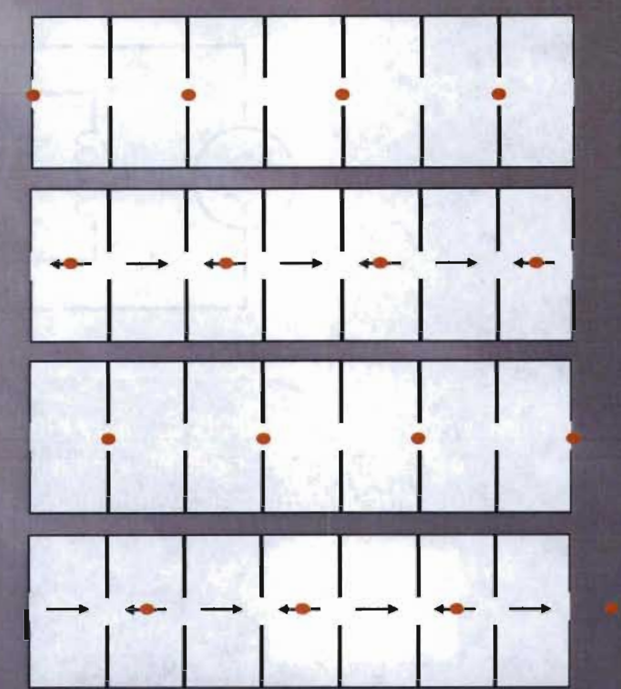

Cavity Quality Factor Q

Stored energy

$$U = \frac{\mu_0}{2}\int |\mathbf{H}|^2 dV$$

Ohmic loss

$$P_l = \frac{R_S}{2}\int |\mathbf{H}|^2 dS$$

Cavity unloaded Q

$$Q_0 = \frac{\omega_0 U}{P_l} = \frac{\omega_0 \mu_0}{R_S}\frac{\int |\mathbf{H}|^2 dV}{\int |\mathbf{H}|^2 dS}$$

$$\frac{Volume}{Surface} \approx \frac{c}{\omega_0}$$

$Z_0 = 377\ \Omega$

$$Q_0 = \frac{Z_0 f_{geometry}}{R_S}$$

Geometric factor

$$G = Q_0 R_S$$

Cavity Q is the ratio of stored energy to power loss per cycle. Stored energy is proportional to volume and power loss is proportional to surface area. Geometric factor depends only on cavity shape, and is independent of material, size or frequency. Typical G is about 270 Ω (the higher the better).

Frequency & Shunt Impedance

Resonance frequency

$$\omega_0 = \frac{1}{\sqrt{LC}}$$

Cavity unloaded Q

$$Q_0 = \omega_0 RC$$

R is shunt impedance, not resistance

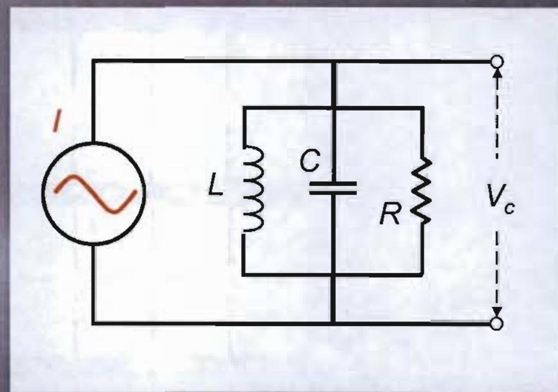

Shunt impedance is a measure of how efficiently a cavity utilizes RF power toward accelerating the beam. Cavity power per unit length is equal to the square of transit-time corrected gradient divided by shunt impedance (MΩ/m).

$$P_c = \frac{(E_0 T)^2}{R}$$

Accelerating Gradients

- Spatial average axial electric field: E_0 $\quad \mathbf{E} = E_0 e^{i\omega t + \vartheta_0}$
- Average structure accelerating gradient, E_{acc} $\quad E_{acc} = E_0 T$
- Packing factor: length of active structure/total length $\quad f_p = \frac{L_{acc}}{L_{total}}$
- Real-estate gradient $\quad E_{real} = E_{acc} f_p$

For cw SRF cavities at 1.3 GHz, the peak on-axis accelerating gradient is about 35 MV/m. The transit-time corrected gradient is about 17 - 20 MV/m. With a packing factor of 0.6, the real-estate gradient is 10 - 12 MV/m.

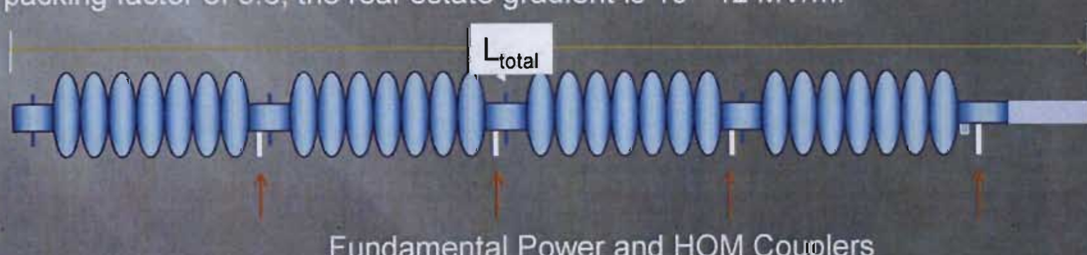

SRF / NCRF Comparison

f_{RF} = 1.3 GHz	SRF Nb (2K)	NCRF Cu (RT)
Q_0	1×10^{10}	2×10^{4}
R/Q	1 kΩ/m	
R_0	1×10^{13} Ω/m	2×10^{7} Ω/m
P_{cav} (@ 5 MV/m)	2.5 W/m	1 MW/m
P_{cav} (@ 20 MV/m)	40 W/m	200 MW/m
τ_{fill}	1 s	5 μs

Courtesy of Tom Powers

RF Superconductivity

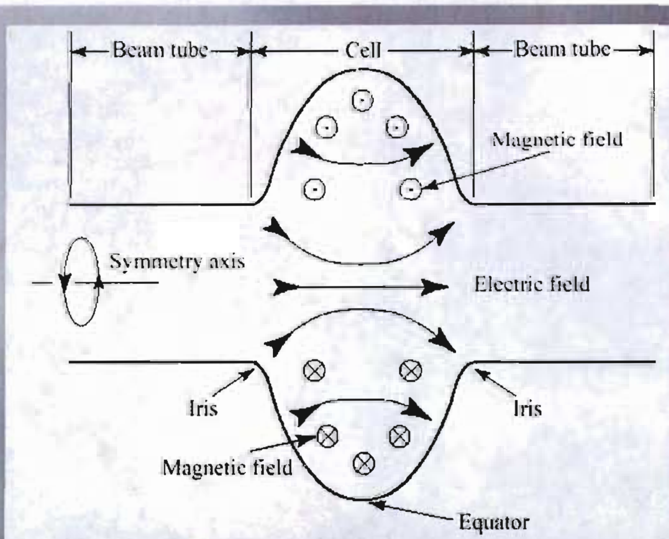

Superconducting RF Cavity

- Low ohmic losses (efficient RF usage)
- Gradient is limited by critical B field

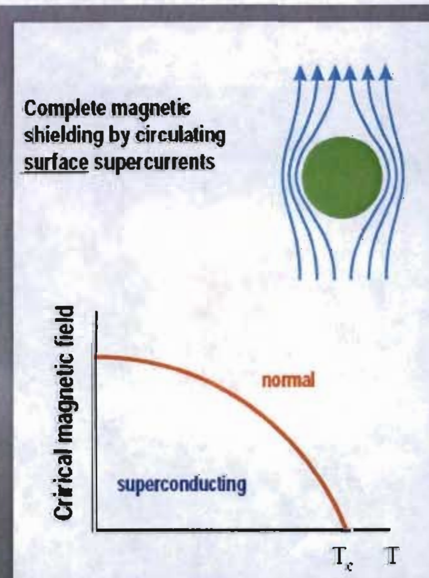

Niobium properties

T_c is 9.2K
At 2K, H_c is ~0.2 T

Surface Resistance of Niobium

$$R_S \approx 2\times10^{-4}\Omega\left(\frac{f}{1.5GHz}\right)^2 \frac{1}{T}\exp\left(\frac{-17.67}{T}\right)+R_{residual}$$

Surface resistance has 2 components:

- BCS resistance (that depends exponentially with -1/T)
- Residual resistance (that depends on surface quality, trapped flux)

Treat Nb surface and shield cavities with mu metal to reduce ambient magnetic field and residual resistance.

Typical R_s for good cavities < 20 nΩ

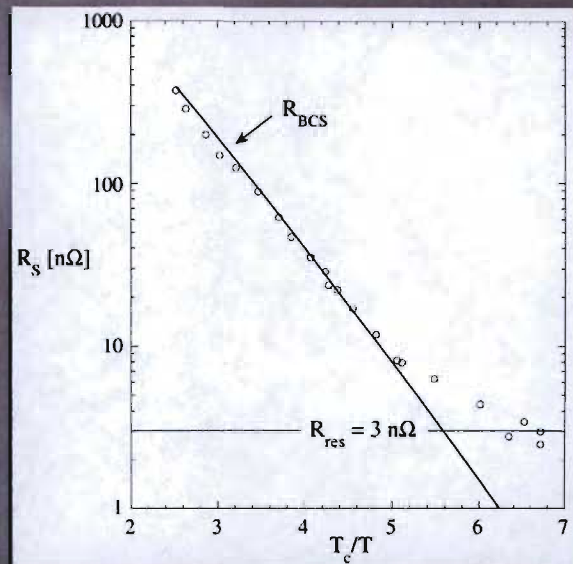

E and B Fields in SRF Cavity

Peak electric field

Peak magnetic field

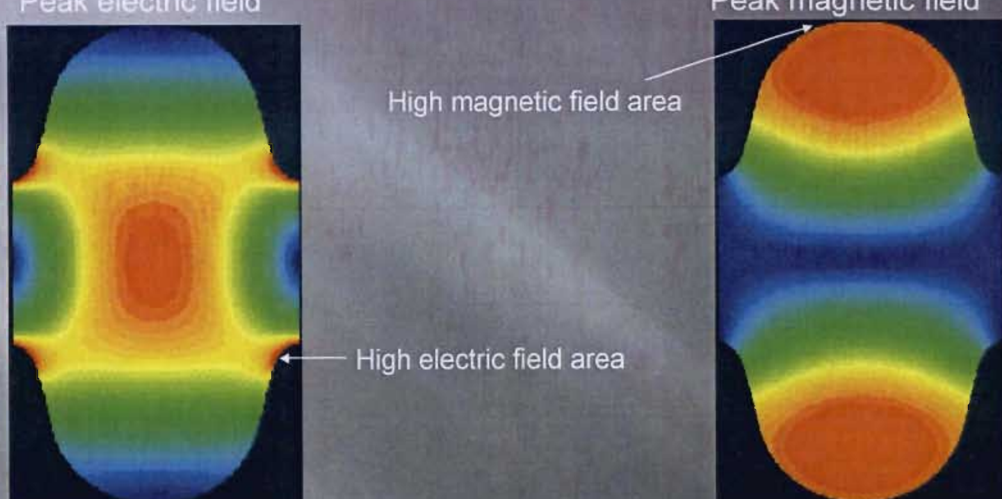

High electric fields cause field emission → Q degradation

High magnetic fields cause RF heating → quenching

Courtesy of J. Sekutowics

SRF Cavity Q versus Gradient

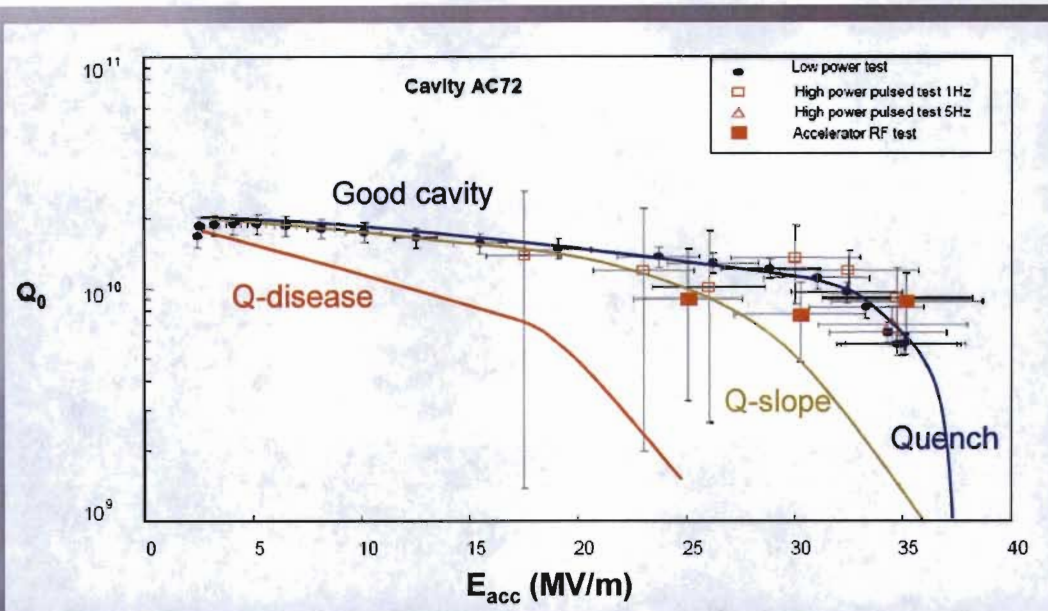

Quenching is caused by surface magnetic exceeding H_c (~100 mT)
Q disease is caused by hydride formation – avoided by cooling quickly or bake
Q slope is caused by surface oxygen – reduced by baking

Loaded Q and Bandwidth

External Q is optimized for a particular beam loading condition (current)

$$Q_{ext} = \frac{E_c}{\left(\frac{R}{Q}\right) I_b \cos\phi_s}$$

Cavity gradient

Off-crest phase

Beam current

~1kΩ

Cavity loaded Q

$$\frac{1}{Q_L} = \frac{1}{Q_0} + \frac{1}{Q_{ext}} \approx \frac{1}{Q_{ext}}$$

Cavity bandwidth

$$\Delta\omega = \frac{\omega_0}{Q_L}$$

For a typical SRF cavity, loaded Q is equal to the external Q which is optimized for a given beam current and off-crest phase. Typical loaded Q is ~10^5, much less than Q_0. Loaded Q determines the cavity bandwidth.

Cryomodules

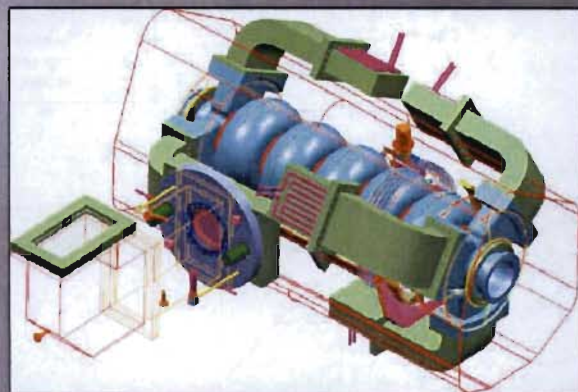

Cryomodules house SRF cavities, RF, vacuum and cryo hardware

- A typical cavity consists of 5 – 9 RF cells
- Each cavity is connected to an RF source with phase & amplitude control
- Each cryomodule houses several cavities
- Other hardware includes RF windows, power couplers, tuner and shields.

from Bob Rimmer's ERL 2007 Presentation

High-Power RF System

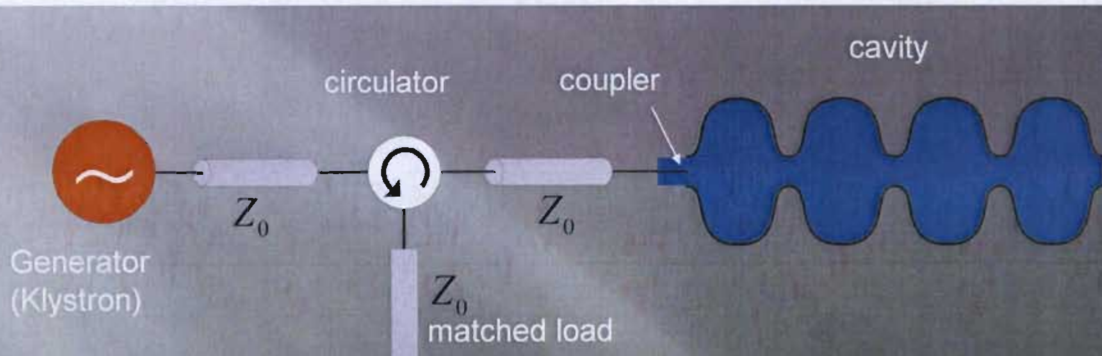

Z_0 = characteristic impedance of transmission line (waveguide)

Klystron power P_{for} sees *matched impedance* Z_0 only at a specific beam current. Otherwise, RF power is reflected from the cavity and redirected into the matched (water-cooled) load.

Conservation of energy: $P_{for} = P_{ref} + P_{cav}$

Wakefields

A relativistic electron bunch drags along electric field lines that are mostly transverse and terminate perpendicular to a perfectly conducting surface.

relativistic electron bunch in beam pipe

The same electron bunch traversing a discontinuity such as a cavity generates wakefields that can disrupt subsequent electron bunches.

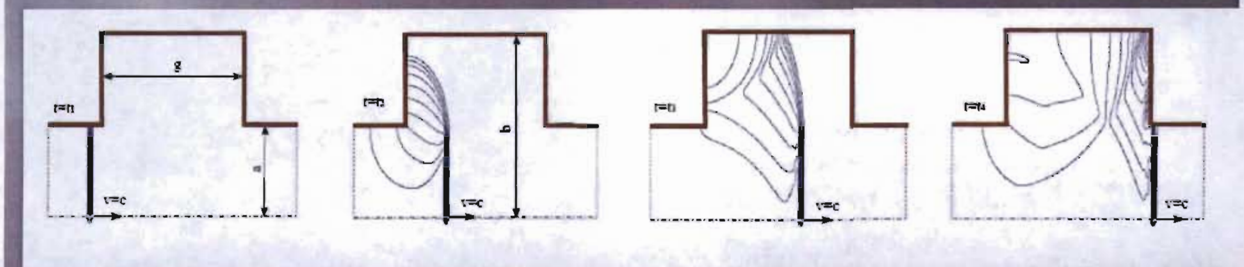

from Paolo Craievich's PhD Thesis

Transverse Wakefields

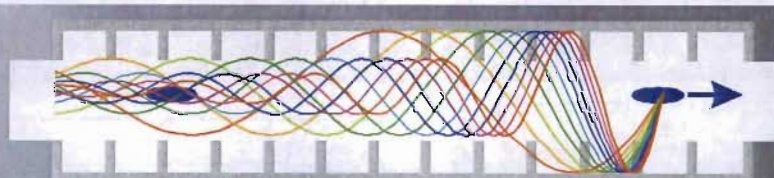

Transverse wake function

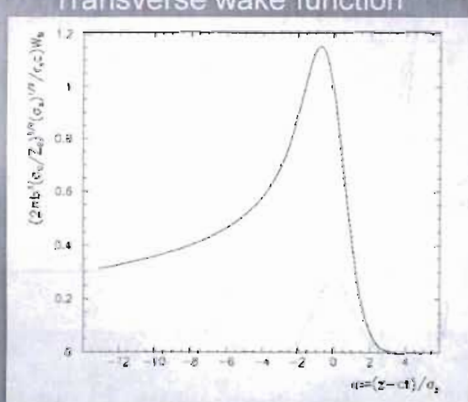

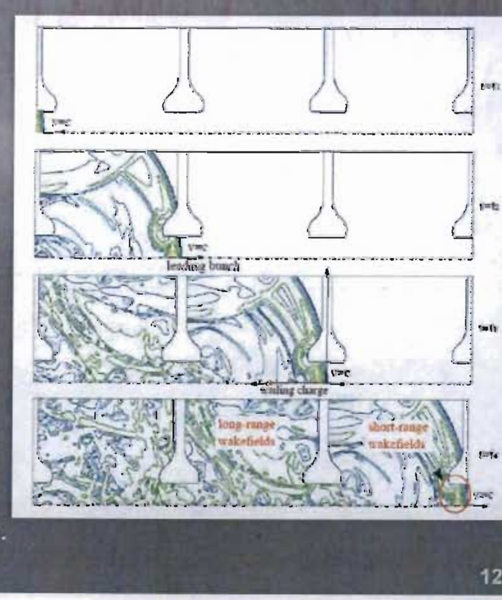

Transverse wakefields couple power into higher order modes (HOM) of accelerator cavities and cause beam breakup instabilities.

Higher Order Modes

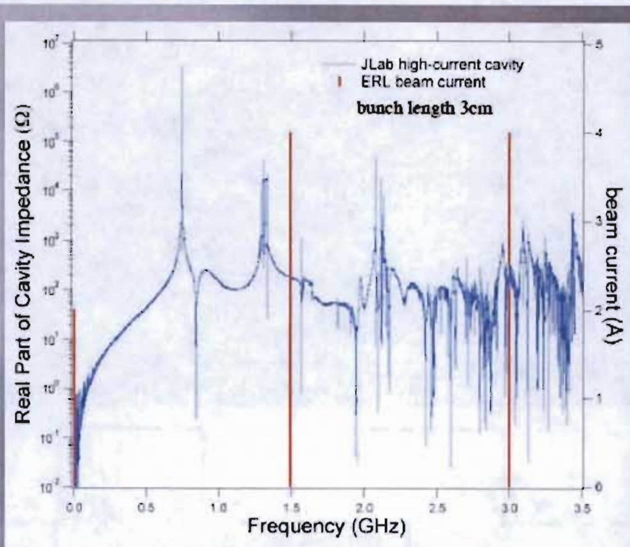

Monopole modes excited by on-axis beam

Higher order mode power

$$P_{HOM} = 2Q_b k_{loss} I_{ave}$$

Q_b : bunch charge

k_{loss} : loss factor (~10 V/pC)

I_{ave} : average current

Higher order modes (HOM) have to be damped to avoid transverse beam deflection that could lead to beam breakup instabilities (BBU).

from Bob Rimmer's ERL 2007 Presentation

Longitudinal Wakefields

Longitudinal wake function

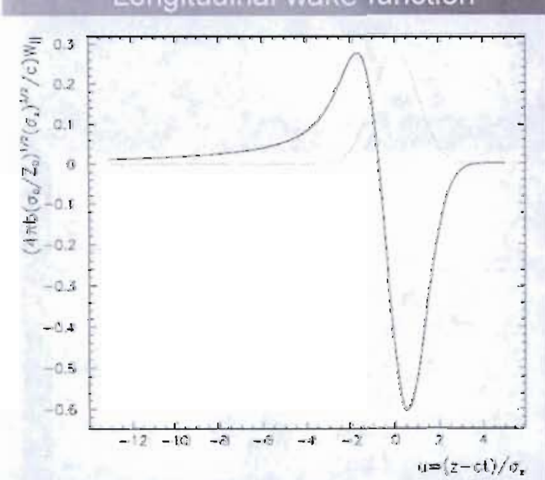

Longitudinal wakefields of different σ_z

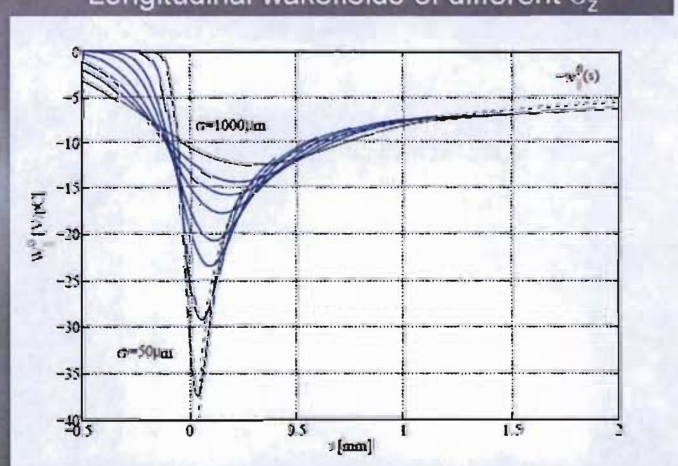

Longitudinal wakefields cause energy depression in the same electron bunch and introduce curvature in energy-phase distribution. Keeping the electron bunch long reduces longitudinal wakefields.

Energy Recovery Linac

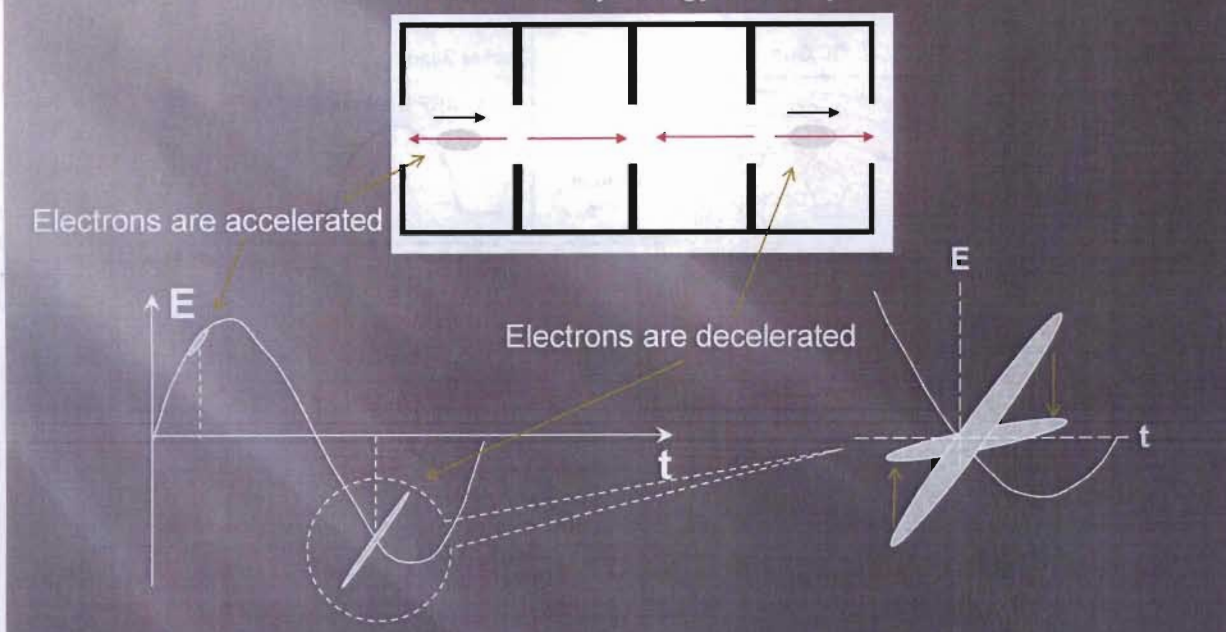

Courtesy of Dave Douglas

Part 7
Electron Injectors

DC Injector and Booster

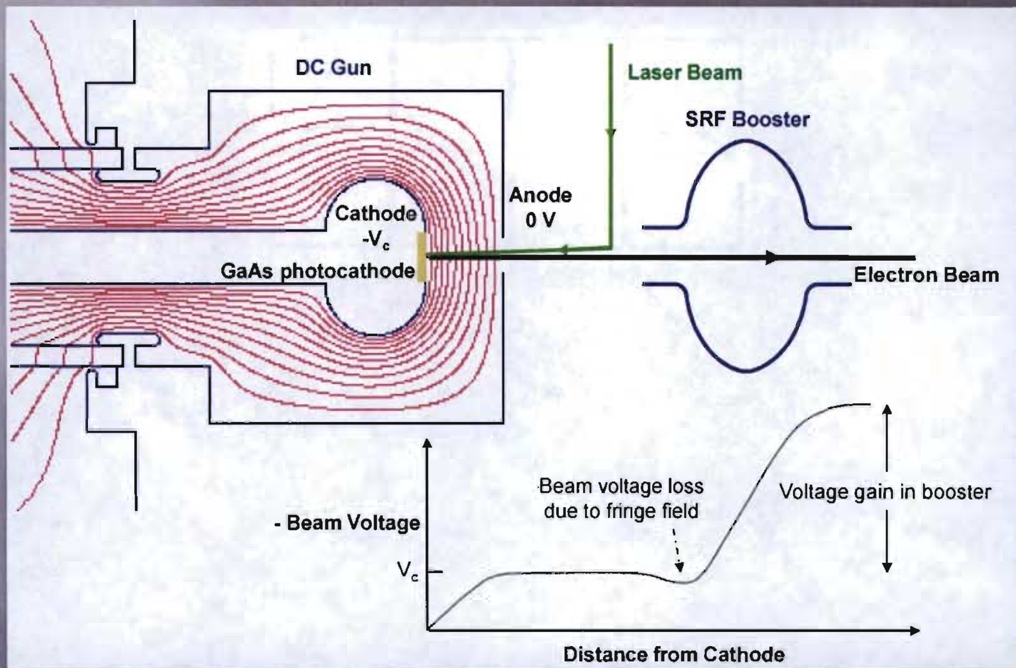

DC Electron Gun

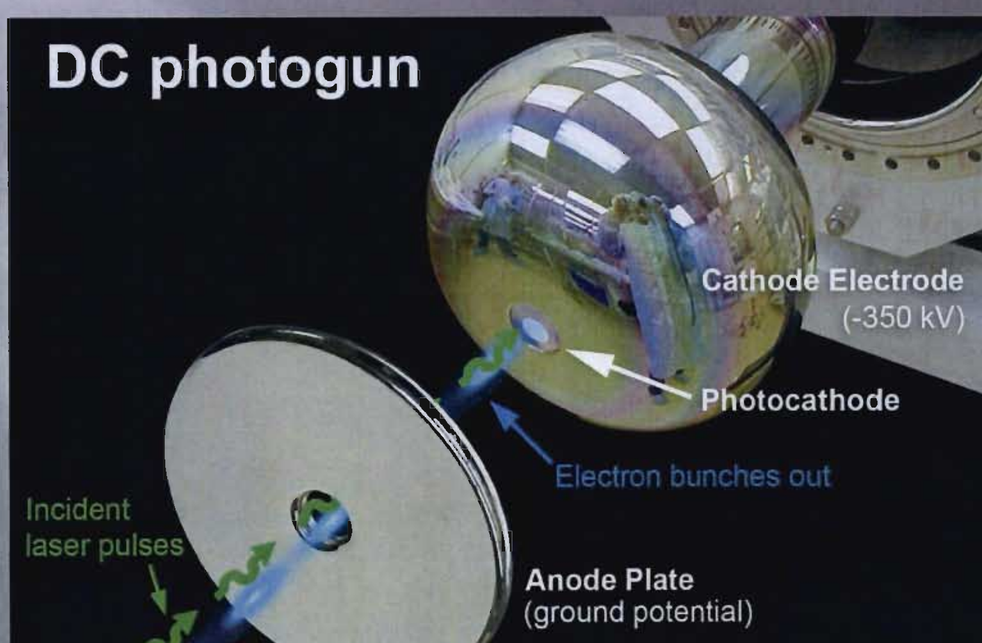

Courtesy of C. Hernandez-Garcia

DC Injector Performance

	DC Gun	Pulsed NCRF	High-duty NCRF	SRF Injector
Gradient (MV/m)	6	100	26	16
Energy (MeV)	0.35	5	2	3
Bunch charge (nC)	0.135	1	5	0.4
Average current (mA)	10	<0.001	32	<1
Transverse emittance (µm)	10	1	10	3
Bunch length (ps)	50	5	20	15
Photocathodes	GaAs	Cu	K_2CsSb	Cs_2Te
Photon energy (eV) **Photon wavelength (nm)**	2.3 530	4.6 266	2.3 530	4.6 266
Photocathode lifetime	days	months	hours	months

GaAs Photocathodes

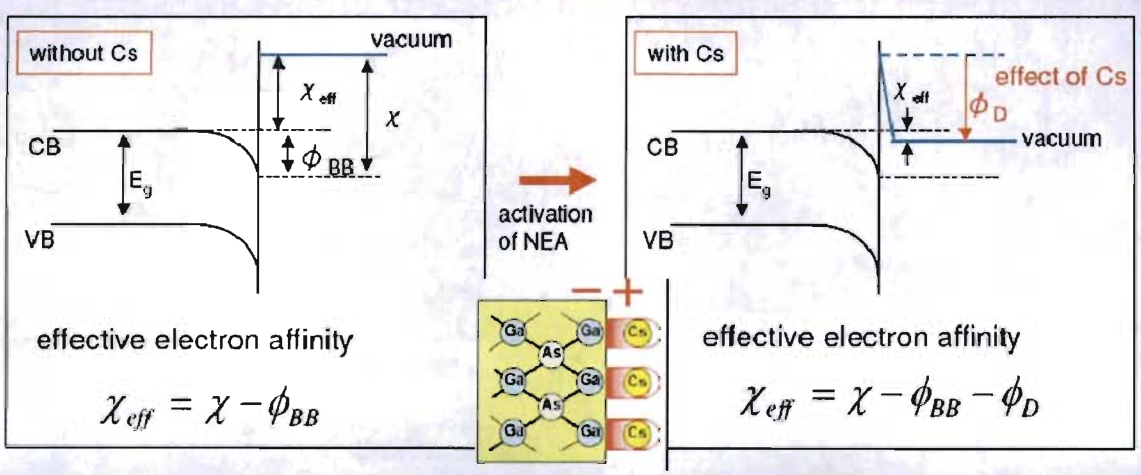

The quantum efficiency (QE) of GaAs cathode is enhanced by adding a monolayer of cesium to the surface. Cesium reduces the effective electron affinity by lowering the vacuum energy level to below the bulk energy level. Cesiated GaAs is thus a negative electron affinity (NEA) photocathode.

RF Injector Schematic

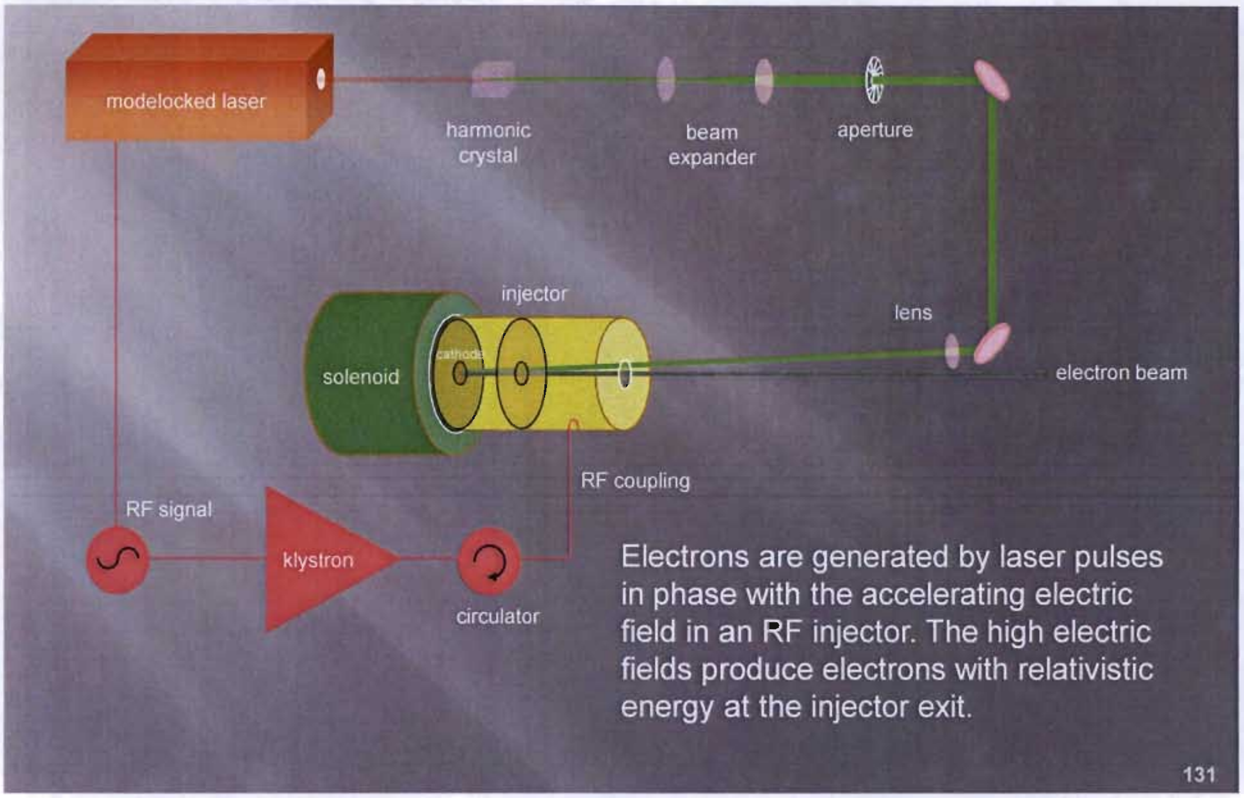

Normal-Conducting RF Injectors

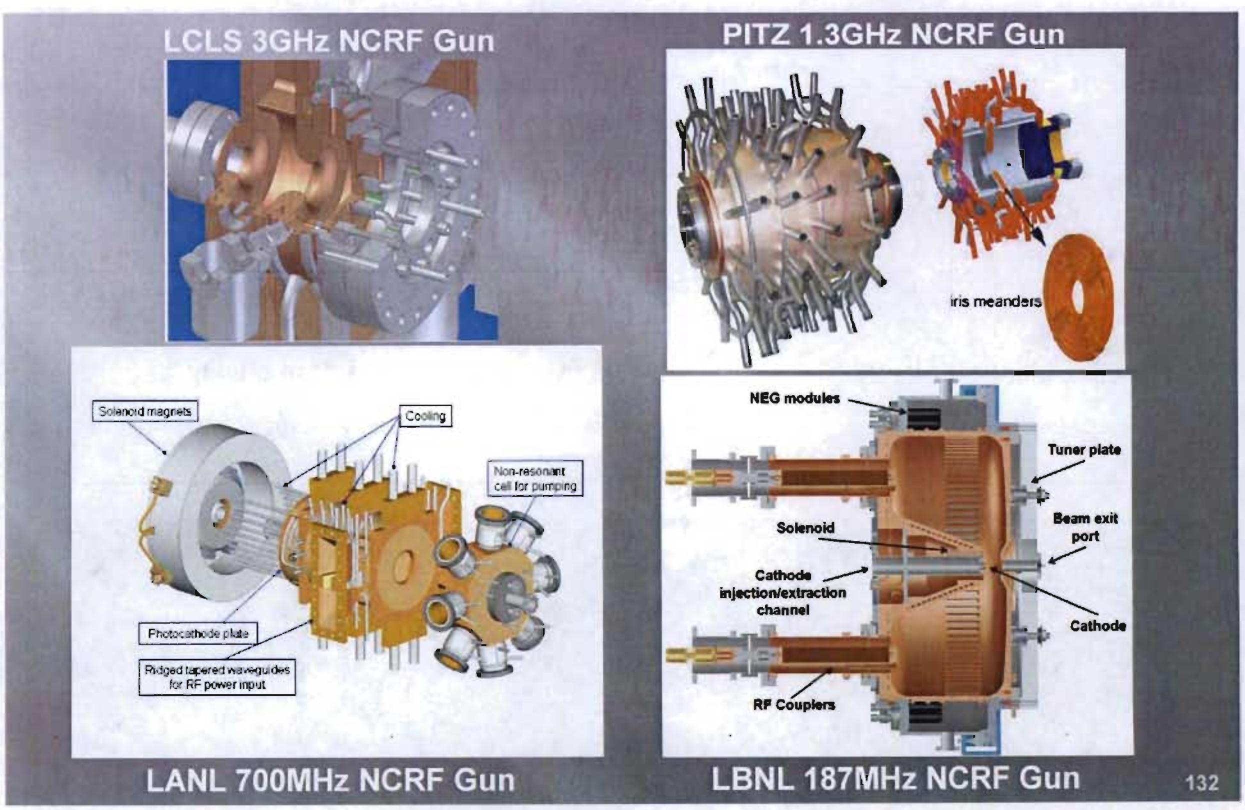

NCRF Injector Performance

	DC Gun	Pulsed NCRF	High-duty NCRF	SRF Injector
Gradient (MV/m)	6	100	26	16
Energy (MeV)	0.35	5	2	3
Bunch charge (nC)	0.135	1	5	0.4
Average current (mA)	10	<0.001	32	<1
Transverse emittance (μm)	10	1	10	3
Bunch length (ps)	50	5	20	15
Photocathodes	GaAs	Cu	K_2CsSb	Cs_2Te
Photon energy (eV) **Photon wavelength (nm)**	2.3 530	4.6 266	2.3 530	4.6 266
Photocathode lifetime	days	months	hours	months

Electron Photoemission from Semiconductor Photocathodes

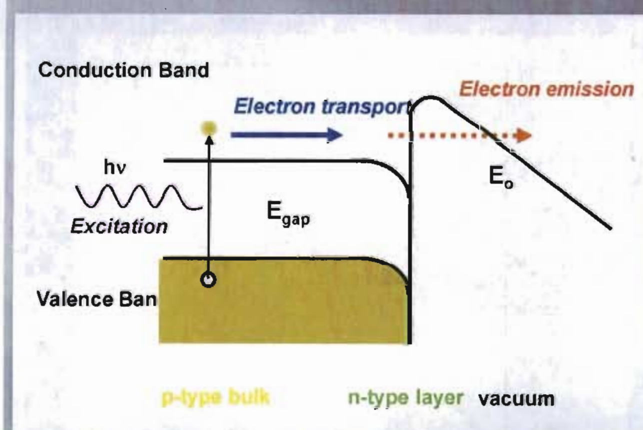

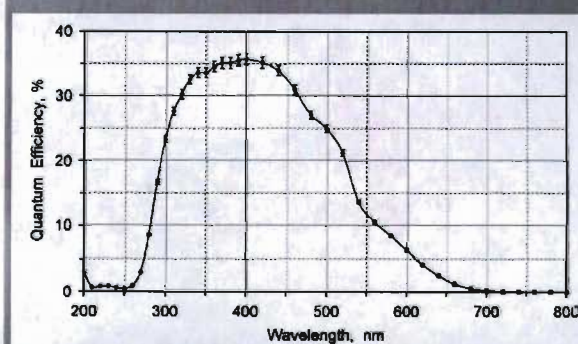

Quantum efficiency of CsK_2Sb

Photoelectron emission from a semiconductor photocathode is a three-step process, involving first **excitation** of electrons from valence band to conduction band, followed by **electron transport** from the bulk to the cathode-vacuum boundary, and finally **electron emission** via tunneling through a potential barrier.

Photocathode Lifetime

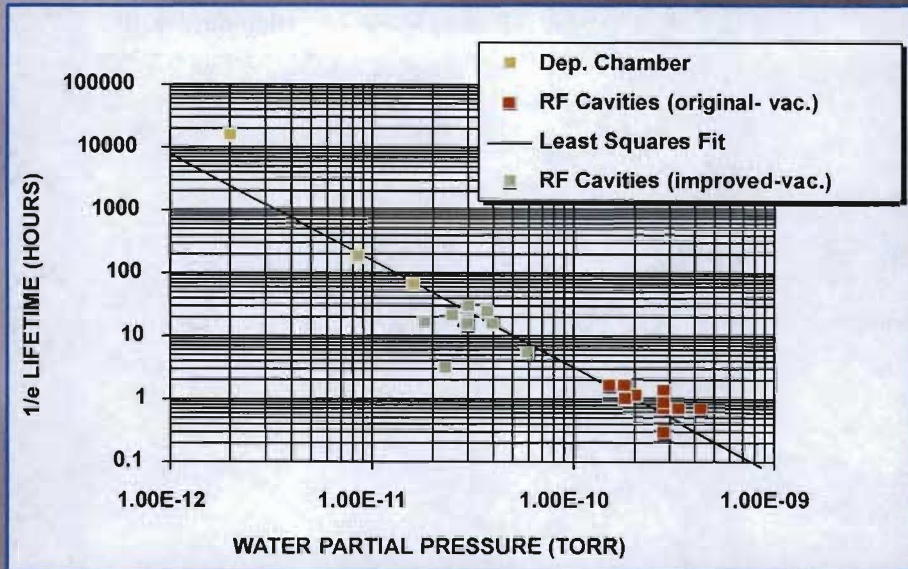

Cesiated cathode lifetime depends strongly on partial pressures of water and other oxygen-containing gases in the RF cavity.

Courtesy of Dave Dowell

Space Charge Limited Emission

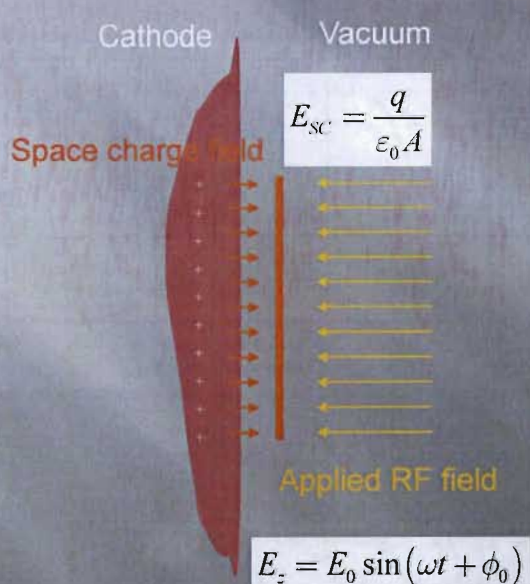

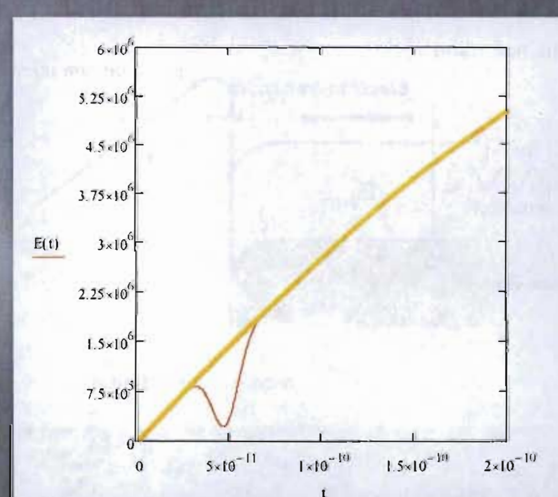

Applied RF field must exceed space charge field to avoid shutting off emission of photoelectrons during the laser pulse.

Emittance Compensation with Solenoid Magnets in NCRF Gun

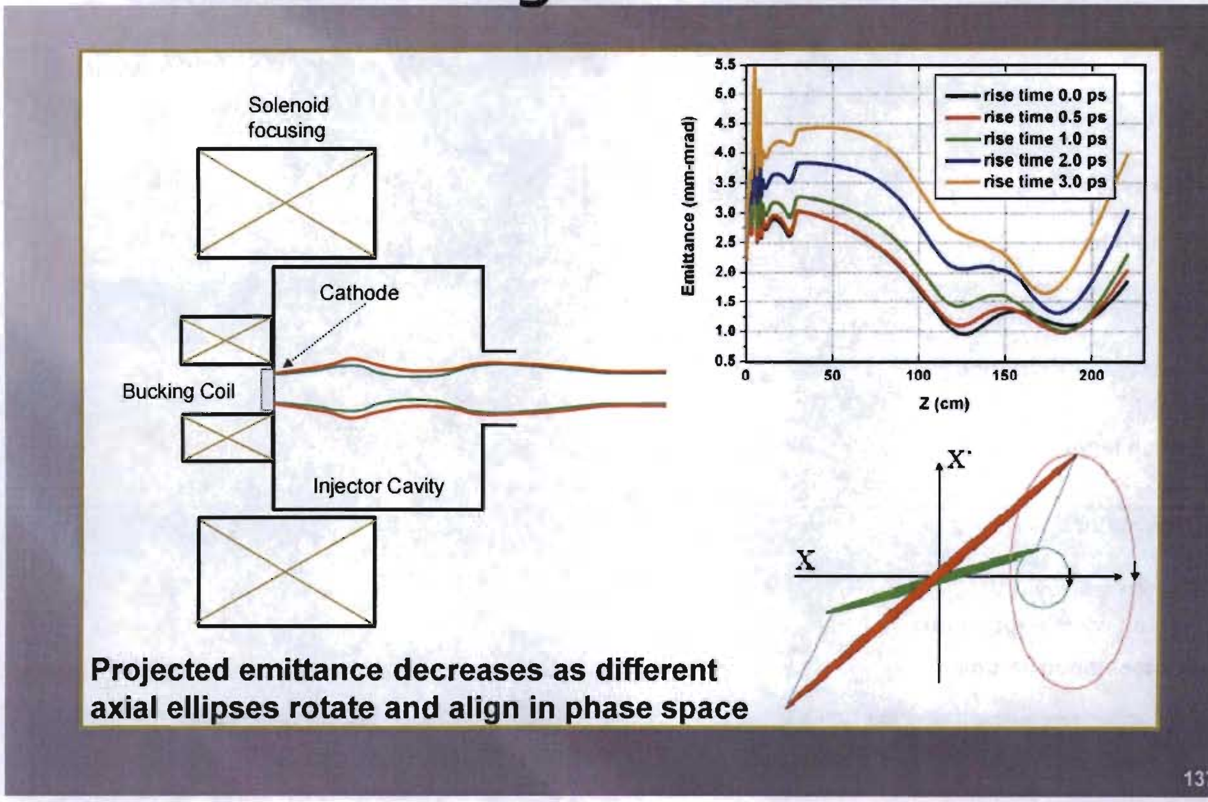

Superconducting RF Injectors

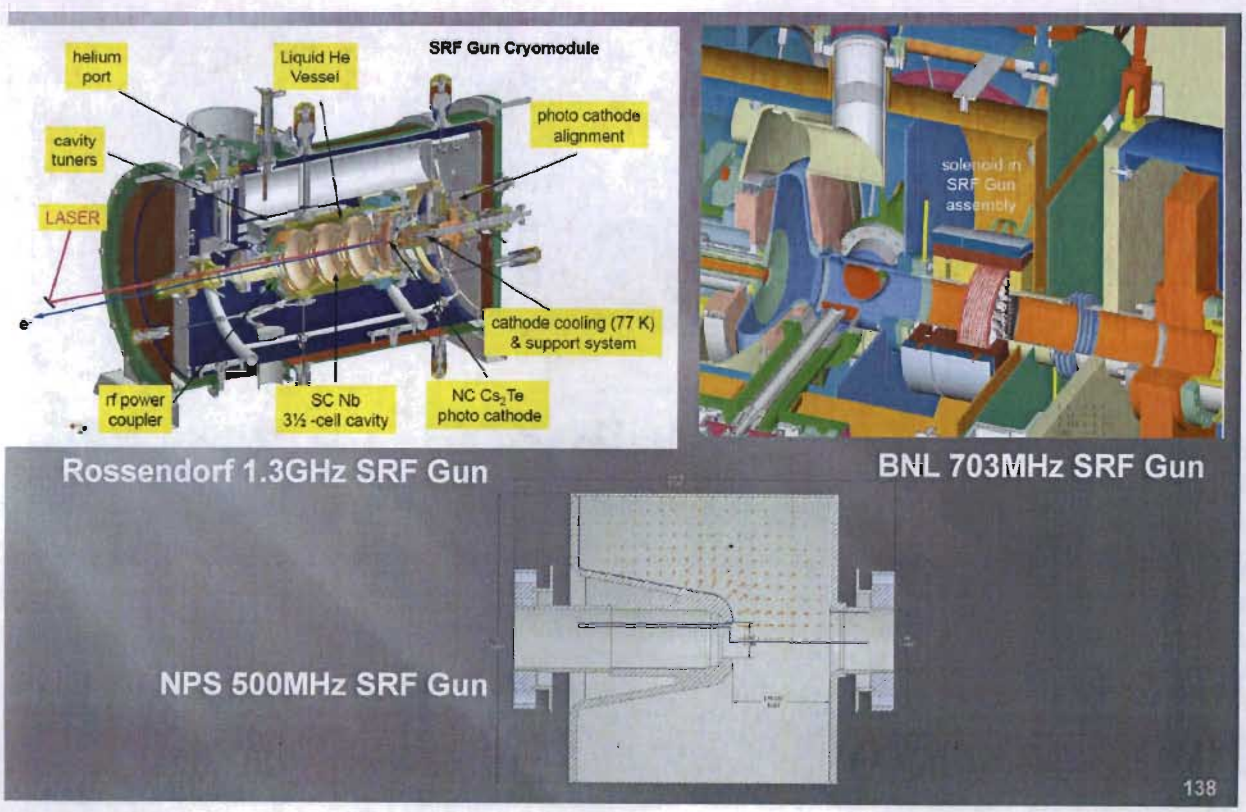

SRF Injector Performance

	DC Gun	Pulsed NCRF	High-duty NCRF	SRF Injector
Gradient (MV/m)	6	100	26	16
Energy (MeV)	0.35	5	2	3
Bunch charge (nC)	0.135	1	5	0.4
Average current (mA)	10	<0.001	32	<1
Transverse emittance (μm)	10	1	10	3
Bunch length (ps)	50	5	20	15
Photocathodes	GaAs	Cu	K_2CsSb	Cs_2Te
Photon energy (eV) Photon wavelength (nm)	2.3 530	4.6 266	2.3 530	4.6 266
Photocathode lifetime	days	months	hours	months

139

Los Alamos
NATIONAL LABORATORY
EST. 1943

Part 8
Backup Slides
Review Materials

140

Physical Constants

Speed of light	c	2.9979×10^{8} m/s	$c = \sqrt{\dfrac{1}{\mu_0 \varepsilon_0}}$
Permeability of vacuum	μ_0	$4\pi \times 10^{-7}$ H/m	
Permittivity of vacuum	ε_0	8.8542×10^{-12} F/m	$\varepsilon_0 = \dfrac{1}{\mu_0 c^2}$
Free space impedance	Z_0	376.73 Ω	$Z_0 = \sqrt{\dfrac{\mu_0}{\varepsilon_0}} = c\mu_0 = \dfrac{1}{c\varepsilon_0}$
Electronic charge	e	1.6022×10^{-19} C	
Electron mass	m_0	9.1094×10^{-31} kg	
Electron rest energy	m_0c^2	0.511 MeV	
Classical electron radius	r_0	2.81794×10^{-15} m	$r_0 = \dfrac{1}{4\pi\varepsilon_0}\dfrac{e^2}{mc^2}$
Alfven current	I_0	1.7×10^{4} A	$I_0 = \dfrac{ec}{r_0} = \dfrac{1}{4\pi\varepsilon_0}\dfrac{m_0c^3}{e}$

Maxwell Equations

Gauss' law for electricity

$$\nabla \cdot \mathbf{E} = \frac{\rho}{\varepsilon_0} \longrightarrow \mathbf{D} = \varepsilon_0 \mathbf{E} \longrightarrow$$

Gauss' law for magnetism

$$\nabla \cdot \mathbf{B} = 0$$

Faraday's law

$$\nabla \times \mathbf{E} = -\frac{\partial \mathbf{B}}{\partial t}$$

Ampere's law

$$\nabla \times \mathbf{B} = \mu_0 \mathbf{J} + \frac{1}{c^2}\frac{\partial \mathbf{E}}{\partial t} \longrightarrow \mathbf{B} = \mu_0 \mathbf{H} \longrightarrow$$

Maxwell Equations in simple forms

$$\nabla \cdot \mathbf{D} = \rho$$

$$\nabla \cdot \mathbf{B} = 0$$

$$\nabla \times \mathbf{E} = -\frac{\partial \mathbf{B}}{\partial t}$$

$$\nabla \times \mathbf{H} = \mathbf{J} + \frac{\partial \mathbf{D}}{\partial t}$$

Special Relativity

1. All inertial frames are completely equivalent with regard to physical phenomena
2. The speed of light in vacuum is the same for all observers in inertial frames of reference.

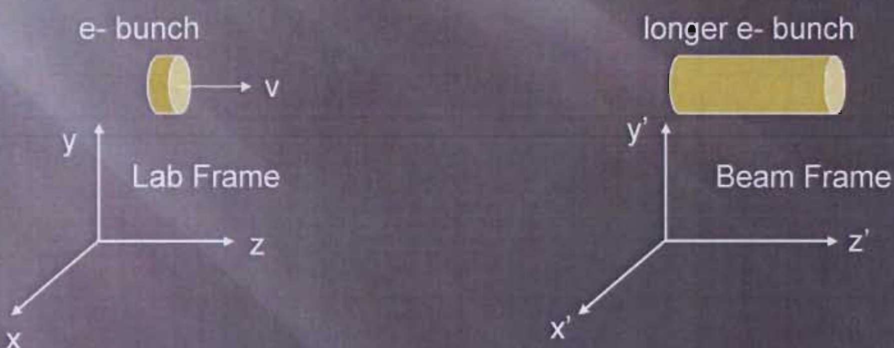

Lorentz Transformation

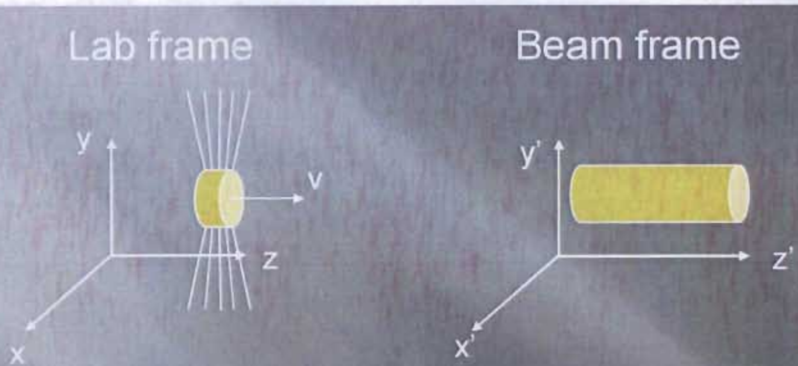

Lorentz factor

$$\gamma = \frac{1}{\sqrt{1-\beta^2}}$$

$$\beta = \frac{v}{c}$$

Transverse dimensions are unchanged

Lengths of moving objects along direction of motion is contracted by γ (**Lorentz contraction**). The proper length of any object in its rest frame is the longest.

Electric field lines are squished together (stronger) in the lab frame and further apart (weaker) in the beam frame.

Wiggler period is contracted by γ in electron beam frame

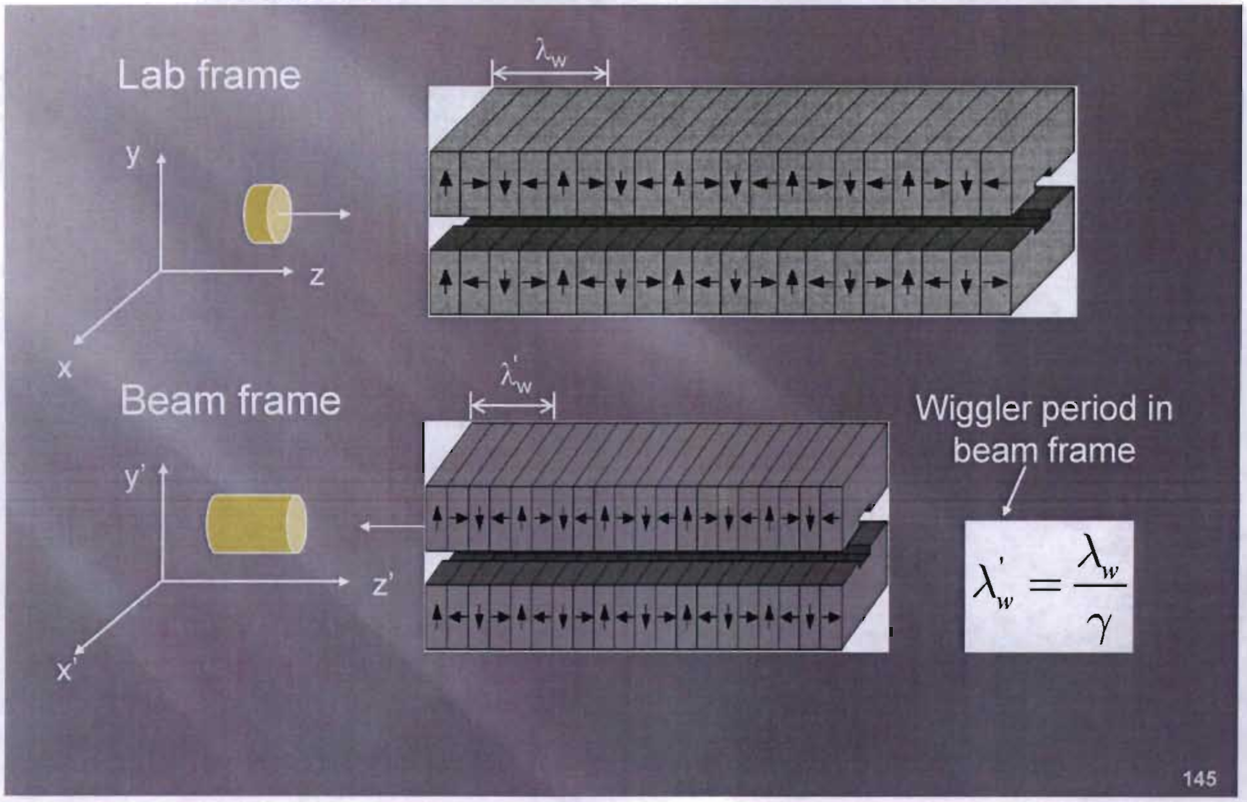

Wiggler field transforms into EM field in electron beam frame

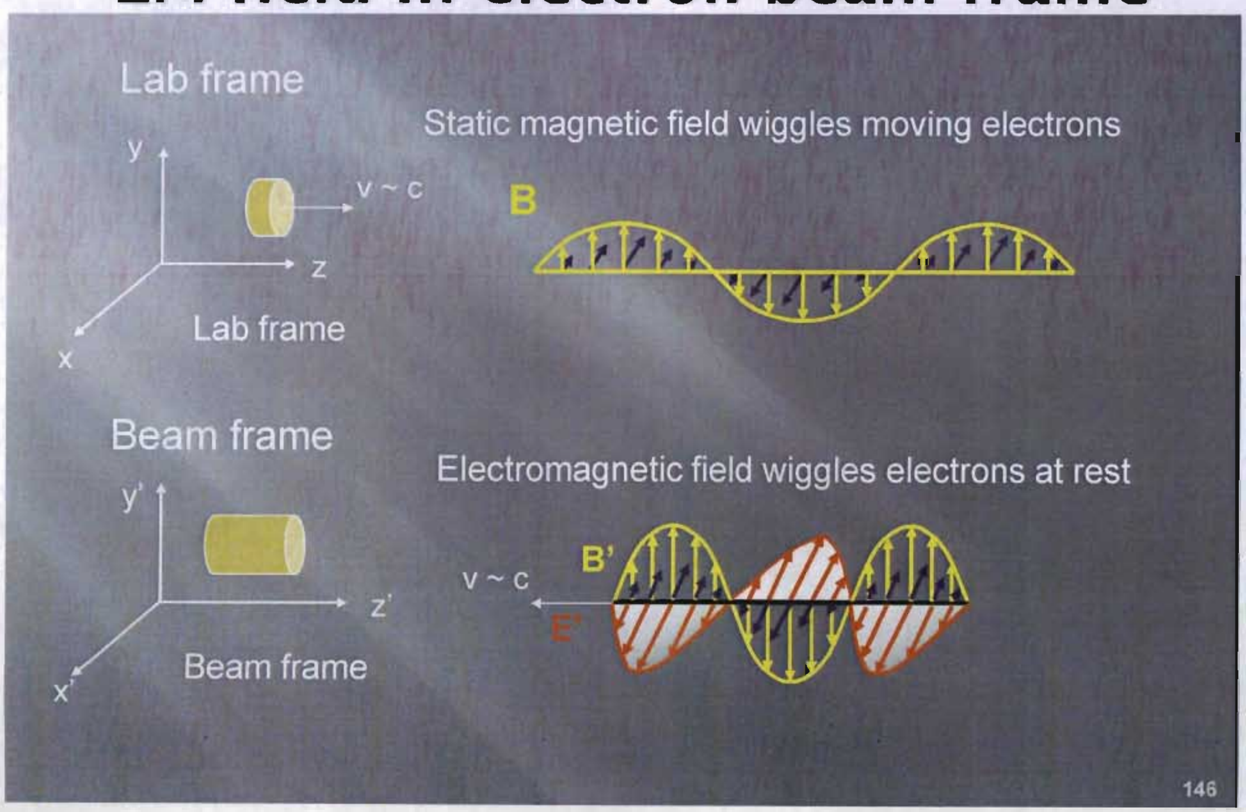

Wiggler EM field causes electrons to radiate real photons at λ'

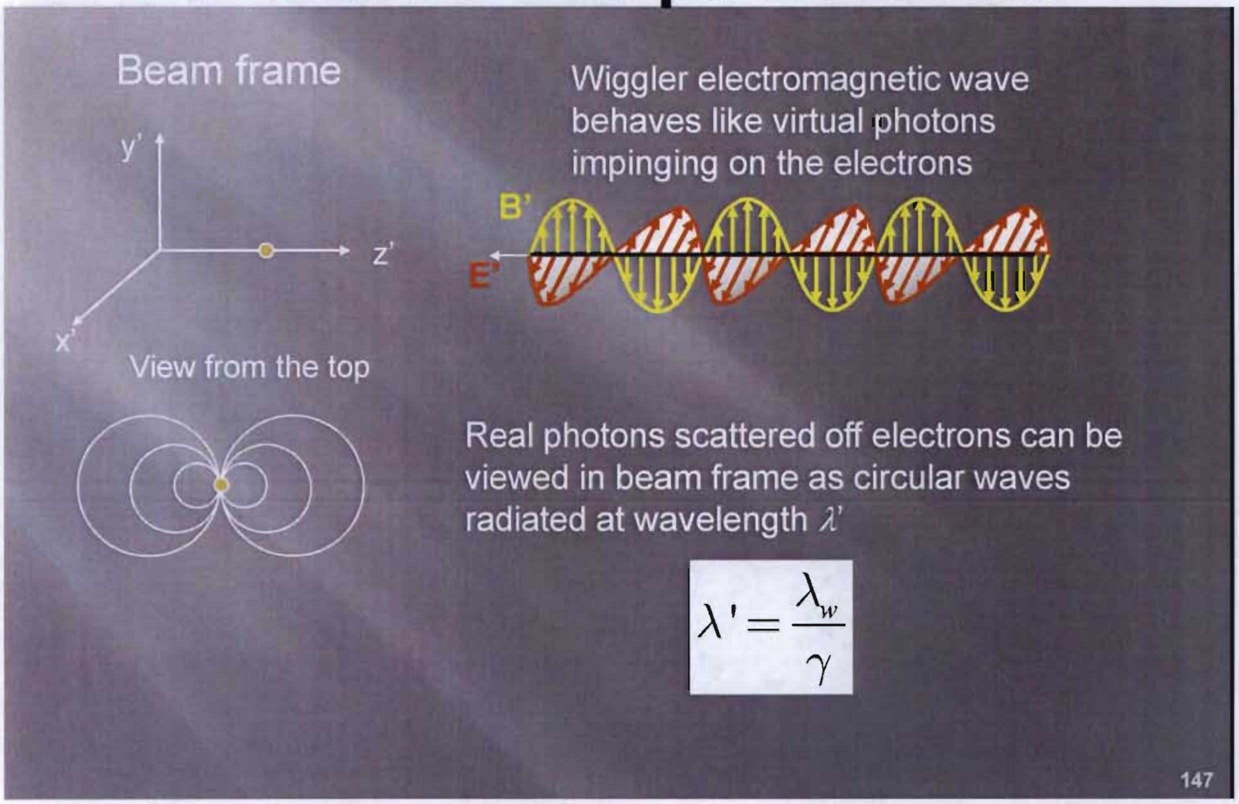

Relativistic Doppler Shifts

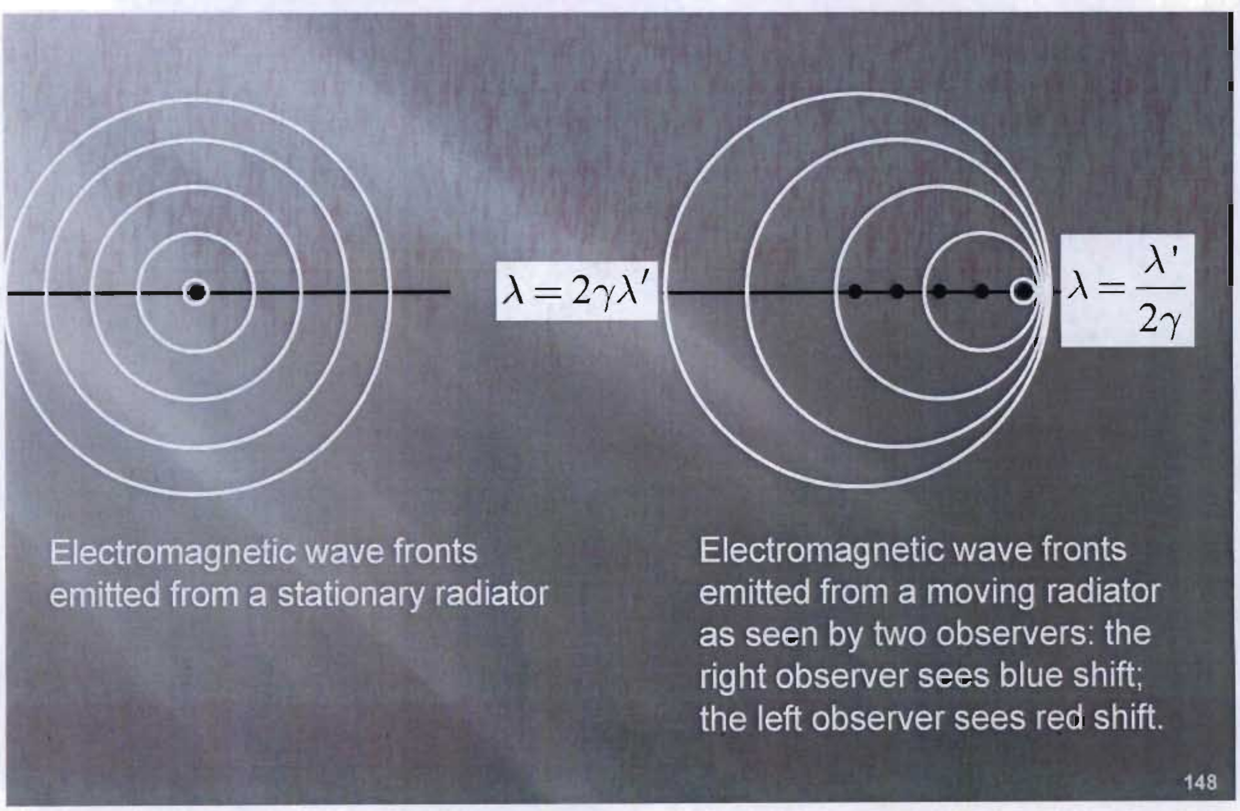

Radiation wavelength is shorter than wiggler period by $2\gamma^2$

Beam frame

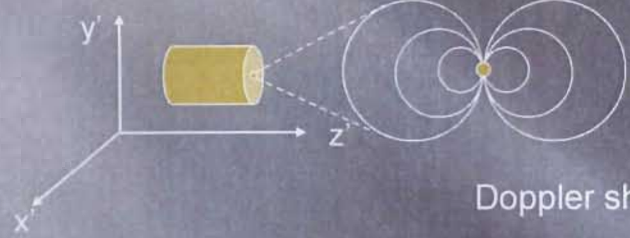

Doppler shift in forward direction

$$\lambda = \frac{\lambda'}{2\gamma}$$

Lab frame

Combine Lorentz contraction and Doppler shift

$$\lambda = \frac{\lambda_w}{2\gamma^2}$$

Relativistic Energy & Momentum

Total energy $E = T + m_0c^2 = \gamma m_0 c^2$

Momentum $p = \beta\gamma m_0 c$

Momentum x speed of light $pc = \beta\gamma m_0 c^2$

$$E^2 = (pc)^2 + (m_0c^2)^2$$